USGS
science for a changing world

Techniques of Water-Resources Investigations
of the United States Geological Survey

CHAPTER D1

APPLICATION OF SURFACE GEOPHYSICS TO GROUND-WATER INVESTIGATIONS

By A. A. R. Zohdy, G. P. Eaton,
and D. R. Mabey

BOOK 2
COLLECTION OF ENVIRONMENTAL DATA

Electrical Methods

By A. A. R. Zohdy

The electrical properties of most rocks in the upper part of the Earth's crust are dependent primarily upon the amount of water in the rock, the salinity of the water, and the distribution of the water in the rock. Saturated rocks have lower resistivities than unsaturated and dry rocks. The higher the porosity of the saturated rock, the lower its resistivity, and the higher the salinity of the saturating fluids, the lower the resistivity. The presence of clays and conductive minerals also reduces the resistivity of the rock.

Two properties are of primary concern in the application of electrical methods: (1) the ability of rocks to conduct an electric current, and (2) the polarization which occurs when an electrical current is passed through them (induced polarization). The electrical conductivity of Earth materials can be studied by measuring the electrical potential distribution produced at the Earth's surface by an electric current that is passed through the Earth or by detecting the electromagnetic field produced by an alternating electric current that is introduced into the Earth. The measurement of natural electric potentials (spontaneous polarization, telluric currents, and streaming potentials) has also found application in geologic investigations. The principal methods using natural energy sources are (1) telluric current, (2) magnetotelluric, (3) spontaneous polarization, and (4) streaming potential.

Telluric Current Method

Telluric currents (Cagniard, 1956; Berdichevskii, 1960; Kunetz; 1957) are natural electric currents that flow in the Earth's crust in the form of large sheets, and that constantly change in intensity and in direction. Their presence is detected easily by placing two electrodes in the ground separated by a distance of about 300 meters (984 feet) or more and measuring the potential difference between them. The origin of these telluric currents is believed to be in the ionosphere and is related to ionospheric tidal effects and to the continuous flow of charged particles from the Sun which become trapped by the lines of force of the Earth's magnetic field.

If the ground in a given area is horizontally stratified and the surface of the basement rocks is also horizontal, then, at any given moment, the density of the telluric current is uniform over the entire area. In the presence of geologic structures, however, such as anticlines, synclines, and faults, the distribution of current density is not uniform over the area. Furthermore, current density is a vector quantity, and the vector is larger when the telluric current flows at right angles to the axis of an anticline than when the current flows parallel to the axis (fig. 1). By plotting these vectors we obtain ellipses over anticlines and synclines and circles where the basement rocks are horizontal. The longer axis of the ellipse is oriented at right angles to the axis of the geologic structure.

The measurement of telluric field intensity is relatively simple. Four electrodes, M, N, M′, and N′ are placed on the surface of the ground at the ends of two intersecting perpendicular lines (fig. 2), and the potential differences are recorded on a potentiometric chart recorder or on an x-y plotter (Yungul, 1968). From these measurements two components E_x and E_y of the telluric field can

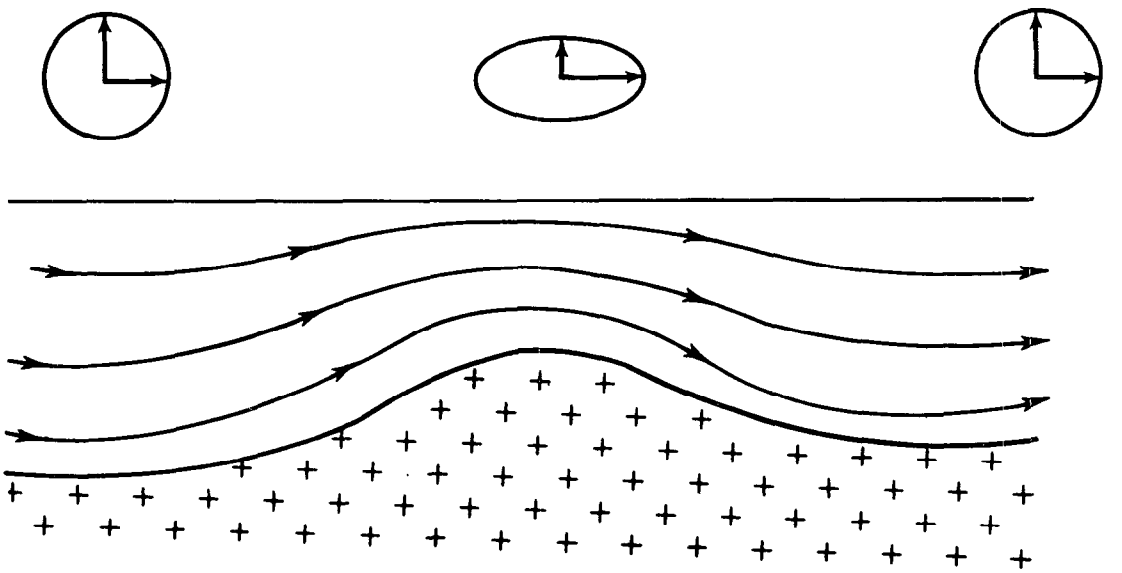

Figure 1.—Flow of telluric current over an anticline. Ellipse and circles indicate telluric field intensity as a function of direction with respect to axis of anticline.

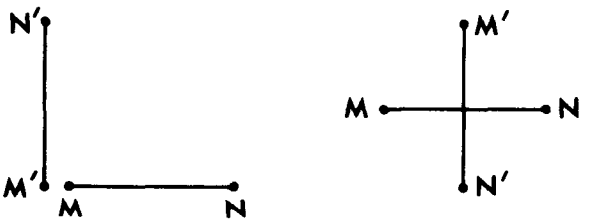

Figure 2.—Examples of electrode arrays for measuring x and y components of telluric field. M, M', N, and N' are potential electrodes.

be computed, and the total field obtained by adding E_x and E_y vectorially.

The intensity and direction of the telluric current field vary with time; therefore, measurements must be recorded simultaneously at two different stations to take into account this variation. One station is kept stationary (base station), and the other is moved to a new location in the field (field station) after each set of measurements. The ratio of the area of the ellipse at the field station to the area of a unit circle (Keller and Frischknecht, 1966) at the base station is calculated mathematically. When a contour map of equal elliptical areas is prepared (Migaux, 1946, 1948; Migaux and others, 1952; Migaux and Kunetz, 1955; Schlumberger, 1939) it reflects the major geologic structures of the basement rocks in very much the same manner as a gravity map or magnetic map. However, a telluric map (fig. 3) delineates rock structure based on differences in electrical resistivity rather than on differences in density or magnetic susceptibility.

Magneto-Telluric Method

The magneto-telluric method (Berdichevskii, 1960; Cagniard, 1953) of measuring resistivity is similar to the telluric current method but has the advantage of providing an estimate of the true resistivity of the layers. Measurements of amplitude variations in the telluric field E_x and the associated magnetic field H_y determine earth resistivity. Magneto-telluric measurements at several frequencies provide information on the variation of resistivity with depth because the depth of penetration of electromagnetic waves is a function of frequency. A limitation of the method is the instrumental difficulty of measuring rapid fluctuations of the magnetic field. Interpretation techniques usually involve comparisons of observed data with theoretical curves. The method is useful in exploration to depths greater than can be

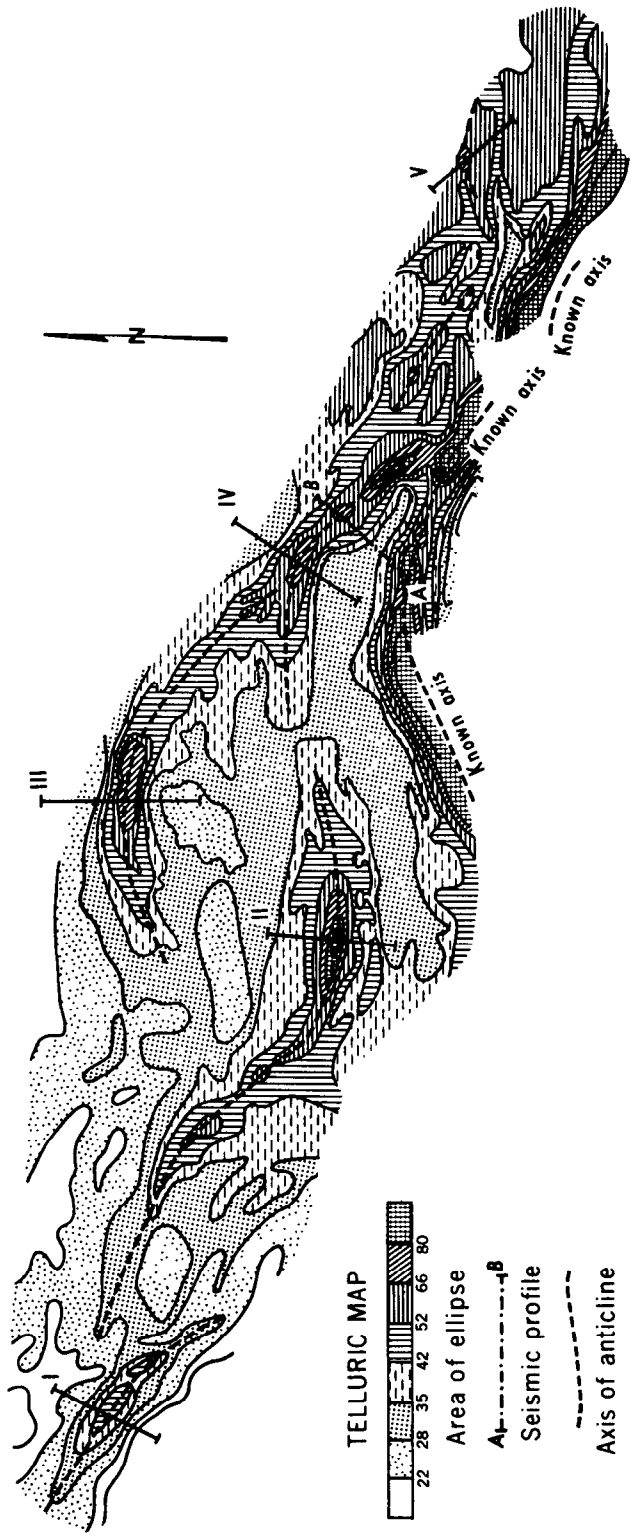

Figure 3.—Telluric map of the Aquitaine basin, France.

reached effectively by methods using artificially induced currents.

To the author's knowledge the telluric and magneto-telluric methods have not been used extensively in the Western Hemisphere; however, the methods have been used extensively in the Eastern Hemisphere by French and Russian geophysicists in petroleum exploration. The use of the methods in ground-water exploration is recommended at present only for reconnaissance of large basins.

Spontaneous Polarization and Streaming Potentials

Spontaneous polarization or self-potential methods involve measurement of electric potentials developed locally in the Earth by electro-chemical activity, electrofiltration activity, or both. The most common use of self-potential surveys has been in the search for ore bodies in contact with solutions of different compositions. The result of this contact is a potential difference and current flow which may be detected at the ground surface. Of more interest to ground-water investigations are the potentials generated by water moving through a porous medium (streaming potentials). Measurements of these potentials have been used to locate leaks in reservoirs and canals (Ogilvy and others, 1969).

Spontaneous potentials generally are no larger than a few tens of millivolts but in some places may reach a few hundred millivolts. Relatively simple equipment can be used to measure the potentials, but spurious sources of potentials often obscure these natural potentials. Interpretation is usually qualitative although some quantitative interpretations have been attempted.

Direct Current-Resistivity Method

In the period from 1912 to 1914 (Dobrin, 1960) Conrad Schlumberger began his pioneering studies which lead to an understanding of the merits of utilizing electrical resistivity methods for exploring the subsurface (Compagnie Générale de Géophysique, 1963). According to Breusse (1963), the real progress in applying electrical methods to ground-water exploration began during World War II. French, Russian, and German geophysicists are mainly responsible for the development of the theory and practice of direct-current electrical prospecting methods.

Definition and Units of Resistivity

It is well known that the resistance R, in ohms, of a wire is directly proportional to its length L and is inversely proportional to its cross-sectional area A. That is:

$$R \propto L/A,$$

or

$$R = \rho \frac{L}{A}, \qquad (1)$$

where ρ, the constant of proportionality, is known as the electrical resistivity or electrical specific resistance, a characteristic of the material which is independent of its shape or size. According to Ohm's law, the resistance is given by

$$R = \Delta V/I, \qquad (2)$$

where ΔV is the potential difference across the resistance and I is the electric current through the resistance.

Substituting equation 1 in equation 2 and rearranging we get

$$\rho = \frac{A}{L}\frac{\Delta V}{I}. \qquad (3)$$

Equation 3 may be used to determine the resistivity ρ of homogeneous and isotropic materials in the form of regular geometric shapes, such as cylinders, parallelopipeds, and cubes. In a semi-infinite material the resistivity at every point must be defined. If the cross-sectional area and length of an element within the semi-infinite material are shrunk to infinitesimal size then the resistivity ρ may be defined as

$$\rho = \frac{\lim_{L \to 0} (\Delta V/L)}{\lim_{A \to 0} (I/A)}$$

or

$$\rho = \frac{E_L}{J} \qquad (4)$$

where E_L is the electric field and J is the current density. To generalize, we write

$$\rho = \frac{E}{J}. \qquad (5)$$

Equation 5 is known as Ohm's law in its differential vectorial form.

The resistivity of a material is defined as being numerically equal to the resistance of a specimen of the material of unit dimensions. The unit of resistivity in the mks (meter-kilogram-second) system is the ohm-meter. In other systems it may be expressed in ohm-centimeter, ohm-foot, or other similar units.

Rock Resistivities

The resistivity ρ of rocks and minerals displays a wide range. For example, graphite has a resistivity of the order of 10^{-6} ohm-m, whereas some dry quartzite rocks have resistivities of more than 10^{12} ohm-m (Parasnis, 1962). No other physical property of naturally occurring rocks or soils displays such a wide range of values.

In most rocks, electricity is conducted electrolytically by the interstitial fluid, and resistivity is controlled more by porosity, water content, and water quality than by the resistivities of the rock matrix. Clay minerals, however, are capable of conducting electricity electronically, and the flow of current in a clay layer is both electronic and electrolytic. Resistivity values for unconsolidated sediments commonly range from less than 1 ohm-m for certain clays or sands saturated with saline water, to several thousand ohm-m for dry basalt flows, dry sand, and gravel. The resistivity of sand and gravel saturated with fresh water ranges from about 15 to 600 ohm-m. Field experience indicates that values ranging from 15 to 20 ohm-m are characteristic of aquifers in the southwestern United States, whereas in certain areas in California the resistivity of fresh-water bearing sands generally ranges from 100 to 250 ohm-m. In parts of Maryland resistivities have been found to range between about 300 and 600 ohm-m, which is about the same range as that for basaltic aquifers in southern Idaho. These figures indicate that the geophysicists should be familiar with the resistivity spectrum in the survey area before he draws conclusions about the distribution of fresh-water aquifers.

Principles of Resistivity Method

In making resistivity surveys a commutated direct current or very low frequency (<1 Hz) current is introduced into the ground via two electrodes. The potential difference is measured between a second pair of electrodes. If the four electrodes are arranged in any of several possible patterns, the current and potential measurements may be used to calculate resistivity.

The electric potential V at any point P caused by a point electrode emitting an electric current I in an infinite homogeneous and isotopic medium of resistivity ρ is given by

$$V = \frac{\rho I}{4\pi R}, \qquad (6)$$

where $R = \sqrt{x^2 + y^2 + z^2}$.

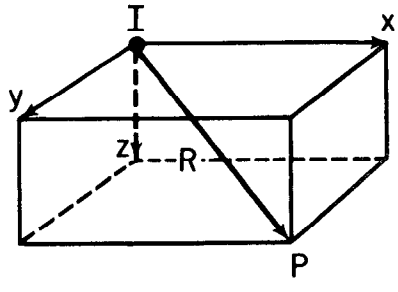

Figure 4.—Diagram showing the relationship between a point source of current I (at origin of coordinates) in an isotropic medium of resistivity ρ and the potential V at any point P. $V = \frac{\rho I}{4\pi R}$, where $R = \sqrt{x^2 + y^2 + z^2}$.

For a semi-infinite medium, which is the simplest Earth model, and with both current and potential point-electrodes placed at the Earth surface ($z = 0$), equation 6 reduces to

$$V = \frac{\rho I}{2\pi\sqrt{x^2 + y^2}} = \frac{\rho I}{2\pi \overline{AM}} \qquad (7)$$

where $\overline{AM}$ is the distance on the Earth surface between the positive current electrode A and the potential electrode M. When two current electrodes, A and B, are used and the potential difference, ΔV, is measured between two measuring electrodes M and N, we get

$V_M^A = \frac{\rho I}{2\pi}\frac{1}{\overline{AM}}$ = potential at M due to positive electrode A,

$V_N^A = \frac{\rho I}{2\pi}\frac{1}{\overline{AN}}$ = potential at N due to positive electrode A,

$V_M^B = \frac{\rho I}{2\pi}\frac{1}{\overline{BM}}$ = potential at M due to negative electrode B,

$V_N^B = \frac{\rho I}{2\pi}\frac{1}{\overline{BN}}$ = potential at N due to negative electrode B,

$V_M^{A,B} = \frac{\rho I}{2\pi}\left(\frac{1}{\overline{AM}} - \frac{1}{\overline{BM}}\right)$ = total potential at M due to A and B,

$V_N^{A,B} = \frac{\rho I}{2\pi}\left(\frac{1}{\overline{AN}} - \frac{1}{\overline{BN}}\right)$ = total potential at N due to A and B,

and, therefore, the net potential difference is:

$$\Delta V_{MN}^{A,B} = V_M^{A,B} - V_N^{A,B} =$$

$$\frac{\rho I}{2\pi}\left(\frac{1}{\overline{AM}} - \frac{1}{\overline{BM}} - \frac{1}{\overline{AN}} + \frac{1}{\overline{BN}}\right). \qquad (8)$$

Rearranging equation 8, we express the resistivity ρ by:

$$\rho = \left(\frac{2\pi}{\frac{1}{\overline{AM}} - \frac{1}{\overline{BM}} - \frac{1}{\overline{AN}} + \frac{1}{\overline{BN}}}\right)\frac{\Delta V}{I}. \qquad (9)$$

Equation 9 is a fundamental equation in direct-current (d-c) electrical prospecting.

The factor $\dfrac{2\pi}{\frac{1}{\overline{AM}} - \frac{1}{\overline{BM}} - \frac{1}{\overline{AN}} + \frac{1}{\overline{BN}}}$ is called the geometric factor of the electrode arrangement and generally is designated by the letter K. Therefore,

$$\rho = K\frac{\Delta V}{I}. \qquad (10)$$

If the measurement of ρ is made over a semi-infinite space of homogeneous and isotropic material, then the value of ρ computed from equation 9 will be the true resistivity of that material. However, if the medium is inhomogeneous and (or) anisotropic then the resistivity computed from equation 9 is called an apparent resistivity $\bar{\rho}$.

The value of the apparent resistivity is a function of several variables: the electrode spacings $\overline{AM}$, $\overline{AN}$, $\overline{BM}$, and $\overline{BN}$, the geometry of the electrode array, and the true resistivities and other characteristics of the subsurface materials, such as layer thicknesses, angles of dip, and anisotropic properties. The apparent resistivity, depending on the electrode configuration and on the geology, may be a crude average of the true resistivities in the section, may be larger or smaller than any of the true resistivities, or may even be negative (Al'pin, 1950; Zohdy, 1969b).

Electrode Configurations

The value of $\bar{\rho}$ (eq. 9) depends on the four distance-variables $\overline{AM}$, $\overline{AN}$, $\overline{BM}$, and $\overline{BN}$. If $\bar{\rho}$ is made to depend on only one distance-variable the number of theoretical curves can be greatly reduced. Several electrode arrays have been invented to fulfill this goal.

Wenner Array

This well-known array was first proposed for geophysical prospecting by Wenner (1916). The four electrodes A, M, N, and B are placed at the surface of the ground along a straight line (fig. 5) so that $\overline{AM} = \overline{MN} = \overline{NB} = a$.

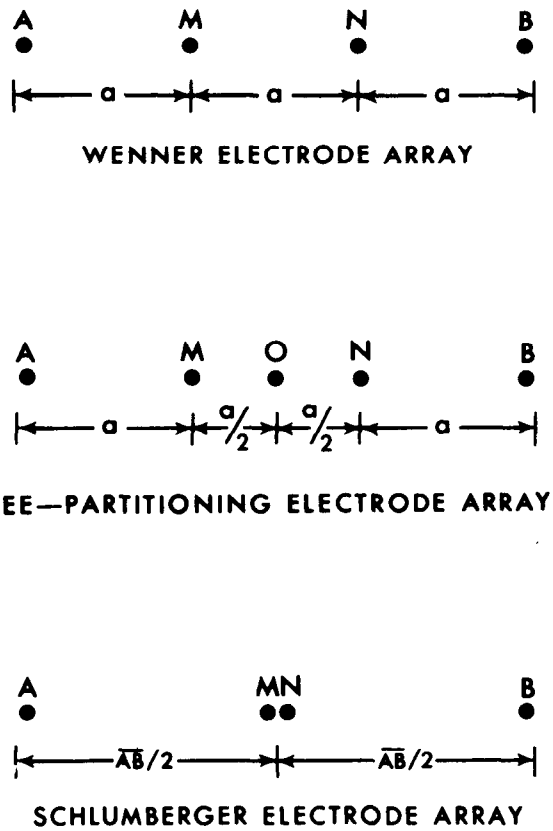

Figure 5.—Wenner, Lee-partitioning, and Schlumberger electrode arrays. A and B are current electrodes, M, N, and O are potential electrodes; a and $\overline{AB}/2$ are electrode spacings.

For the Wenner array, equation 9 reduces to:

$$\bar{\rho}_w = 2\pi a \frac{\Delta V}{I}. \qquad (11)$$

Thus the resistivity $\bar{\rho}_w$ is a function of the single distance-variable, a. The Wenner array is widely used in the Western Hemisphere.

Lee-Partitioning Array

This array is the same as the Wenner array, except that an additional potential electrode O is placed at the center of the array between the potential electrodes M and N. Measurements of the potential difference are made between O and M and between O and N. The formula for computing the Lee-partitioning apparent resistivity is given by

$$\bar{\rho}_{L.P.} = 4\pi a \frac{\Delta V}{I}$$

where ΔV is the potential difference between O and M or O and N. This array has been used extensively in the past (Van Nostrand and Cook, 1966).

Schlumberger Array

This array is the most widely used in electrical prospecting. Four electrodes are placed along a straight line on the Earth surface (fig. 5) in the same order, AMNB, as in the Wenner array, but with $\overline{AB} \geqq 5\overline{MN}$. For any linear, symmetric array AMNB of electrodes, equation 9 can be written in the form:

$$\bar{\rho} = \pi \frac{(\overline{AB}/2)^2 - (\overline{MN}/2)^2}{\overline{MN}} \frac{\Delta V}{I}, \qquad (12)$$

but if $\overline{MN} \to 0$, then equation 12 can be written as

$$\bar{\rho}_s = \pi (\overline{AB}/2)^2 \frac{E}{I} \qquad (13)$$

where $E = \lim_{\overline{MN} \to 0} \frac{\Delta V}{\overline{MN}}$ = electric field.

Conrad Schlumberger defined the resistivity in terms of the electric field E rather than the potential difference ΔV (as in the Wenner array). It can be seen from equation 13 that the Schlumberger apparent resistivity $\bar{\rho}_s$ is a function of a single distance-variable $(\overline{AB}/2)$. In practice it is possible to measure $\bar{\rho}_s$ according to equation 13, but only in an approximate manner. The apparent resistivity $\bar{\rho}_s$ usually is calculated by using equation 12 provided that $\overline{AB} \geqq 5\overline{MN}$ (Deppermann, 1954).

Dipole-Dipole Arrays

The use of dipole-dipole arrays in electrical prospecting has become common since the 1950's, particularly in Russia, where Al'pin (1950) developed the necessary theory. In a dipole-dipole array, the distance between the current electrodes A and B (current dipole) and the distance between the potential

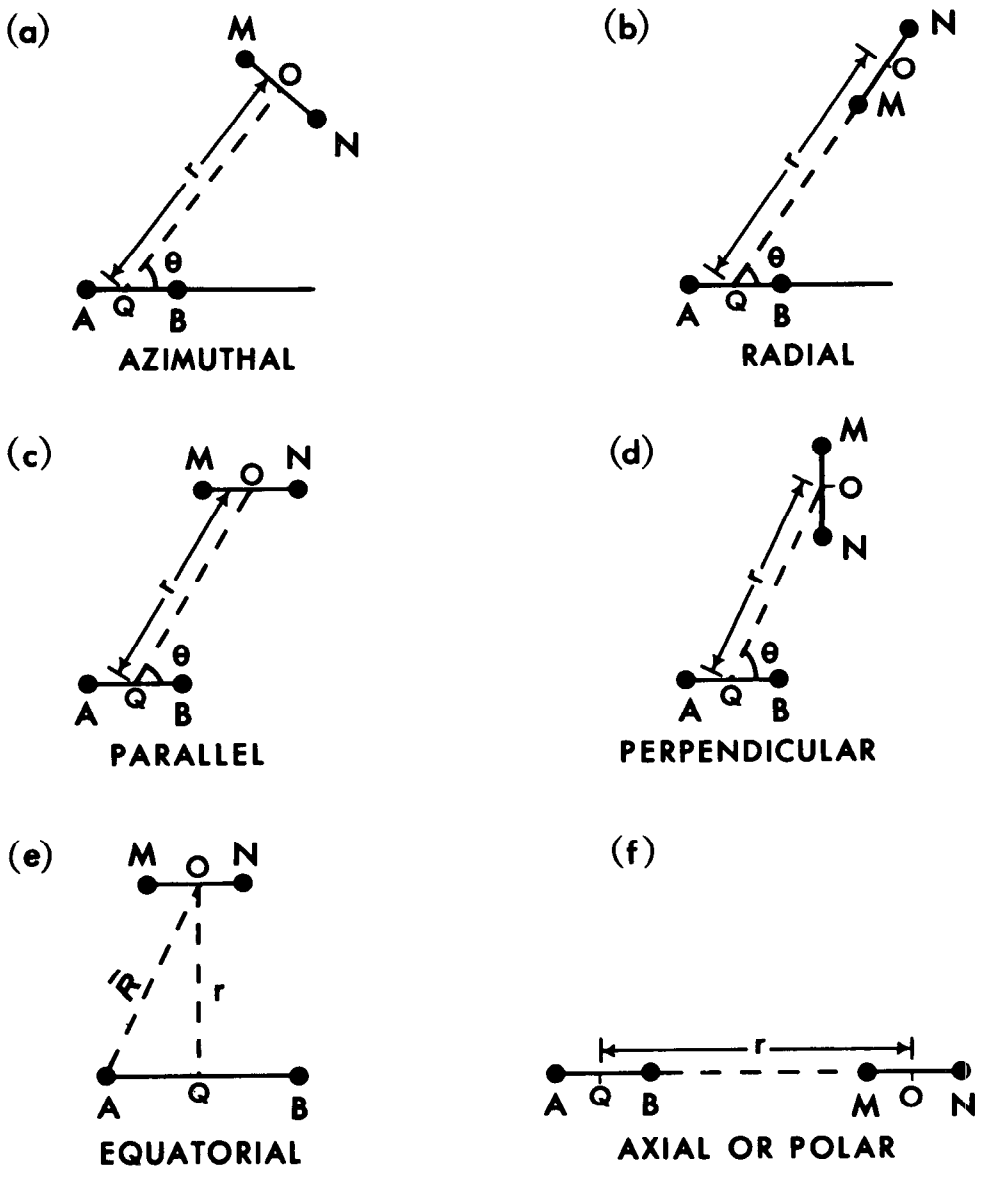

Figure 6.—Dipole-dipole arrays. The equatorial is a bipole-dipole array because AB is large.

electrodes M and N (measuring dipole) are significantly smaller than the distance r, between the centers of the two dipoles. Figure 6 (a, b, c, and d) shows the four basic dipole-dipole arrays that are recognized: azimuthal, radial, parallel, and perpendicular. When the azimuth angle θ formed by the line r and the current dipole AB equals $\frac{\pi}{2}$, the azimuthal array and the parallel array reduce to the equatorial array, and when $\theta = 0$ the parallel and radial arrays reduce to the polar (or axial) array. It can be shown (Al'pin, 1950; Bhattacharya and Patra, 1968; Keller and Frischknecht, 1966) that the electric field due to a dipole at a given point is inversely proportional to the cube of the distance r and that for a given azimuth angle θ the value of the apparent resistivity $\overline{\rho}$ is a function of the single distance-variable r.

Of the various dipole-dipole arrays, the equatorial array in its bipole-dipole form ($\overline{AB}$

is large and $\overline{MN}$ is small) has been used more often than the other dipole-dipole arrays. By enlarging the length of the current dipole, that is, by making it a bipole, the electric current required to generate a given potential difference ΔV at a given distance r from the center of the array, is reduced. Furthermore the apparent resistivity remains a function of the single distance variable, $\overline{R} = \sqrt{(\overline{AB}/2)^2 + r^2}$, (Berdichevskii and Petrovskii, 1956). The equatorial array has been used extensively by Russian geophysicists in petroleum exploration (Berdichevskii and Zagarmistr, 1958). Recently it has been used in ground-water investigations in the United States (Zohdy and Jackson, 1968 and 1969; Zohdy, 1969a).

Electrical Sounding and Horizontal Profiling

Electrical sounding is the process by which depth investigations are made, and horizontal profiling is the process by which lateral variations in resistivity are detected. However, the results of electrical sounding and of horizontal profiling often are affected by both vertical and horizontal variations in the electrical properties of the ground.

If the ground is comprised of horizontal, homogeneous, and isotropic layers, electrical sounding data represent only the variation of resistivity with depth. In practice, however, the electrical sounding data are influenced by both vertical and horizontal heterogeneities. Therefore, the execution, interpretation, and presentation of sounding data should be such that horizontal variations in resistivity can be distinguished easily from vertical ones.

The basis for making an electrical sounding, irrespective of the electrode array used, is that the farther away from a current source the measurement of the potential, or the potential difference, or the electric field is made, the deeper the probing will be. It has been stated in many references on geophysical prospecting that the depth of probing depends on how far apart two current electrodes are placed, but this condition is not necessary for sounding with a dipole-dipole array. Furthermore, when sounding with a Wenner or Schlumberger array, when the distance between the current electrodes is increased, the distance between the current and the potential electrodes, at the center of the array, is increased also. It is this latter increase that actually matters.

In electrical sounding with the Wenner, Schlumberger, or dipole-dipole arrays, the respective electrode spacing a, $\frac{\overline{AB}}{2}$, or r, is increased at successive logarithmic intervals and the value of the appropriate apparent resistivity, $\overline{\rho}_w$, $\overline{\rho}_s$, or $\overline{\rho}_D$, is plotted as a function of the electrode spacing on logarithmic-coordinate paper. The curve of $\overline{\rho} = f\left(a, \frac{\overline{AB}}{2}, \text{or } r\right)$ is called an electrical sounding curve.

In horizontal profiling, a fixed electrode spacing is chosen (preferably on the basis of studying the results of electrical soundings), and the whole electrode array is moved along a profile after each measurement is made. The value of apparent resistivity is plotted, generally, at the geometric center 0 of the electrode array. Maximum apparent resistivity anomalies are obtained by orienting the profiles at right angles to the strike of the geologic structure. The results are presented as apparent resistivity profiles (fig. 7) or apparent resistivity maps (fig. 8), or both. In making horizontal profiles it is recommended that at least two different electrode spacings be used, in order to aid in distinguishing the effects of shallow geologic structures from the effects of deeper ones (fig. 9). In figure 9, the effect of shallow geologic features is suppressed on the profile made with the larger spacing, whereas the effect of deeper features is retained.

In certain surveys, the two current electrodes may be placed a large distance apart (1—6 km) and the potential electrodes moved along the middle third of the line AB. This method of horizontal profiling has been

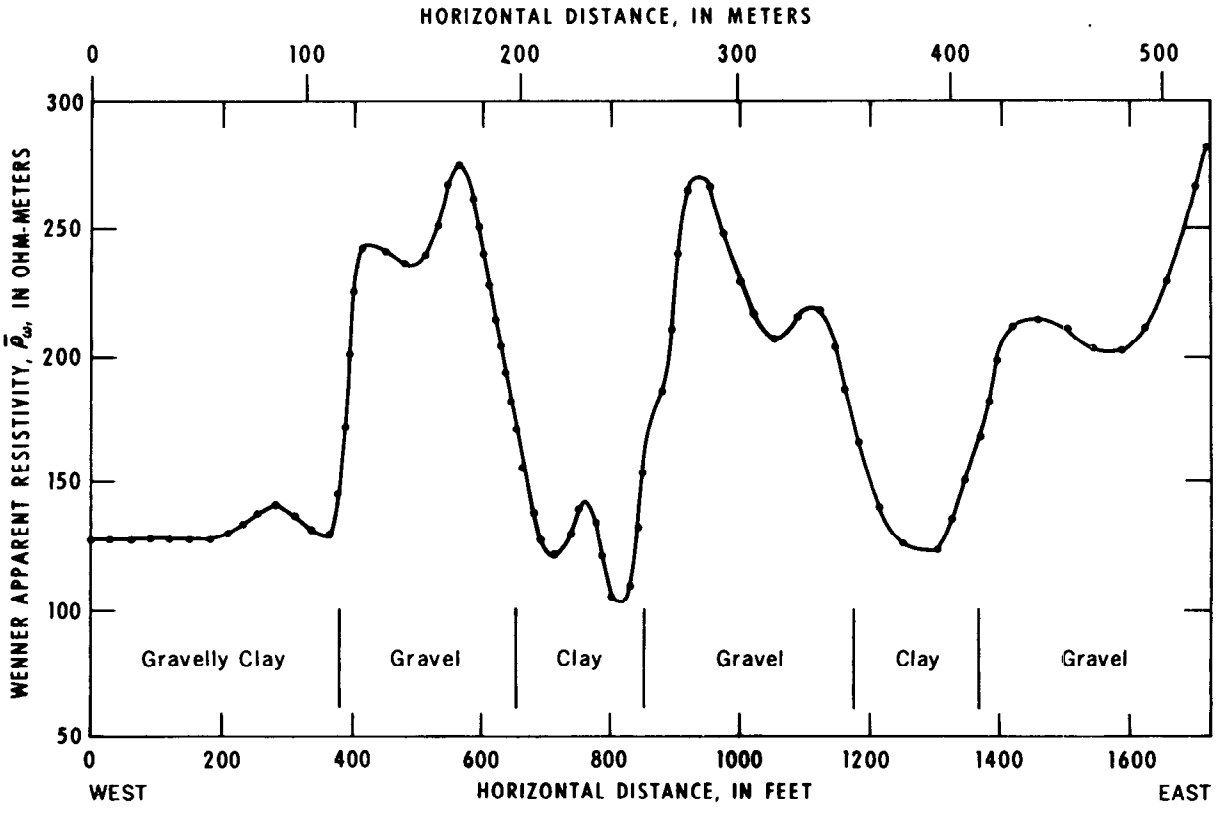

Figure 7.—Horizontal profile and interpretations over a shallow gravel deposit in California (Zohdy, unpub. data, 1964; Zohdy, 1964) using Wenner array at a = 9.15 meters.

called the Schlumberger AB profile (Kunetz, 1966; Lasfargues, 1957); in Canada and in parts of the United States it is referred to sometimes as the "Brant array" (fig. 10a). A modification of this procedure where the potential electrodes are moved not only along the middle third of the line AB but also along lines laterally displaced from and parallel to AB (fig. 10b) is called the "Rectangle of Resistivity Method" (Breusse and Astier, 1961; Kunetz, 1966). The lateral displacement of the profiles from the line AB may be as much as $\frac{\overline{AB}}{4}$.

Another horizontal profiling technique, used by many mining geophysicists, has been given the name "dipole-dipole" method, although it does not approximate a true dipole-dipole. The lengths of the current and potential "dipoles" are large in comparison to the distance between their centers. This arrangement introduces an extra variable in the calculation of theoretical curves and makes quantitative interpretation of the results difficult.

Practically all types of the common electrode arrays have been used in horizontal profiling, including pole-dipole (Hedstrome, 1932; Logn, 1954) and dipole-dipole arrays (Blokh, 1957 and 1962).

The interpretation of horizontal profiling data is generally qualitative, and the primary value of the data is to locate geologic structures such as buried stream channels, veins, and dikes. Quantitative interpretation can be obtained by making a sufficient number of profiles with different electrode spacings and along sets of traverses of different azimuths. Best interpretative results are obtained generally from a combination of horizontal profiling and electrical sounding data.

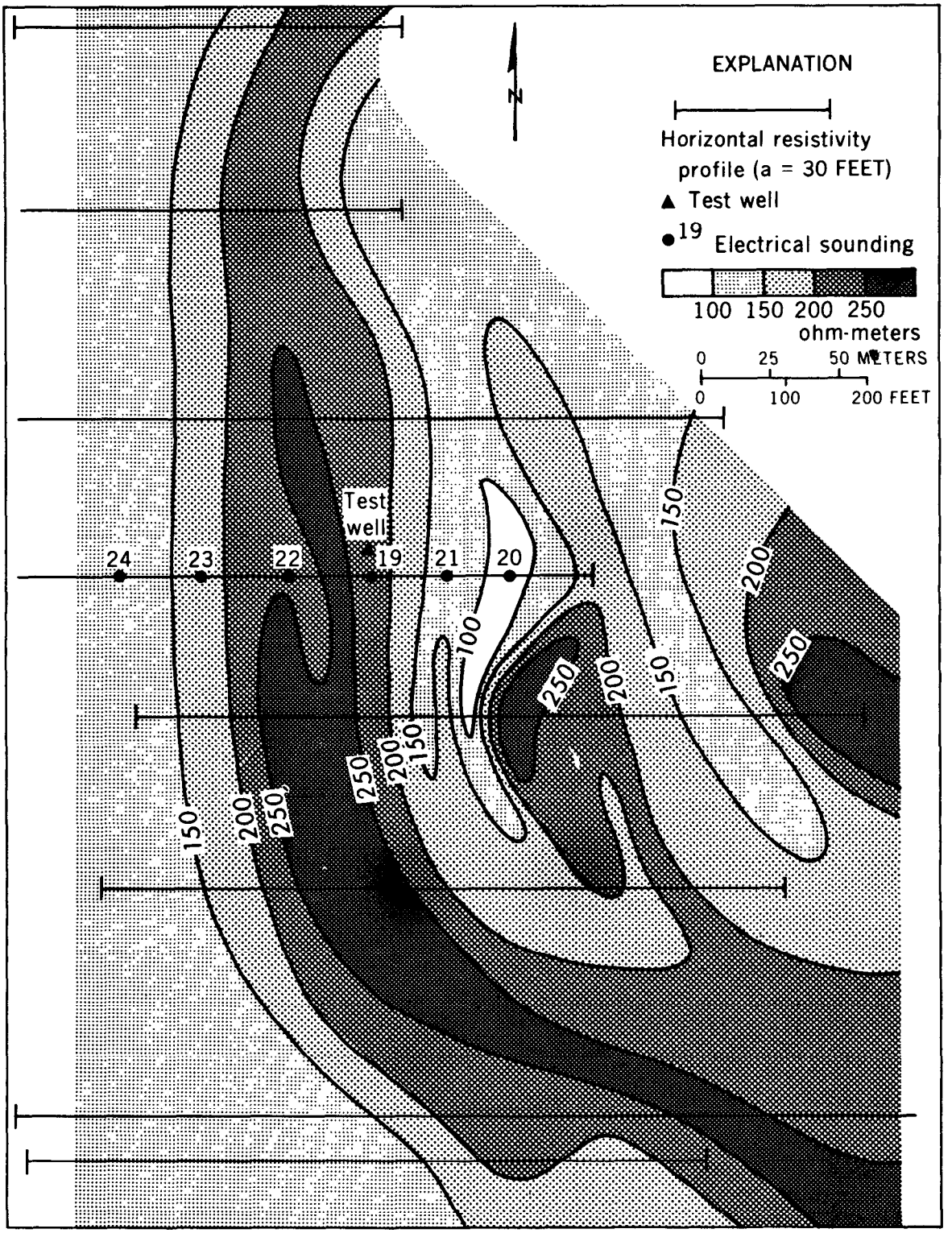

Figure 8.—Apparent-resistivity map near Campbell, Calif. Unpublished data obtained by Zohdy (1964) using Wenner array. Crosshatched areas are buried stream channels containing thick gravel deposits. Stippled areas are gravelly clay deposits.

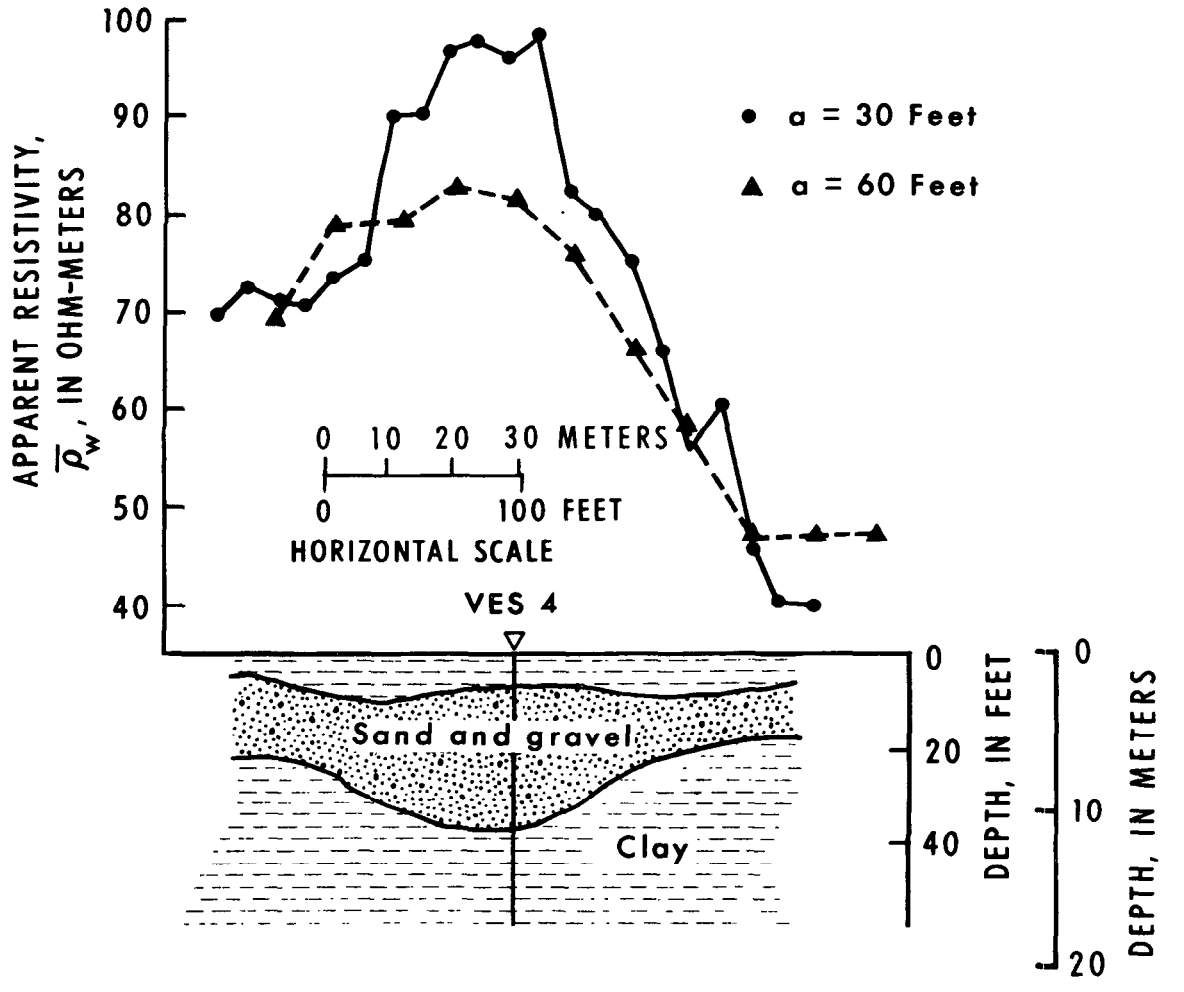

Figure 9.—Horizontal profiles over a buried stream channel using two electrode spacings: a = 9.15 meters (30 feet) and a = 18.3 meters (60 feet) (after Zohdy, 1964). VES 4 marks the location of an electrical sounding used to aid in the interpretation of the profiles.

Comparison of Wenner, Schlumberger, and Dipole-Dipole Measurements

The Schlumberger and the Wenner electrode arrays are the two most widely used arrays in resistivity prospecting. There are two essential differences between these arrays: (1) In the Schlumberger array the distance between the potential electrodes $\overline{MN}$ is small and is always kept equal to, or smaller than, one-fifth the distance between the current electrodes $\overline{AB}$; that is, $\overline{AB} \geq 5\overline{MN}$. In the Wenner array $\overline{AB}$ is always equal to $3\overline{MN}$. (2) In a Schlumberger sounding, the potential electrodes are moved only occasionally, whereas in a Wenner sounding they and the current electrodes are moved after each measurement.

As a direct consequence of these two differences the following facts are realized:

1. Schlumberger sounding curves portray a slightly greater probing depth and resolving power than Wenner sounding curves for equal AB electrode spacing. The maximum and the minimum values of apparent resistivity on a theoretical Schlumberger curve ($\overline{MN} \rightarrow 0$) appear on the sounding

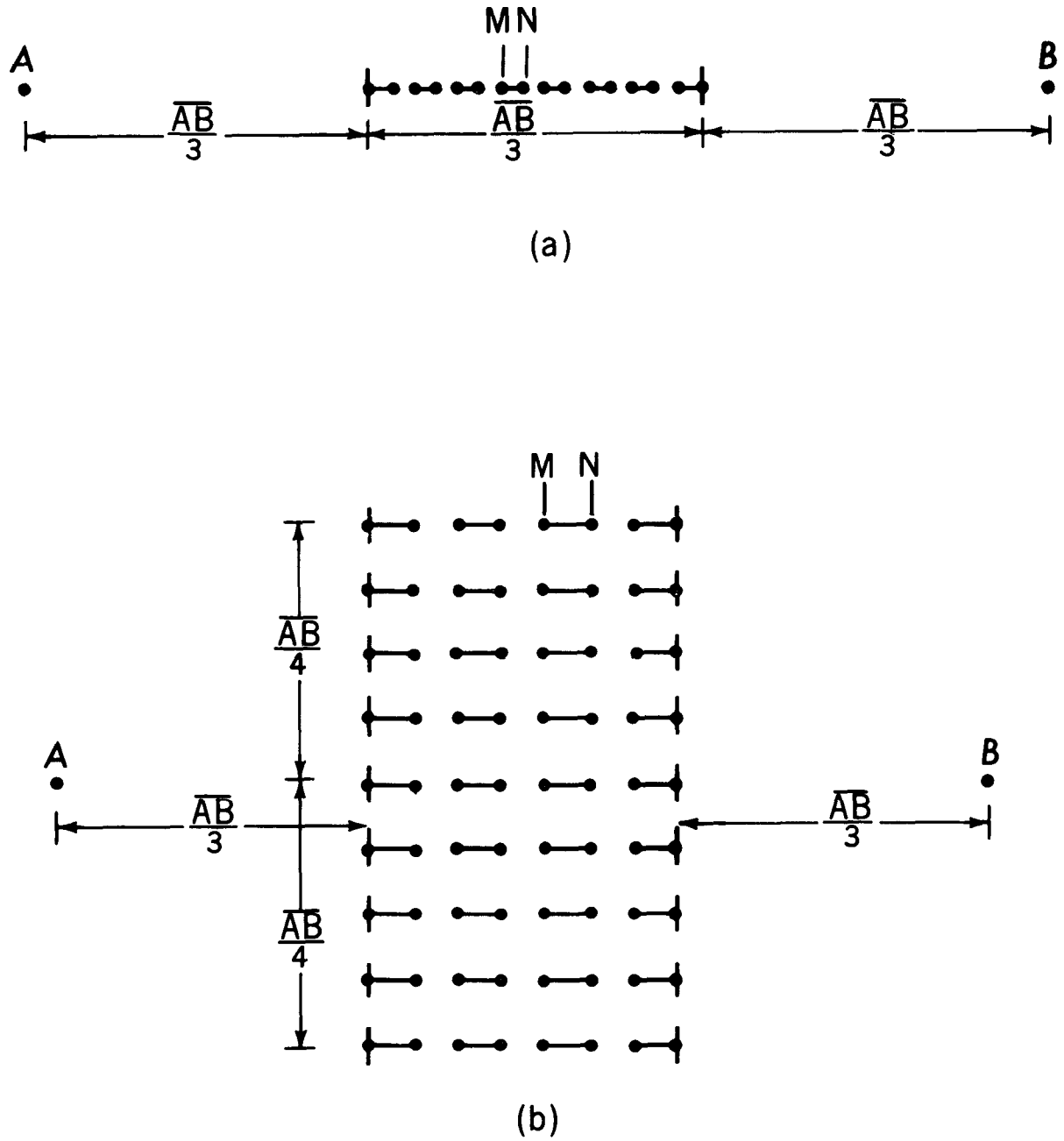

Figure 10.—Electrode arrays, for (a) Schlumberger $\overline{AB}$ profile, also called Brant array and (b) rectangle of resistivity.

curve at shorter electrode spacings and are slightly more accentuated than on a Wenner curve (fig. 11). This fact was proved theoretically by Depperman (1954), discussed by Unz (1963), and practically illustrated by Zohdy (1964). A true comparison between the two types of sounding curves is made by standardizing the electrode spacing for the two arrays; that is, both apparent resistivities $\overline{\rho}_w$ and $\overline{\rho}_s$ should be plotted as a function of $\overline{AB}/2$, or $\overline{AB}/3$, or $\overline{AB}$.

2. The manpower and time required for mak-

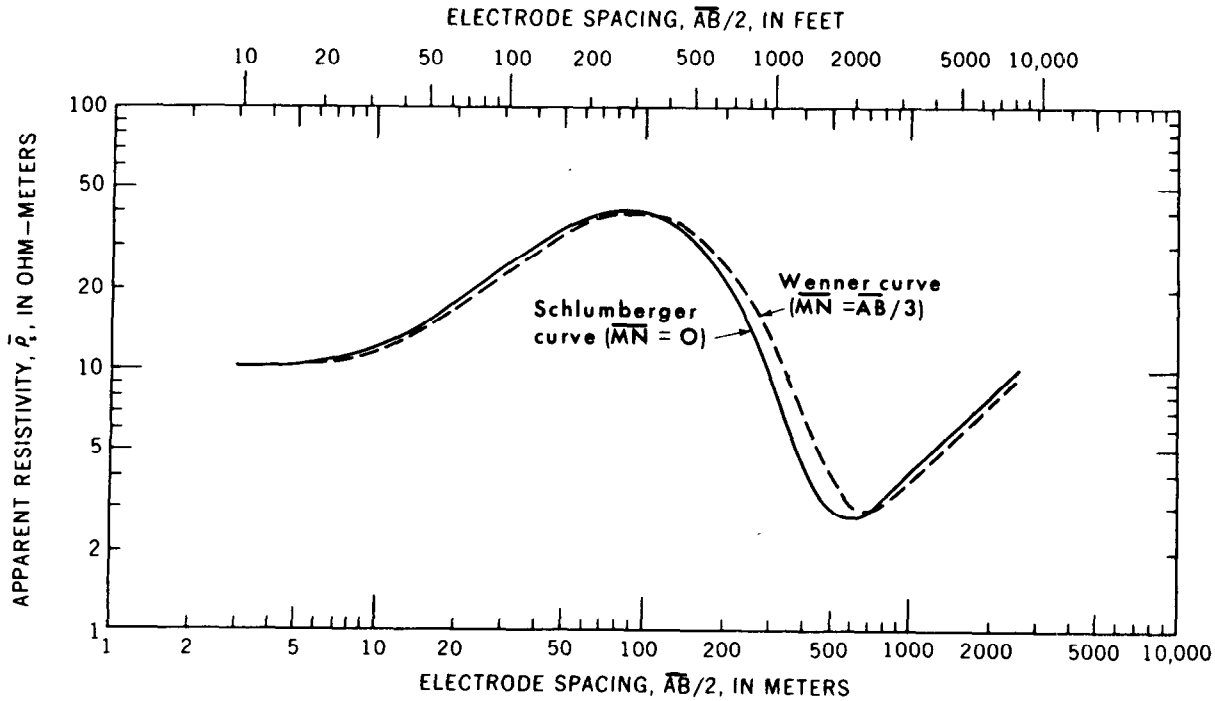

Figure 11.—Comparison between four-layer Schlumberger and Wenner sounding curves. Electrode spacing is $\overline{AB}/2$ for both curves.

ing Schlumberger soundings are less than that required for making Wenner soundings.

3. Stray currents in industrial areas and telluric currents that are measured with long spreads affect measurements made with the Wenner array more readily than those made with the Schlumberger array.
4. The effects of near-surface, lateral inhomogeneities are less apt to affect Schlumberger measurements than Wenner measurements. Furthermore, the effect of lateral variations in resistivity are recognized and corrected more easily on a Schlumberger curve than on a Wenner curve.
5. A drifting or unstable potential difference is created upon driving two metal stakes into the ground. This potential difference, however, becomes essentially constant after about 5–10 minutes. Fewer difficulties of this sort are encountered with the Schlumberger array than with the Wenner array.
6. A Schlumberger sounding curve, as opposed to a theoretical curve, is generally discontinuous. The discontinuities result from enlarging the potential electrode spacing after several measurements. This type of discontinuity on the Schlumberger sounding field curve is considered as another advantage over Wenner sounding field curves, because if the theoretical assumption of a horizontally stratified laterally homogeneous and isotropic Earth is valid in the field, then the discontinuities should occur in a theoretically prescribed manner (Depperman, 1954). The Schlumberger curve then can be rectified and smoothed accordingly as shown in figure 12. Any deviation of the Schlumberger sounding field curve from the theoretically prescribed pattern of discontinuities would indicate lateral inhomogeneities or errors in measurements. The effect of lateral inhomogeneities on a Schlumberger curve can be removed by shifting the displaced segments of the curve upward or downward to where they should be in relation to the other segments of the curve. Such information is usually unobtainable from Wenner sounding curves and there is no systematic way of smoothing the ob-

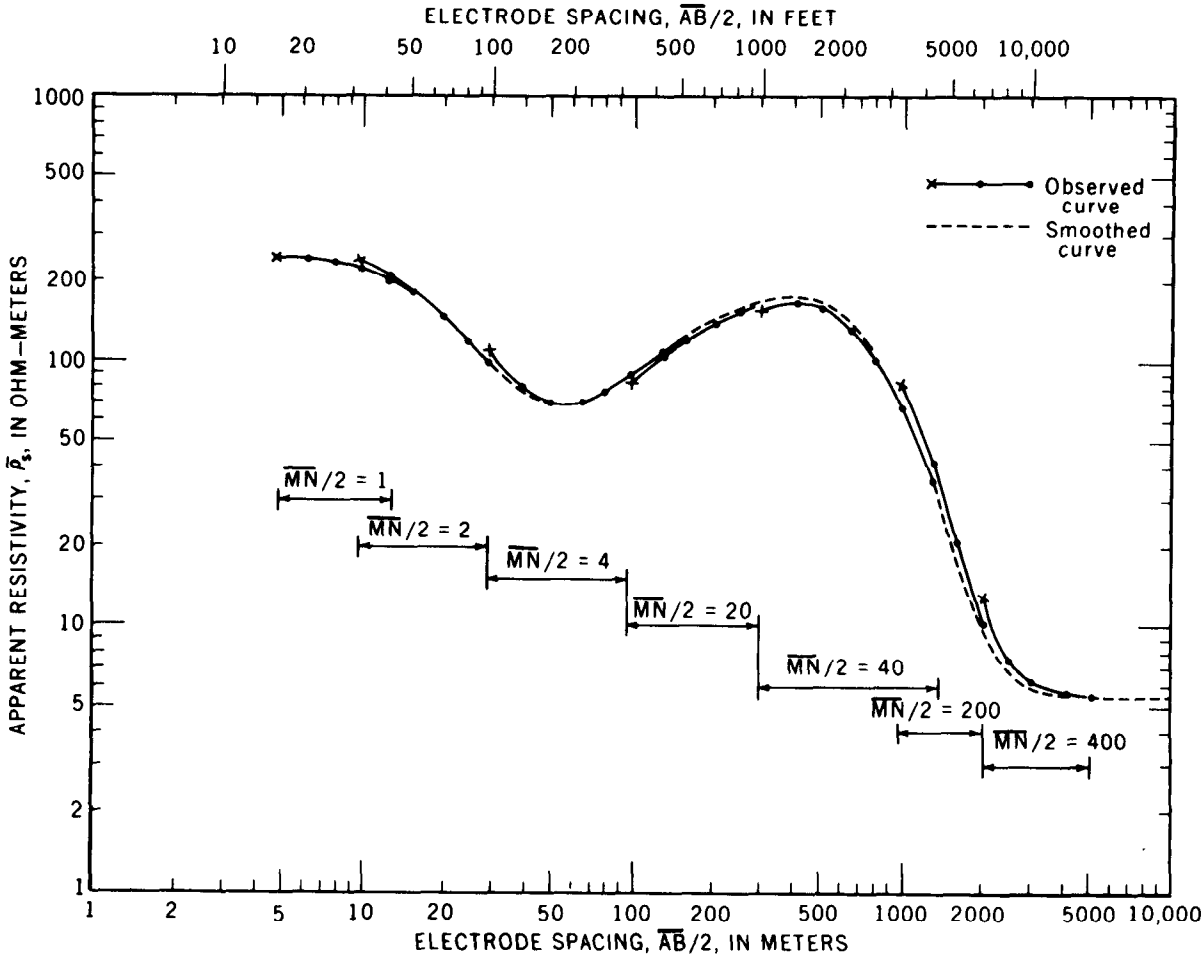

Figure 12.—Correct displacements on a Schlumberger sounding curve and method of smoothing.

served data. With the Lee-partitioning method, it is possible to obtain an indication of lateral changes in subsurface conditions or of errors in measurements, but there is no simple method that would reduce the observed data so that it would correspond to a horizontally homogeneous Earth.

The advantages of the Wenner array are limited to the following: (1) The relative simplicity of the apparent resistivity formula $\bar{\rho}_w = 2\pi a\ (\Delta V/I)$, (2) the relatively small current values necessary to produce measurable potential differences, and (3) the availability of a large album of theoretical master curves for two-, three-, and four-layer Earth models (Mooney and Wetzel, 1956).

The above comparison indicates that it is advantageous to use the Schlumberger array rather than the Wenner array for making electrical resistivity soundings. The use of the Schlumberger array is recommended not only because of the above listed advantages but also, and perhaps more important, because the interpretation techniques are developed more fully and they are more diversified for Schlumberger sounding curves than for Wenner sounding curves.

With the invention of dipole-dipole arrays and their use in the Soviet Union and the United States, their following advantages over the Schlumberger array became recognized: (1) Relatively short AB and MN lines are used to explore large depths, which reduces field labor and increases productivity, (2) problems of current leakage (Dakhnov, 1953; Zohdy, 1968b) are reduced to a mini-

mum, (3) bilateral investigations are possible and therefore more detailed information on the direction of dip of electrical horizons is obtainable, and (4) problems of inductive coupling and associated errors are minimized.

Among the disadvantages of dipole methods are: (1) The requirement of a large generator to provide ample amounts of current, especially in deep exploration, and (2) special knowledge and special theoretical developments and materials are required to interpret most of the data obtained by dipole-dipole arrays. Generally one cannot use the experience gained in using Schlumberger or Wenner arrays to obtain or to interpret dipole sounding data in a straightforward way.

Problem of Defining Probing Depth

A favorite rule-of-thumb in electrical prospecting is that the electrode spacing is equal to the depth of probing. This rule-of-thumb is wrong and leads to erroneous interpretations. Its origin probably stems from the fact that when using direct current in probing a homogeneous and isotropic semi-infinite medium, there is a definite relation between the spacing $\overline{AB}$ separating the current electrodes and the depth to which any particular percentage of the current penetrates. For example, 50 percent of the current penetrates to a depth equal to $\overline{AB}/2$ and 70 percent to a depth equal to $\overline{AB}$. Therefore the greater the current electrode separation, the greater the amount of current that penetrates to a given depth. This relation is governed by the equation (Weaver, 1929; Jakosky, 1950)

$$I_z/I_t = \frac{2}{\pi} \tan^{-1}(2z/\overline{AB}),$$

where I_z = current confined between depth 0 and z,

I_t = total current penetrating the ground, and

$\overline{AB}$ = distance separating current electrodes.

This current-depth relation for a homogeneous and isotropic Earth cannot be used as a general rule-of-thumb to establish a so-called "depth of penetration" or "probing depth" that also applies to a stratified or an inhomogeneous Earth. For an inhomogeneous medium the percentage of the total current that penetrates to a given depth z depends not only upon the electrode separation but also upon the resistivities of the Earth layers. This fact was discussed by Muskat (1933), Muskat and Evinger (1941), Evjen (1944), Orellana (1960), 1961), and others. Furthermore, the above relation does not include the apparent resistivity nor the true resistivity (or resistivities) of the medium. Consequently it is of no value in interpreting apparent resistivity data. In fact, in resistivity interpretation we do not care about the percentage of current that penetrates to a given depth or the percentage of current that exists at a given distance as long as we can make measurements of the total current I_t and of the potential difference ΔV from which the apparent resistivity can be calculated.

Many investigators, however, still use the above rule-of-thumb in making their interpretations, with variable degrees of fortuitous success and more often failure. Perhaps this rule-of-thumb is of some value when the geophysicist has to decide on an electrode spacing for horizontal profiling over a buried structure, but a better choice can be made after making a few soundings in the area.

Advantages of Using Logarithmic Coordinates

Electrical sounding data should be plotted on logarithmic coordinates with the electrode spacing on the abscissa and the apparent resistivity on the ordinate. The advantages of plotting the sounding data on logarithmic coordinates are:

1. Field data can be compared with precalculated theoretical curves for given

Earth models (curve-matching procedure).

2. The form of an electrical sounding curve does not depend on the resistivity and thickness of the first layer provided that the ratios $\frac{\rho_2}{\rho_1}, \frac{\rho_3}{\rho_1}, \ldots, \frac{\rho_n}{\rho_1}$, and the ratios $\frac{h_2}{h_1}, \frac{h_3}{h_1}, \ldots, \frac{h_n}{h_1}$, remain constant from model to model, where $\rho_1, \rho_2, \rho_3, \ldots, \rho_n$, are the resistivities and $h_1, h_2, h_3, \ldots, h_n$, are the thicknesses of the first, second, third, and n^{th} layers, respectively. When the absolute values of ρ and h change but the ratios $\frac{\rho_i}{\rho_1}$ and $\frac{h_i}{h_1}$, where $i = 2, 3, \ldots, n$, remain constant, the position of the curve is merely displaced vertically for changes in ρ, and horizontally for changes in h (fig. 13). Consequently, two curves with different values of ρ, and h, (but with the same values of $\frac{\rho_2}{\rho_1}$ and $\frac{h_2}{h_1}$) can be superposed by translating one curve on top of the other (while the ordinate and abscissa axes remain parallel). This is the essence of the curve-matching method. Furthermore, in the computation of theoretical sounding curves the thickness and resistivity

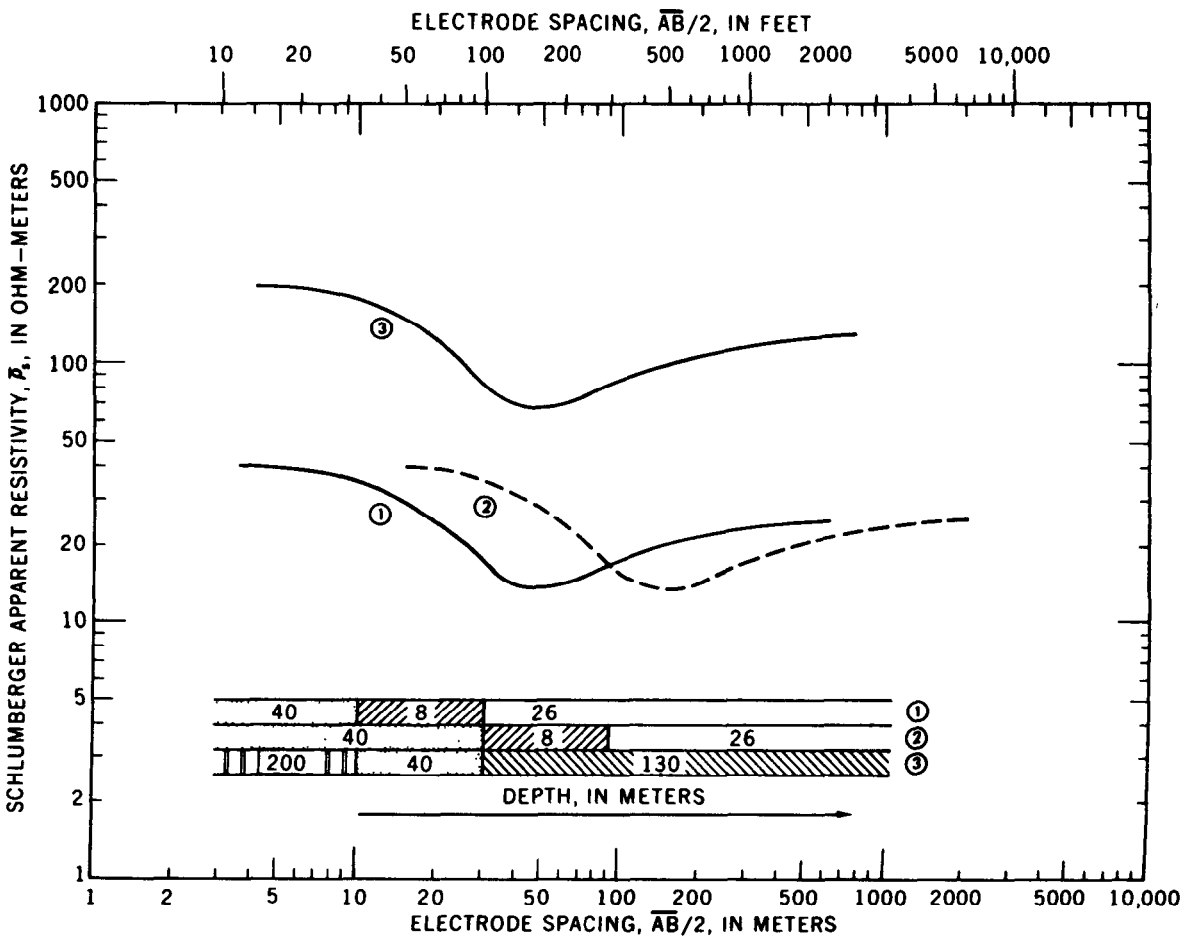

Figure 13.—Logarithmic plot of sounding curves. The layers in model 2 are three times as thick as model 1; the layer resistivities in model 3 are five times as large as model 1; however, the shapes of all three curves are identical.

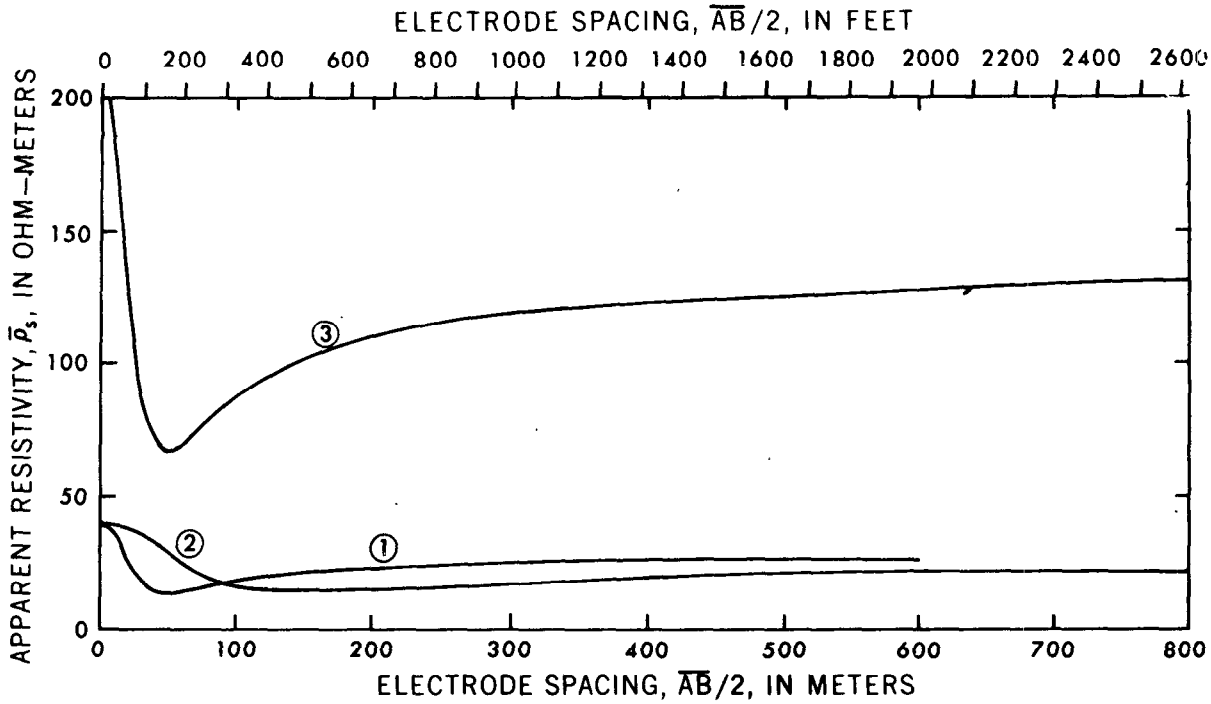

Figure 14.—Linear plot of sounding curves. Earth models are the same as in figure 13. Curve form is not preserved.

of one of the layers can be assumed equal to unity, which eliminates two parameters in the calculation of a sounding curve for a given Earth model.

When sounding curves are plotted on linear coordinates, the form, as well as the position, of the curve varies as a function of ρ_1 and h_1, even when the ratios $\frac{\rho_2}{\rho_1}$ and $\frac{h_2}{h_1}$ remain constant (fig. 14).

3. The use of logarithmic coordinates, on the one hand, suppresses the effect of variations in the thickness of layers at large depths, and it also suppresses variations of high resistivity values. On the other hand, it enhances the effect of variations in the thickness of layers at shallow depths, and it enhances the variations of low resistivity values. These properties are important because the determination of the thickness of a layer to within ±10 meters (±32.8 feet) when that layer is at a depth of several hundred meters is generally acceptable, whereas a precision to within one meter is desirable when the layer is at a depth of only a few tens of meters. Similarly, the determination of the resistivity of a conductive layer (less than about 20 ohm-m) to the nearest ohm-m is necessary for determining its thickness accurately, whereas for a resistive layer (more than about 200 ohm-m), the determination of its resistivity to within one ohm-m is unimportant.
4. The wide spectrum of resistivity values measured under different field conditions and the large electrode spacings necessary for exploring the ground to moderate depths make the use of logarithmic coordinates a logical choice.

Geoelectric Parameters

A geologic section differs from a geoelectric section when the boundaries between geologic layers do not coincide with the boundaries between layers characterized by

different resistivities. Thus, the electric boundaries separating layers of different resistivities may or may not coincide with boundaries separating layers of different geologic age or different lithologic composition. For example, when the salinity of ground water in a given type of rock varies with depth, several geoelectric layers may be distinguished within a lithologically homogeneous rock. In the opposite situation layers of different lithologies or ages, or both, may have the same resistivity and thus form a single geoelectric layer.

A geoelectric layer is described by two fundamental parameters: its resistivity ρ_i and its thickness h_i, where the subscript i indicates the position of the layer in the section ($i = 1$ for the uppermost layer). Other geoelectric parameters are derived from its resistivity and thickness. These are:

1. Longitudinal unit conductance, $S_i = h_i/\rho_i$,
2. Transverse unit resistance, $T_i = h_i\rho_i$,
3. Longitudinal resistivity, $\rho_L = h_i/S_i$,
4. Transverse resistivity, $\rho_t = T_i/h_i$, and
5. Anisotropy, $\lambda = \sqrt{\rho_t/\rho_L}$.

For an isotropic layer $\rho_t = \rho_L$ *and* $\lambda = 1$. These secondary geoelectric parameters are particularly important when they are used to describe a geoelectric section consisting of several layers.

For n layers, the total longitudinal unit conductance is

$$S = \sum_{i=1}^{n} \frac{h_i}{\rho_i} = \frac{h_1}{\rho_1} + \frac{h_2}{\rho_2} + \ldots \frac{h_n}{\rho_n};$$

the total transverse unit resistance is

$$T = \sum_{i=1}^{n} h_i\rho_i = h_1\rho_1 + h_2\rho_2 + \ldots + h_n\rho_n;$$

the average longitudinal resistivity is

$$\rho_L = \frac{H}{S} = \frac{\sum_{1}^{n} h_i}{\sum_{1}^{n} \frac{h_i}{\rho_i}};$$

the average transverse resistivity is

$$\rho_t = \frac{T}{H} = \frac{\sum_{i}^{n} h_i\rho_i}{\sum_{i}^{n} h_i};$$

and the anisotropy is

$$\lambda = \sqrt{\frac{\rho_t}{\rho_L}} = \frac{\sqrt{TS}}{H}.$$

The parameters S, T, ρ_L, ρ_t, and λ are derived from consideration of a column of unit square cross-sectional area (1×1 meter) cut out of a group of layers of infinite lateral extent (fig. 15). If current flows vertically only through the column, then the layers in the column will behave as resistors connected in series, and the total resistance of the column of unit cross-sectional area will be:

$$R = R_1 + R_2 + R_3 + \ldots + R_n,$$

or

$$R = \rho_1 \frac{h_1}{1\times1} + \rho_2 \frac{h_2}{1\times1} + \ldots + \rho_n \frac{h_n}{1\times1} = \sum_{i}^{n} \rho_i h_i = T.$$

The symbol T is used instead of R to indicate that the resistance is measured in a direction transverse to the bedding and also because

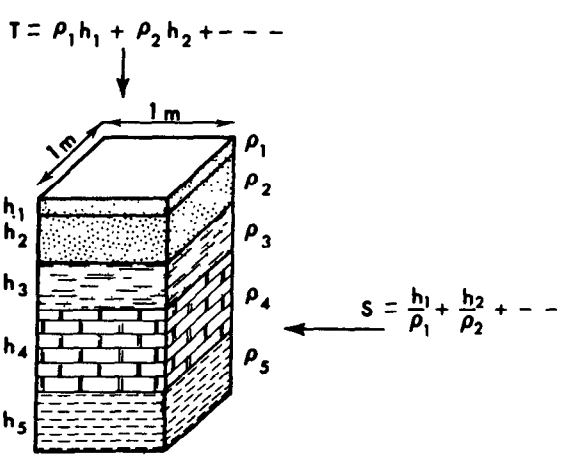

Figure 15.—Columnar prism used in defining geoelectric parameters of a section. Patterns are arbitrary. ρ = resistivity, h = thickness, S = total longitudinal conductance, T = total transverse resistance.

the dimensions of this "unit resistance" are usually expressed in ohm-m^2 instead of ohms.

If the current flows parallel to the bedding, the layers in the column will behave as resistors connected in parallel and the conductance will be

$$S = \frac{1}{R} = \frac{1}{R_1} + \frac{1}{R_2} + \ldots + \frac{1}{R_n},$$

or

$$S = \frac{1 \times h_1}{\rho_1 \times 1} + \frac{1 \times h_2}{\rho_2 \times 1} + \ldots + \frac{1 \times h_n}{\rho_n \times 1} = \frac{h_1}{\rho_1} + \frac{h_2}{\rho_2} + \ldots + \frac{h_n}{\rho_n}.$$

The dimensions of the longitudinal unit conductance are m/ohm-m = 1/ ohm = mho. It is interesting to note that the quantity $S_i = \frac{h_i}{\rho_i} = \sigma_i h_i$, where σ_i is the conductivity (inverse of resistivity), is analogous to transmissivity $T_i = K_i b_i$ used in ground-water hydrology, where K_i is the hydraulic conductivity of the i^{th} layer and b_i is its thickness.

The parameters T and S were named the "Dar Zarrouk" parameters by Maillet (1947).

In this manual we shall refer to T and S as the transverse resistance and the longitudinal conductance; the word "unit" is omitted for brevity.

In the interpretation of multilayer electrical sounding curves, the evaluation of S or T is sometimes all that can be determined uniquely. There are simple graphical methods for the determination of these parameters from sounding curves. The study of the parameters S, T, ρ_L, ρ_t, and λ is an integral part of the analysis of electrical sounding data and also is the basis of important graphical procedures (for example, the auxiliary point method) for the interpretation of electrical sounding curves (Kalenov, 1957; Orellana and Mooney, 1966; Zohdy, 1965).

Types of Electrical Sounding Curves Over Horizontally Stratified Media

The form of the curves obtained by sounding over a horizontally stratified medium is a function of the resistivities and thicknesses of the layers, as well as of the electrode configuration.

Homogeneous and isotropic medium.—If the ground is composed of a single homogeneous and isotropic layer of infinite thickness and finite resistivity then, irrespective of the electrode array used, the apparent resistivity curve will be a straight horizontal line whose ordinate is equal to the true resistivity ρ_1 of the semi-infinite medium.

Two-layer medium.—If the ground is composed of two layers, a homogeneous and isotropic first layer of thickness h_1 and resistivity ρ_1, underlain by an infinitely thick substratum ($h_2 = \infty$) of resistivity ρ_2, then the sounding curve begins, at small electrode spacings, with a horizontal segment ($\bar{\rho} \cong \rho_1$). As the electrode spacing is increased, the curve rises or falls depending on whether $\rho_2 > \rho_1$ or $\rho_2 < \rho_1$, and on the electrode configuration used. At electrode spacings much larger than the thickness of the first layer, the sounding curve asymptotically approaches a horizontal line whose ordinate is equal to ρ_2. The electrode spacing at which the apparent resistivity $\bar{\rho}$ asymptotically approaches the value ρ_2 depends on three factors: the thickness of the first layer h_1, the value of the ratio ρ_2/ρ_1, and the type of electrode array used in making the sounding measurements.

The dependence of the electrode spacing on the thickness of the first layer is fairly obvious. The larger the thickness of the first layer, the larger the spacing required for the apparent resistivity to be approximately equal to the resistivity of the second layer. This is true for any given electrode array and for any given resistivity ratio. However, for most electrode arrays, including the conventional Schlumberger, Wenner, dipole equatorial and dipole polar arrays, when $\rho_2/\rho_1 > 1$, larger electrode spacings are required for $\bar{\rho}$ to be approximately equal to ρ_2 than when $\rho_2/\rho_1 < 1$. Figure 16 shows a comparison between two Schlumberger sounding curves obtained over two-layer Earth models in which $h_1 = 1$ meter (3.28 feet), $\rho_2/\rho_1 = 10$, and $\rho_2/\rho_1 = 0.1$. Figure 17 shows the dif-

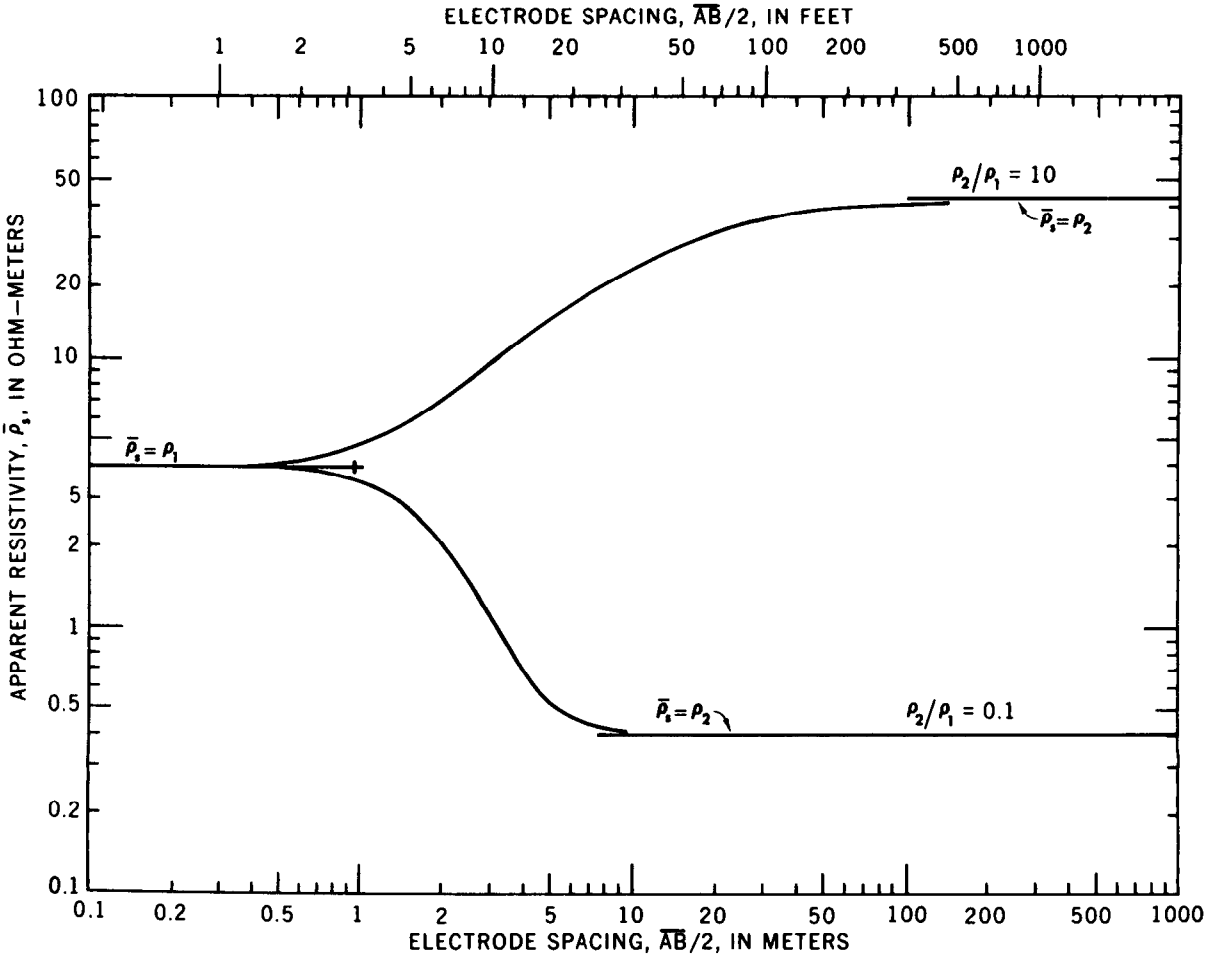

Figure 16.—Comparison between two-layer Schlumberger curves for $\rho_2/\rho_1 = 10$ and 0.1; $h_1 = 1$ meter (3.28 feet) for both curves.

ference in the form of sounding curves, and the asymptotic approach of $\bar{\rho}$ to ρ_1 and to ρ_2 as a function of electrode array for $h_1 = 1$ meter, $\rho_2/\rho_1 = 9$, and $\rho_2/\rho_1 = 0.2$. The comparison is made between equatorial and polar-dipole sounding curves.

Three-layer medium.—If the ground is composed of three layers of resistivities ρ_1, ρ_2, and ρ_3, and thicknesses h_1, h_2, *and* $h_3 = \infty$, the geoelectric section is described according to the relation between the values of ρ_1, ρ_2, and ρ_3. There are four possible combinations between the values of ρ_1, ρ_2, and ρ_3. These are:

$\rho_1 > \rho_2 < \rho_3$ ____H-type section,
$\rho_1 < \rho_2 < \rho_3$ ___A-type section,
$\rho_1 < \rho_2 > \rho_3$ ____K-type section,
$\rho_1 > \rho_2 > \rho_3$ ____Q-type section.

The use of the letters H, A, K, and Q to describe the relation between ρ_1, ρ_2, and ρ_3 in the geoelectric section is very convenient and also is used to describe the corresponding sounding curves. For example, we talk about an H-type electrical sounding curve to indicate that it is obtained over a geoelectric section in which $\rho_1 > \rho_2 < \rho_3$. H-, A-, K-, and Q-type Schlumberger sounding curves are shown in figure 18.

Multilayer-medium.— If the ground is composed of more than three horizontal layers of resistivities ρ_1, ρ_2, ρ_3, . . . ρ_n and thicknesses h_1, h_2, h_3, . . . $h_n = \infty$, the geoelectric section is described in terms of relationship between the resistivities of the layers, and the letters H, A, K, and Q are

used, in combination, to indicate the variation of resistivity with depth. In four-layer geoelectric sections, there are eight possible relations between ρ_1, ρ_2, ρ_3, and ρ_4:

$\rho_1 > \rho_2 < \rho_3 < \rho_4$ ----HA-type section,
$\rho_1 > \rho_2 < \rho_3 > \rho_4$ ----HK-type section,
$\rho_1 < \rho_2 < \rho_3 < \rho_4$ ----AA-type section
$\rho_1 < \rho_2 < \rho_3 > \rho_4$ ----AK-type section,
$\rho_1 < \rho_2 > \rho_3 < \rho_4$ ----KH-type section,
$\rho_1 < \rho_2 > \rho_3 > \rho_4$ ----KQ-type section,
$\rho_1 > \rho_2 > \rho_3 < \rho_4$ ----QH-type section,
$\rho_1 > \rho_2 > \rho_3 > \rho_4$ ----QQ-type section.

Examples of Schlumberger electrical sounding curves for three of these eight types of four-layer models are shown in figure 19.

For a five-layer geoelectric section there are 16 possible relationships between ρ_1, ρ_2, ρ_3, ρ_4, and ρ_5, and, therefore, there are 16 types of five-layer electrical sounding curves. Each of these 16 geoelectric sections may be described by a combination of three letters. For example, an HKH section is one in which $(\rho_1 > \rho_2 < \rho_3 > \rho_4 < \rho_5)$. In general, an n-layer section (where $n \geq 3$) is described by (n-2) letters.

Electrical Sounding Over Laterally Inhomogeneous Media

Lateral inhomogeneities in the ground affect resistivity measurements in different ways. The effect depends on (1) the size of the inhomogeneity with respect to its depth of burial, (2) the size of the inhomogeneity with respect to the size of the electrode array, (3) the resistivity contrast between the inhomogeneity and the surrounding media, (4) the type of electrode array used, (5) the geometric form of the inhomogeneity, and (6) the orientation of the electrode array with respect to the strike of the inhomogeneity.

The simplest type of a lateral inhomogeneity, from the geometric and mathematical points of view, is that of a vertical plane boundary separating two homogeneous and isotropic media of resistivities ρ_1 and ρ_2. Although this Earth model is ideal and does not exist commonly in nature, its study serves to illustrate the general form of the resistivity anomaly to be expected over a

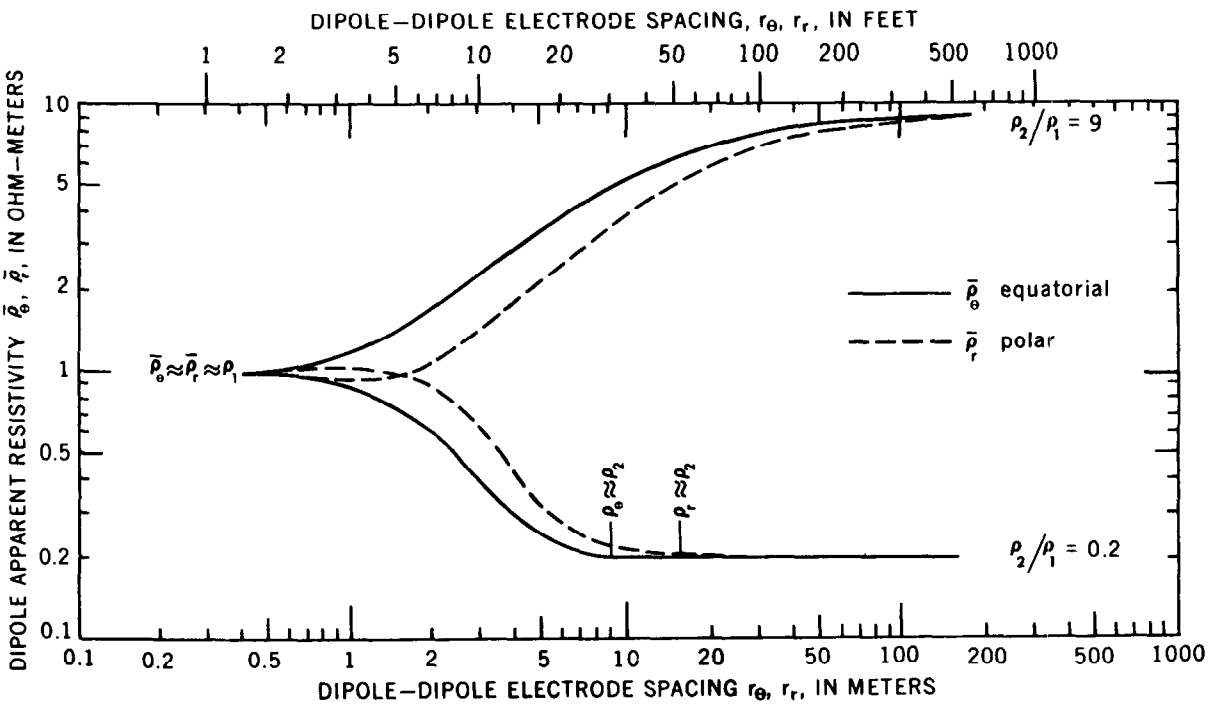

Figure 17.—Comparison between two-layer azimuthal (or equatorial) and radial (or polar) sounding curves ($h_1 = 1$ meter (3.28 feet), $\rho_2/\rho_1 = 9$ or 0.2).

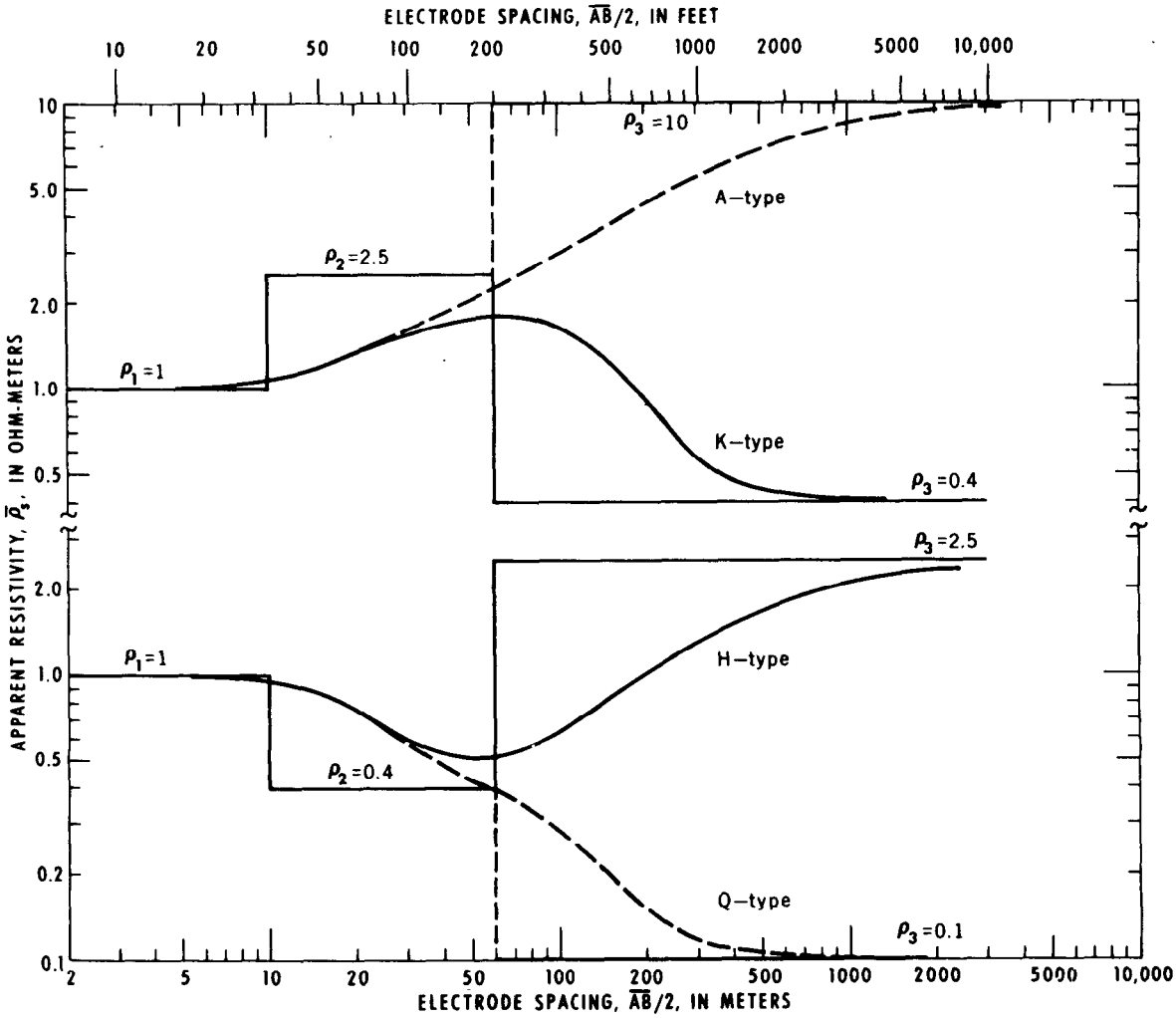

Figure 18.—Examples of the four types of three-layer Schlumberger sounding curves for three-layer Earth models.

large variety of more complicated lateral inhomogeneities.

The electrical sounding curves obtained with an ideal Schlumberger array ($\overline{MN}\rightarrow 0$) oriented at different angles to the surface trace of a vertical contact (Zohdy, 1970) are shown in figure 20. The most important feature on the sounding curves that indicates the presence of the lateral inhomogeneity is the formation of a cusp which is well developed whenever the sounding line makes an azimuth angle close to 90° with the surface trace of the vertical plane boundary. The Wenner sounding curves for azimuth angles of 0° to 90° are shown in figure 21. The Wenner curves are more complicated than the Schlumberger curves because a potential electrode crosses the contact. The effects of such things as dipping, vertical and horizontal contacts, and pipe lines have been described in the literature for different electrode arrays (Kunetz, 1966; Al'pin and others, 1966).

Limitations of the Resistivity Method

The interpretation of a multilayer sounding curve generally is not unique. This means that a given electrical sounding curve can correspond to a variety of subsurface distributions of layer thicknesses and resistivities. Furthermore, several other limitations

are inherent in the conventional methods of electrical sounding and these are considered in the following sections.

Equivalence of K-type curves.—Consider two three-layer sections of the K type ($\rho_1 < \rho_2 > \rho_3$). If ρ_1 in one section equals ρ_1' in the other section, $\rho_3 = \rho_3'$, and $T_2 = \rho_2 h_2 = T_2' = \rho_2' h_2'$, then the sounding curves for both sections will be practically identical (fig. 22, curves a and b).

This type of equivalence is known as equivalence by T and it also applies approximately to Q-type curves.

Equivalence of H-type curves.— Consider two three-layer sections of the H type ($\rho_1 > \rho_2 < \rho_3$). If ρ_1 in one section equals ρ_1' in the other section, $\rho_3 = \rho_3'$ and $S_2 = h_2/\rho_2 = S_2' = h_2'/\rho_2'$, then the sounding curves for both sections (fig. 22, curves c and d) will be practically identical (equivalence by S). The equivalence by S also applies to sounding curves of the A type ($\rho_1 < \rho_2 < \rho_3$).

For both equivalence by T and equivalence by S, there is a certain range, depending on the ratios ρ_2/ρ_1 and h_2/h_1, where the two sounding curves coincide very closely. Special nomograms published by Pilayev (1948) define this range, which is referred to as the domain of the principle of equivalence. These charts were published in the books of Bhattacharya and Patra (1968), Dakhnov (1953), Golovtsin (1963), Kalenov (1957),

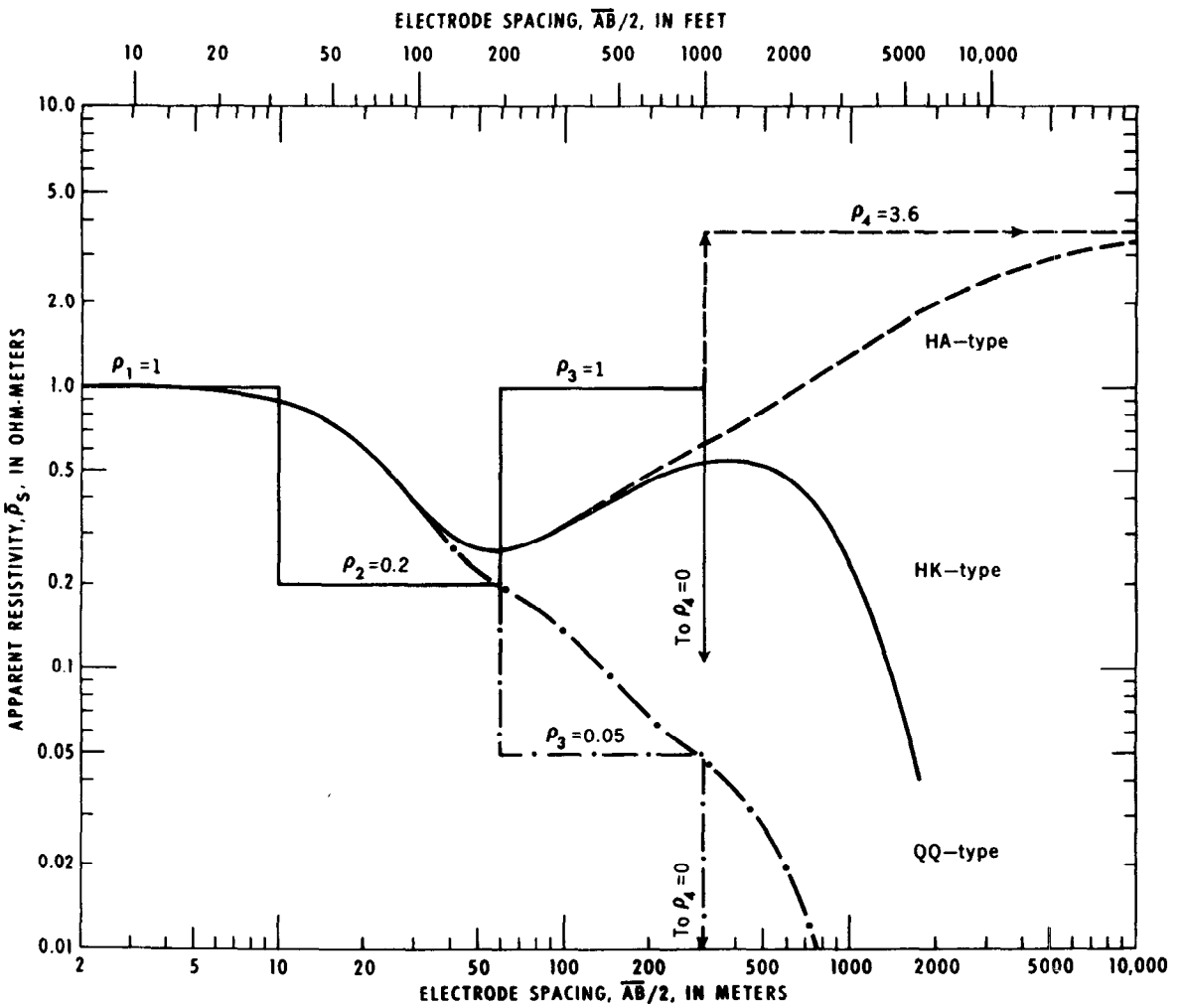

Figure 19.—Examples of three of the eight possible types of Schlumberger sounding curves for four-layer Earth models.

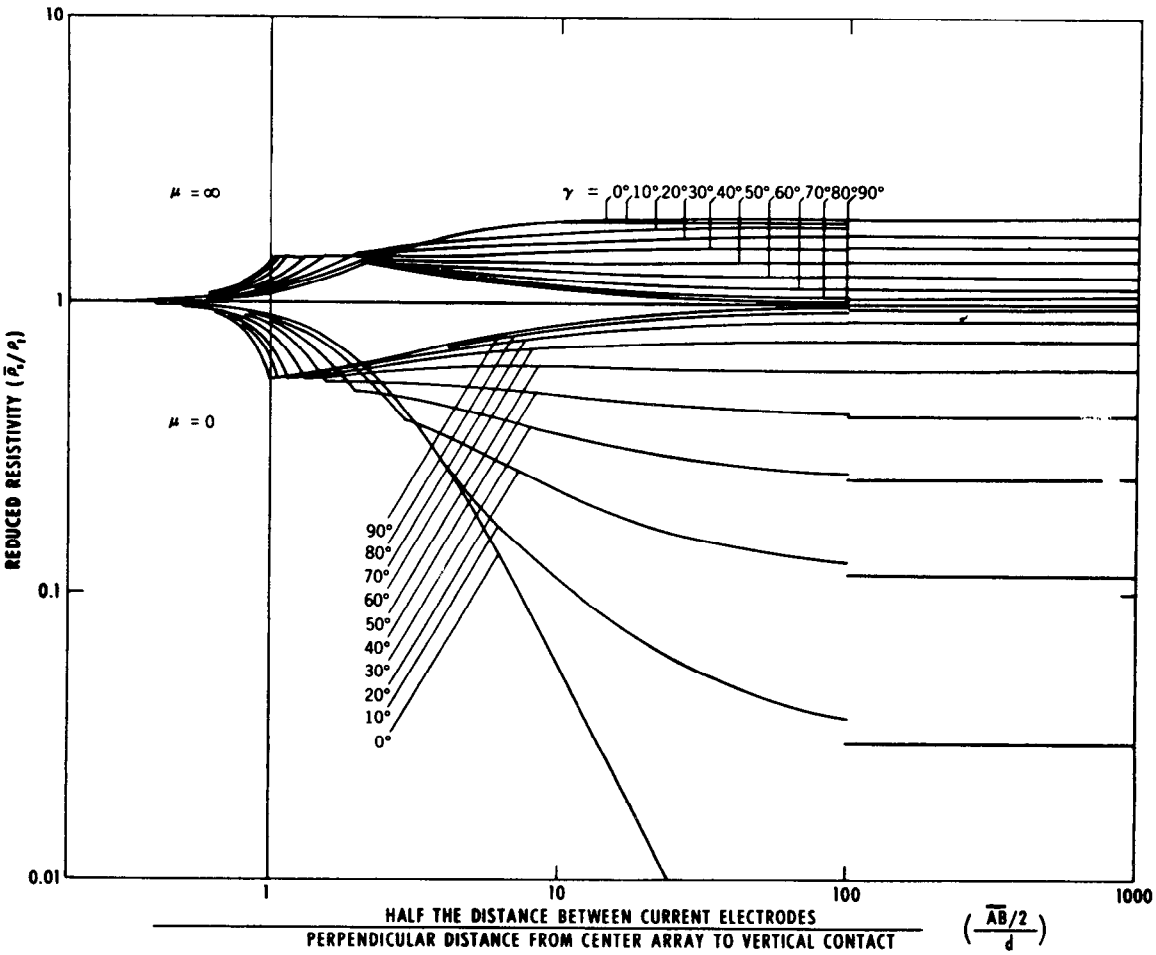

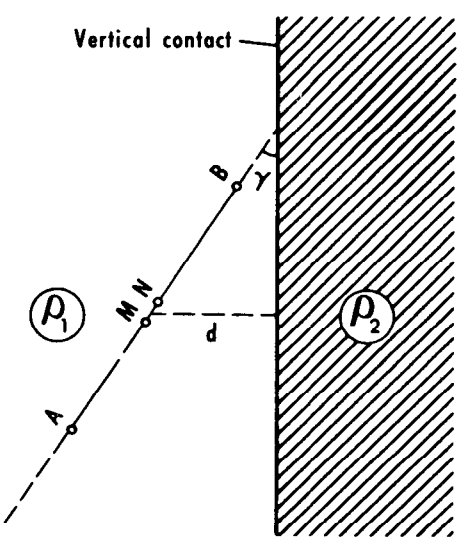

Figure 20.—Examples of the variation of Schlumberger sounding curves across a vertical contact at various azimuths. $\overline{AB}/2$, electrode spacing; d, perpendicular distance from center of array 0 to surface trace of vertical contact; $\bar{\rho}$, apparent resistivity; ρ, true resistivity; γ, azimuth angle (after Zohdy, 1970).

and Keller and Frischknecht (1966).

Approximate equivalence of sounding curves of sections with horizontal or vertical contacts, or both, to sounding curves of sections with horizontal boundaries only.— The form of sounding curves obtained over sections with horizontal and (or) vertical or inclined contacts can be quite similar to curves obtained over sections with horizontal contacts only. This is true when the sounding line is parallel to the strike of the vertical (or inclined) contact. Depending on the ratio d/h of the perpendicular distance from the center of the sounding line to the surface trace of the vertical contact d to the thickness of the top layer h, one may obtain sounding curves that are equivalent to curves obtained over a three, or more, horizontally-layered Earth model (fig. 22, curves e and f). This type of equivalence is resolved easily by making crossed soundings (soundings having the same center but expanded at right angles to one another). The forms of the two sounding curves are so different from one another that it is easy to realize the presence of a lateral heterogeneity in the ground (see curve e', fig. 22). The expansion of the Lee-partitioning array parallel to the strike of a vertical or inclined contact does not yield data that are indicative of the presence of the lateral heterogeneity, and the making of a crossed sounding is required.

Approximate equivalence between two multilayer sections.—A sounding curve obtained over a four- or five-layer section may be nearly equivalent to one obtained over a three-layer section. Generally this is attributed to the so-called principle of suppression (Maillet, 1947). The error, caused by the effect, in interpreting the depth of contacts is sometimes referred to as pseudoanisotropy (Genslay and Rouget, 1937; Flathe, 1955, 1963). An example of this type of equivalence is shown in figure 22, curves g and h.

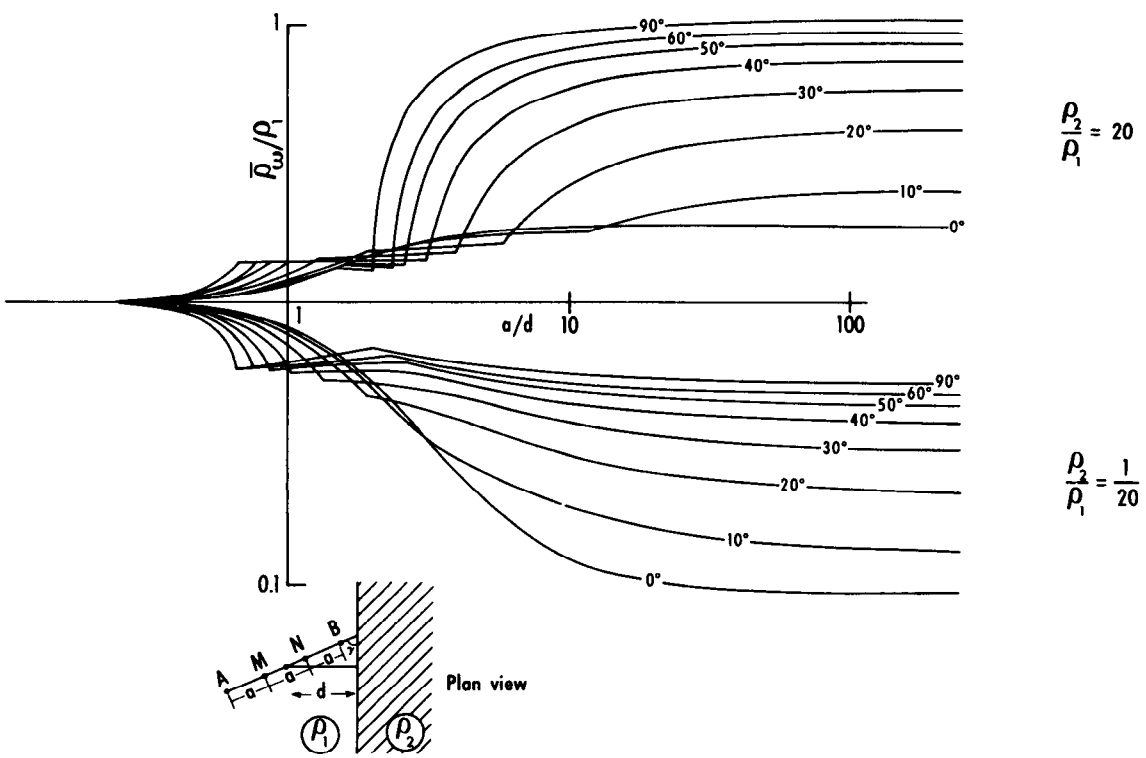

Figure 21.—Examples of the variation of Wenner sounding curves across a vertical contact at various azimuths. Unpublished data calculated by Zohdy, 1970. a, Wenner spacing; d, perpendicular distance from center of array to surface trace of vertical contact; $\overline{\rho}$, apparent resistivity; ρ, true resistivity.

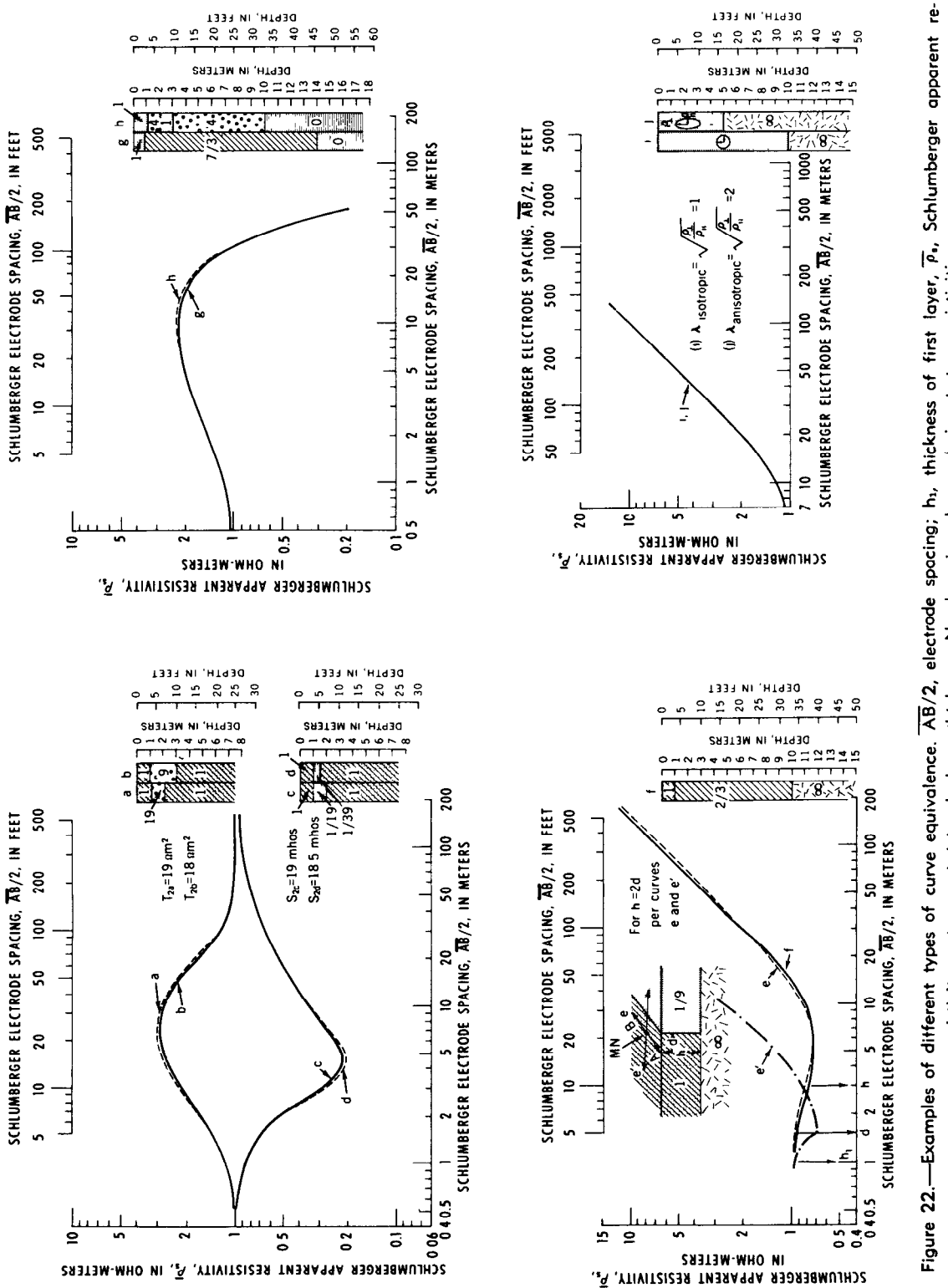

Figure 22.—Examples of different types of curve equivalence. $\overline{AB}/2$, electrode spacing; h_1, thickness of first layer, $\overline{\rho}_a$, Schlumberger apparent resistivity; ρ, true resistivity; h, layer thickness. Numbers in columns designate true resistivities.

Equivalence between isotropic and anisotropic media.—The equivalence between an isotropic layer and an anisotropic layer is exact when the equivalent layer has microanisotropic properties. In practice, depths are generally overestimated by a factor equal to the coefficient of anisotropy $\lambda = \sqrt{\frac{\rho_\perp}{\rho_\parallel}}$, where $\rho_\perp$ and $\rho_\parallel$ are the resistivities perpendicular to, and parallel to, the bedding, respectively (fig. 22, curves i and j). Values of λ generally range from 1.1 to 1.3 and rarely exceed 2.

Monotonic change in resistivity.—When the resistivity of the subsurface layers increases or decreases monotonically (A-, AA-, Q-, or QQ-type sections), the sounding curve may resemble a curve of a simple two-layer Earth model (principle of suppression), unless the thicknesses of the layers increase significantly with depth. Recently, two new methods for making so-called differential soundings have been introduced (Rabinovich, 1965; Zohdy, 1969) whereby the resolving power of the sounding curve is greatly improved for A- and Q-type sections.

Relative thickness of a layer.—The detectability of a layer of given resistivity depends on its relative thickness, which is defined as the ratio of the bed thickness to its depth of burial. The smaller the relative thickness of a given layer, the smaller the chance of its detectability on a sounding curve. In four-layer (or more) Earth models the so-called "effective relative thickness" of a layer (Flathe, 1963), which is defined as the ratio of the layer thickness to the product of the pseudoanisotropy, and the total thickness of the layers above it must be considered. For example, a layer 50 meters (164 feet) thick at a depth of 10 meters (32.8 feet) has a relative thickness of 5, which is quite favorable for its detection on a sounding curve. However, if the top 10 meters (32.8 feet) are composed of two layers of thicknesses of 2 meters (6.56 feet) and 8 meters (26.2 feet) and resistivities of 10 ohm-m and 1,000 ohm-m, respectively, then the pseudoanisotropy λ of the top two layers is 4.1. Therefore, the effective relative thickness is $50/(4.1\times10) \cong 1.22$, which is considerably smaller than the relative thickness of 5 previously calculated. The resistivity of the 50 meter (164 feet) third layer and of the underlying layers also play an important role in the detectability of the layer on the sounding curve.

The limitations to interpretation mentioned above should not be discouraging to the geophysicist nor should they persuade the reader to consider the interpretation of sounding data as an entirely hopeless endeavor. All geophysical methods that are based on potential theory (electrical, gravity, and magnetic methods) lack unique solutions. In practice, it is by correlation of several sounding curves, by making crossed soundings, by sounding with different arrays, by traversing the area with horizontal resistivity profiles, by knowledge of its general geology, and by recognition of the electrical properties of the rocks in the studied area that correct interpretations are achieved. When drilling information is available it is advisable to make parametric electrical soundings near the wells in order to determine the resistivity parameters of the layers using accurately determined layer thicknesses. Then using these known resistivity parameters, we can determine the layer thicknesses in areas where drilling information is lacking.

Analysis of Electrical Sounding Curves

When an area is investigated, the sounding curves generally are not all of the same type (H, A, K, Q, and HA, for example). Furthermore, all the curves may not be interpretable in terms of horizontally stratified media. In this section we shall describe some of the qualitative and quantitative methods of interpretation of electrical sounding data.

Qualitative Interpretation

The qualitative interpretation of sounding data involves the following:

1. Study of the types of the sounding curves obtained and notation of the areal distribution of these types on a map of the survey area.
2. Preparation of apparent-resistivity maps. Each map is prepared by plotting the apparent resistivity value, as registered on the sounding curve, at a given electrode spacing (common to all soundings) and contouring the results (fig. 23).
3. Preparation of apparent-resistivity sec-

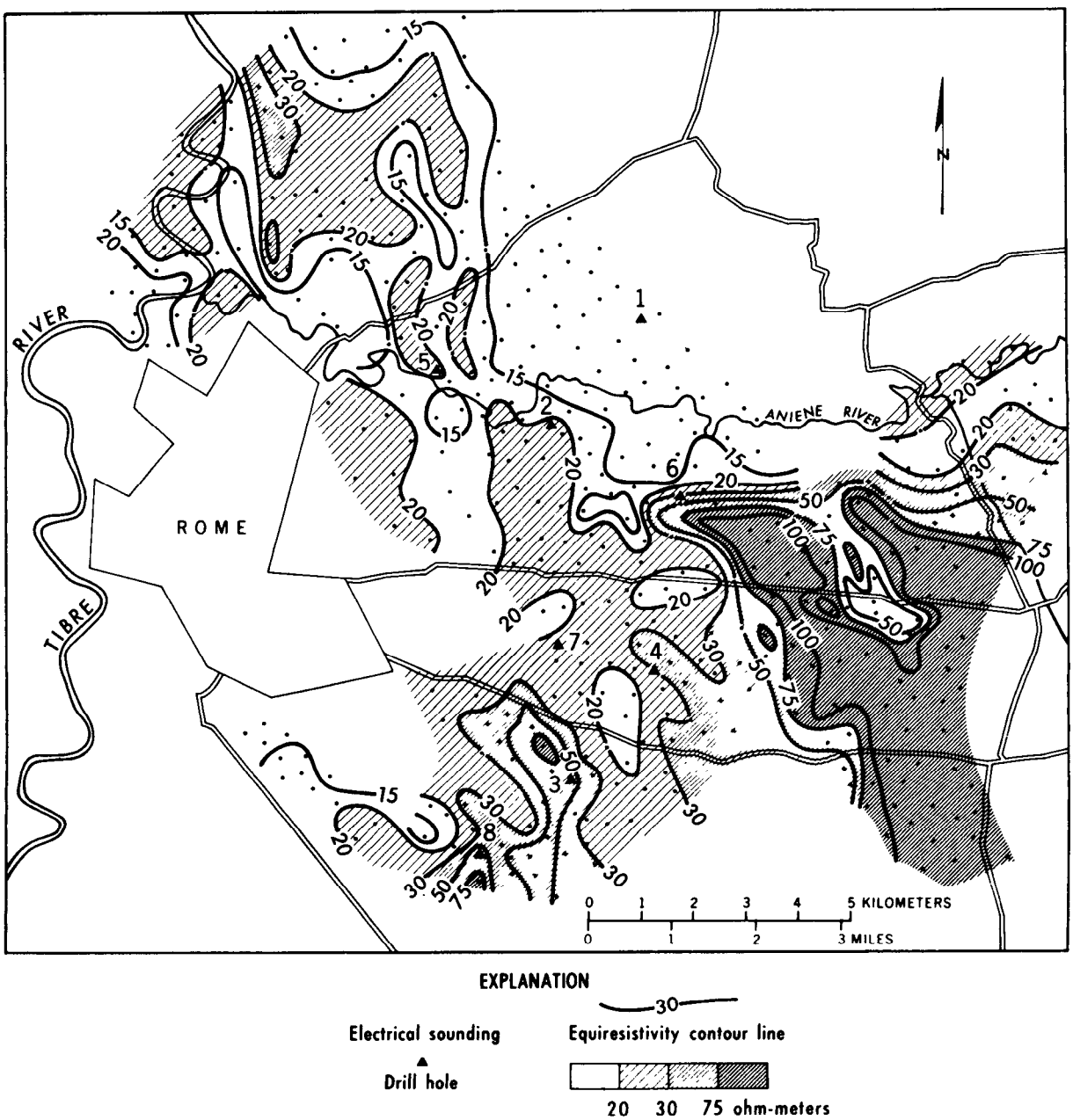

Figure 23.—Map of apparent resistivity near Rome, Italy (after Breusse, 1961a).

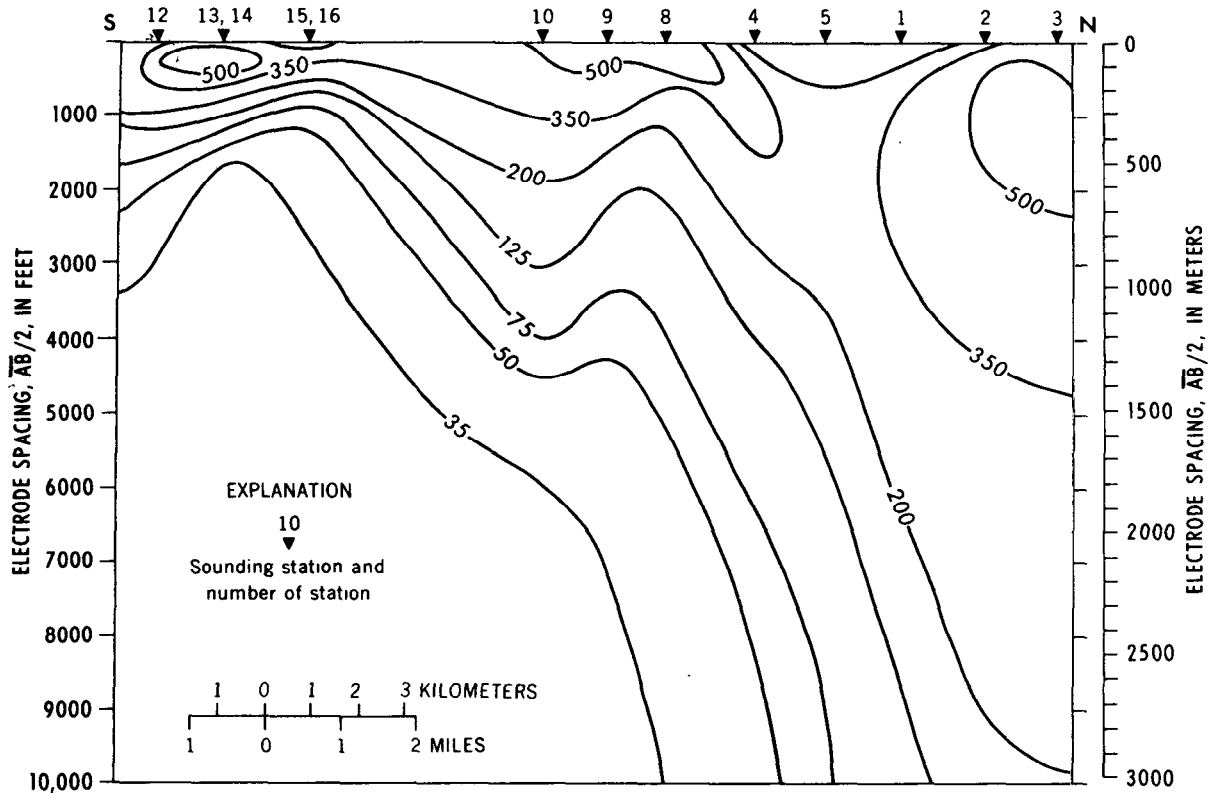

Figure 24.—Section of apparent resistivity near Minidoka, Idaho. Values on contour lines designate apparent resistivities in ohm-meters. Snake River basalt thickens toward the north.

tions. These sections are constructed by plotting the apparent resistivities, as observed, along vertical lines located beneath the sounding stations on the chosen profile. The apparent resistivity values are then contoured (fig. 24). Generally a linear vertical scale is used to suppress the effect of near-surface layers.

4. Preparation of profiles of apparent-resistivity values for a given electrode spacing, profiles of the ordinate or abscissa of the values of the minimum point $\overline{\rho}_{min}$ for H-type sections, profiles of the ordinate or absicissa of the maximum point $\overline{\rho}_{max}$ for K-type sections, profiles of ρ_L values, and profiles of S and T values.

These maps, sections, and profiles constitute the basis of the qualitative interpretation which should precede quantitative interpretation of the electrical sounding data. It should be noted, however, that an apparent resistivity map for a given electrode spacing (fig. 23) does not represent the areal variation of resistivity at a depth equal to that electrode spacing, it merely indicates the general lateral variation in electrical properties in the area. For example, an area on the map having high apparent resistivity values may correspond to a shallow high resistivity bedrock, it may indicate thickening in a clean sand and gravel aquifer saturated with fresh water, or it may indicate the presence of high resistivity gypsum or anhydrite layers in the section.

Determination and Use of Total Transverse Resistance, T, from Sounding Curves

In three-layer sections of the K type, the value of transverse resistance of the second layer can be determined approximately from a Schlumberger sounding curve (fig. 25) by multiplying the ordinate value of the maxi-

mum point ($\overline{\rho_s}_{max}$) by the corresponding abscissa value of $\overline{AB}/2$ (Kunetz, 1966). The value of T_2' thus determined generally is underestimated (fig. 25), especially when the real value T_2' is large and is approximately equal to the total transverse resistance of the upper two layers $T = T_1 + T_2 \cong T_2$, (with, $T_1 \leq 10\%\ T_2$).

The total transverse resistance of the upper two layers $T = T_1 + T_2 = \rho_1 h_1 + \rho_2 h_2$ is determined approximately by another graphical technique (Dzhavarof and Biramova, 1965). The intercept of a straight line tangent to the Schlumberger sounding curve and inclined to the abscissa axis at an angle of 135° (or -45°) with the horizontal line for $\overline{\rho}=1$ ohm-m is approximately equal to T (fig. 25). The value of $T' \cong T$ by this graphical method generally is overestimated. Therefore, for large values of T and where $T_2 \cong T$, the average of the values of T'_2 and T' is close to the true value of T (fig. 25). This is especially true when $\rho_3/\rho_1 << 1$. Where the value of T increases from one sounding station to the next, this generally means that the thickness of the resistive layer in the section (gravel, basalt, etc.) also increases. However the increase in T might be caused also by an increase in the resistivity values. A north-south profile of graphically determined values of total transverse resistance east of Minidoka, Idaho, (fig. 26) is an excellent qualitative indication that the Snake River basalt increases in thickness appreciably from south to north.

Determination of Total Longitudinal Conductance, S, From Sounding Curves

In H, A, KH, HA, and similar type sections the terminal branch on the sounding curve often rises at an angle of 45°. This usually indicates igneous or metamorphic rocks of very high resistivity (>1,000 ohm-m). However, in the presence of conductive sedimentary rocks saturated with salt water (ρ<5 ohm-m) the so-called "electric basement" of high resistivity rocks may correspond to sandstones or limestones having resistivities of only 200–500 ohm-m. The total longitudinal conductance S is determined

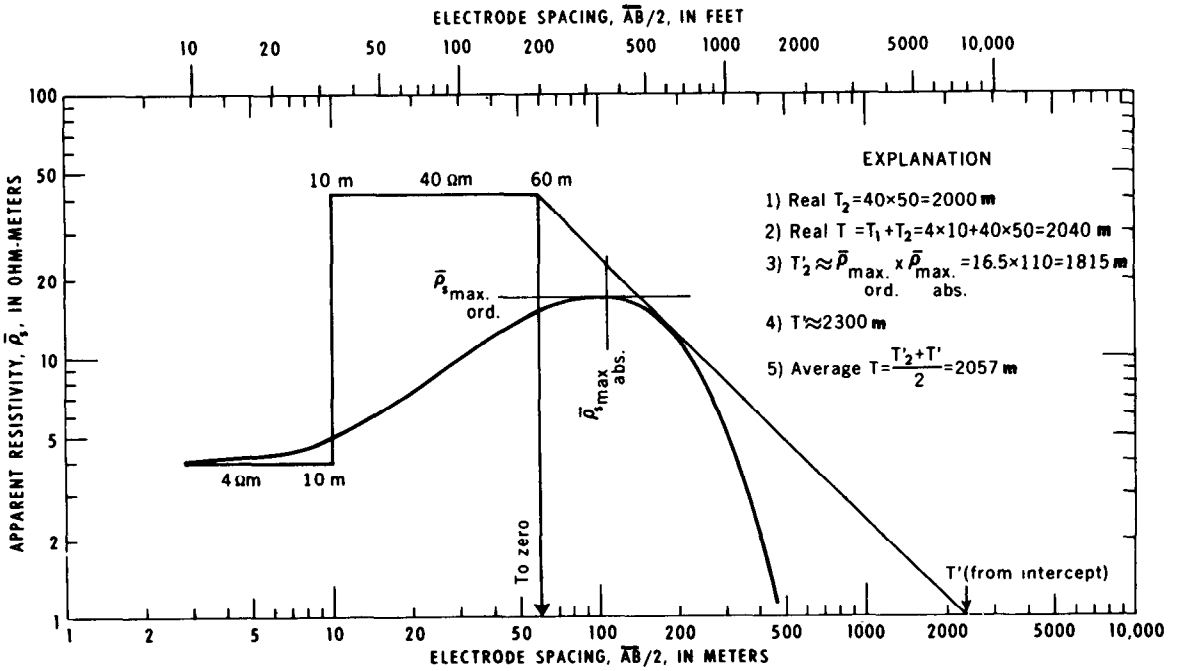

Figure 25.—Graphical determination of total transverse resistance from a K-type Schlumberger sounding curve. ρ_1 = 4 ohm-meters, ρ_2 = 40 ohm-meters, ρ_3 = 0 ohm-meters, h_1 = 10 meters (32.8 feet), h_2 = 50 meters (164 feet), $h_3 = \infty$.

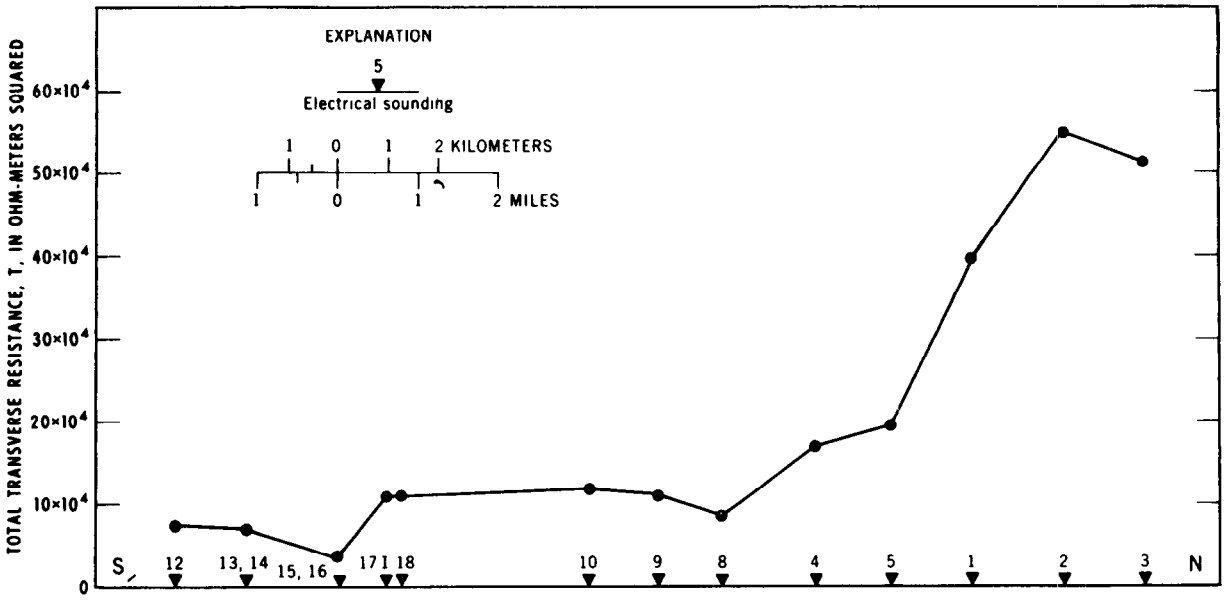

Figure 26.—Profile of total transverse resistance values, T, in ohm-meters squared, near Minidoka, Idaho. High values indicate thickening of basalt layers. Data obtained by Zohdy (1969).

from the slope of the terminal branch of a Schlumberger curve, rising at an angle of 45° (here called the *S*-line). It should be remembered that the slope of a rectilinear branch inclined to the abscissa at 45° is not necessarily equal to unity when the curve is plotted on logarithmic paper. The value of *S* is numerically equal to the inverse of the slope of this line (Kalenov, 1957; Keller and Frischknecht, 1966), and it is usually determined, very quickly, by the intercept of the extension of the *S*-line with the horizontal line, $\overline{\rho}_s = 1$ ohm-m (fig. 27). The determination of *S* by this method is as accurate as a graphical procedure can be, and is valid irrespective of the number of layers that overlie the high resistivity layer provided the terminal branch rises at an angle of 45°. When the resistivity of the bottom layer is not sufficiently high to make the terminal branch rise at an angle of 45°, other methods are used for the graphical determination of *S* (Berdichevskii, 1957; Orellana, 1966; Orellana and Mooney, 1966; Zohdy, 1968). Increases in the value of *S* from one sounding station to the next indicate an increase in the total thickness of the sedimentary section, a decrease in average longitudinal resistivity (ρ_L), or both.

Determination of Average Longitudinal Resistivity, ρ_L, from a Sounding Curve

As the value of longitudinal conductance *S* can be determined easily from a Schlumberger sounding curve, graphical methods for the evaluation of average longitudinal resistivity (ρ_L) from the sounding curve were sought so that the total depth *H* to the high resistivity bedrock could be calculated from the simple relation $H = S\rho_L$. It was found (Zagarmistr, 1957) that for three-layer sections of the H type, the value of the apparent resistivity at the minimum point ($\overline{\rho}_{r\,min}$) on a polar dipole-dipole curve is approximately equal to ρ_L, provided that the thickness of the middle low resistivity layer is at least 3 times as large as the thickness of the first layer ($h_2 \geq 3h_1$). This was found to be valid for all values of $\mu = \frac{\rho_2}{\rho_1}$ (Zagarmistr, 1957; Berdichevskii and Zagarmistr, 1958). Using formulas developed by Al'pin and by Tsekov (Al'pin, 1958; Zagarmistr, 1957; Zohdy, 1969a), Schlumberger and equatorial sounding curves can be transformed into polar dipole sounding curves (fig. 28). The average longitudinal resistivity then can be determined and the thickness of the section can be calculated.

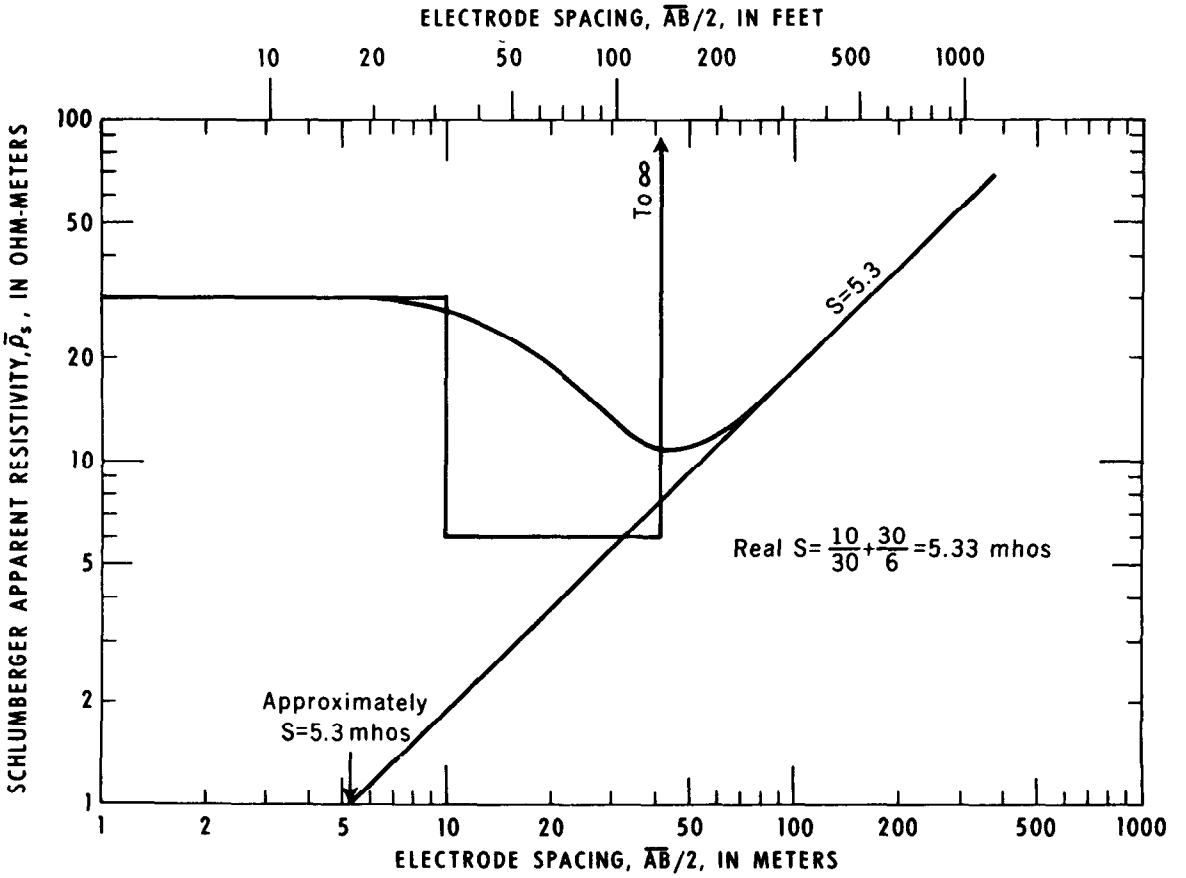

Figure 27.—Graphical determination of total longitudinal conductance S from an H-type Schlumberger sounding curve.

Average longitudinal resistivity also may be determined from borehole induction logs of wells in the area.

Distortion of Sounding Curves by Extraneous Influences

Electrical sounding curves may be distorted by lateral inhomogeneities in the ground, by errors in measurements, or by equipment failure. It is important to realize the cause of various common distortions on sounding curves.

Formation of cusps.—The formation of a cusp on a Schlumberger sounding curve generally is caused by a lateral heterogeniety, by current leakage from poorly insulated cables, by electrode spacing errors, or by errors in calculation (Zohdy, 1968b). When plotting data in the field, it is advisable to check for current leakage whenever a cusp is formed on the sounding curve. A resistive lateral inhomogeneity, in the form of a sand lens or a near-surface caliche layer, produces a cusp like the one shown in curve *A*, figure 29; and a conductive inhomogeneity, in the form of a buried pipe or a clay pocket, produces a cusp as the one shown in curve *B*, figure 29.

Sharp maximum.—The maximum or peak value on a K-type sounding curve is always gentle and broad, and should never have a sharp curvature where the ground is horizontally homogeneous. The formation of a sharp peak (fig. 30) generally is indicative of the limited lateral extent of the buried (middle) resistive layer (Alfano, 1959).

Curve discontinuities.—Two types of discontinuities are observed on Schlumberger sounding curves. The first type is observed when the spacing $\overline{MN}$ is enlarged (with $\overline{AB}$

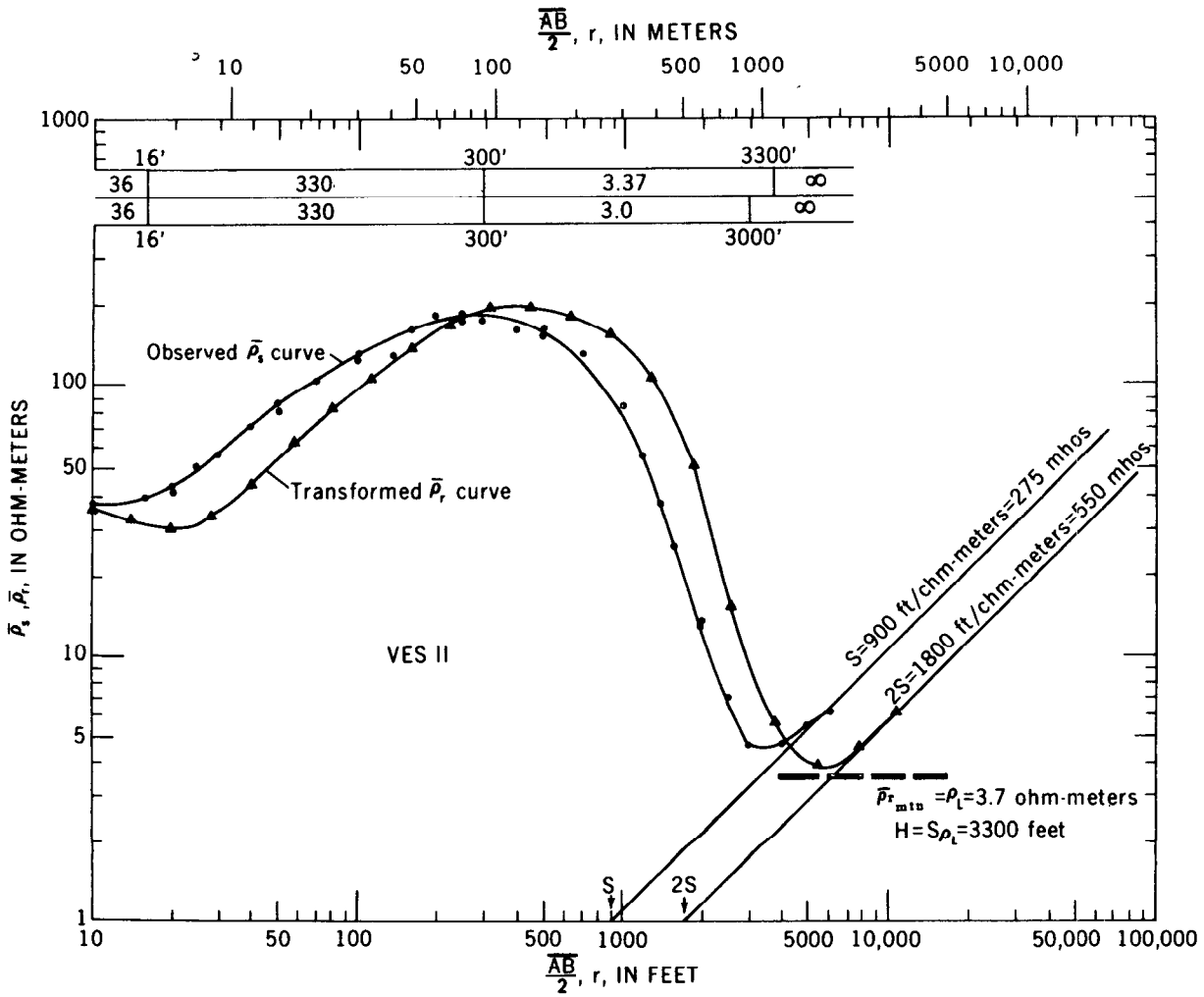

Figure 28.—Transformation of a Schlumberger KH-type curve into a polar dipole-dipole curve to evaluate $\bar{\rho}_{r_{min}} = \rho_L$ and $H = S\rho_L$ (after Zohdy, 1969a). Reproduced with permission of "Geophysics."

constant) and the value of the apparent resistivity, for the larger $\overline{MN}$ spacing, does not conform to the theoretical magnitude for such a change in $\overline{MN}$ (Deppermann, 1954). The repetition of such a discontinuity when $\overline{MN}$ is changed to a larger spacing for the second time indicates a lateral inhomogeneity of large dimensions. This type of discontinuity also may indicate current leakage, electrode spacing errors (Zohdy, 1968b), or that the input impedance of the potential-difference measuring device is not sufficiently high. Examples of the discontinuities that are not in conformity with the assumption of a horizontally homogenous Earth are shown in figure 31. When the discontinuities are not severe, the curve can be corrected easily by shifting the distorted segment of the curve vertically to where it should be.

The second type of discontinuity is less common and occurs during the expansion of the current electrode spacing $\overline{AB}$ when sounding with a Schlumberger array. In general, the curve is displaced downward, that is, the value of the apparent resistivity at the larger AB is much less than the previous reading (fig. 32). This type of discontinuity generally is caused by a narrow, shallow, dike-like structure which is more resistant than

the surrounding media and whose width is small in comparison to the electrode spacing (Kunetz, 1955, 1966; Zohdy, 1969a). The abscissa value at which the discontinuity on the sounding curve occurs is equal to the distance from the sounding center to the dike-like structure.

Quantitative Interpretation

Several methods are used in the quantitative interpretation of electrical sounding curves. These methods are classified as analytical methods, semiempirical methods, and empirical methods.

Analytical Methods of Interpretation

The analytical methods are based on the calculation of theoretical sounding curves that match the observed curves. There are several catalogues of theoretical master curves calculated for a variety of Earth structures, most of which represent horizontally stratified media. Mooney and Wetzel (1956) published an extensive catalogue of master curves for Wenner soundings over two-, three-, and four-layer Earth models. The Mooney-Wetzel album, now out of print, has several shortcomings that limit its usefulness (Zohdy, 1964).

Two problems are encountered in the calculation of theoretical sounding curves and in their application for the interpretation of field data. First, the calculation of the apparent resistivity value at each electrode spacing involves the evaluation of a difficult integral (Stefanesco and others, 1930) or the summation of an infinite series (Hummel, 1929). Thus the use of a high speed digital computer is almost always necessary for the calculation of theoretical sounding curves.

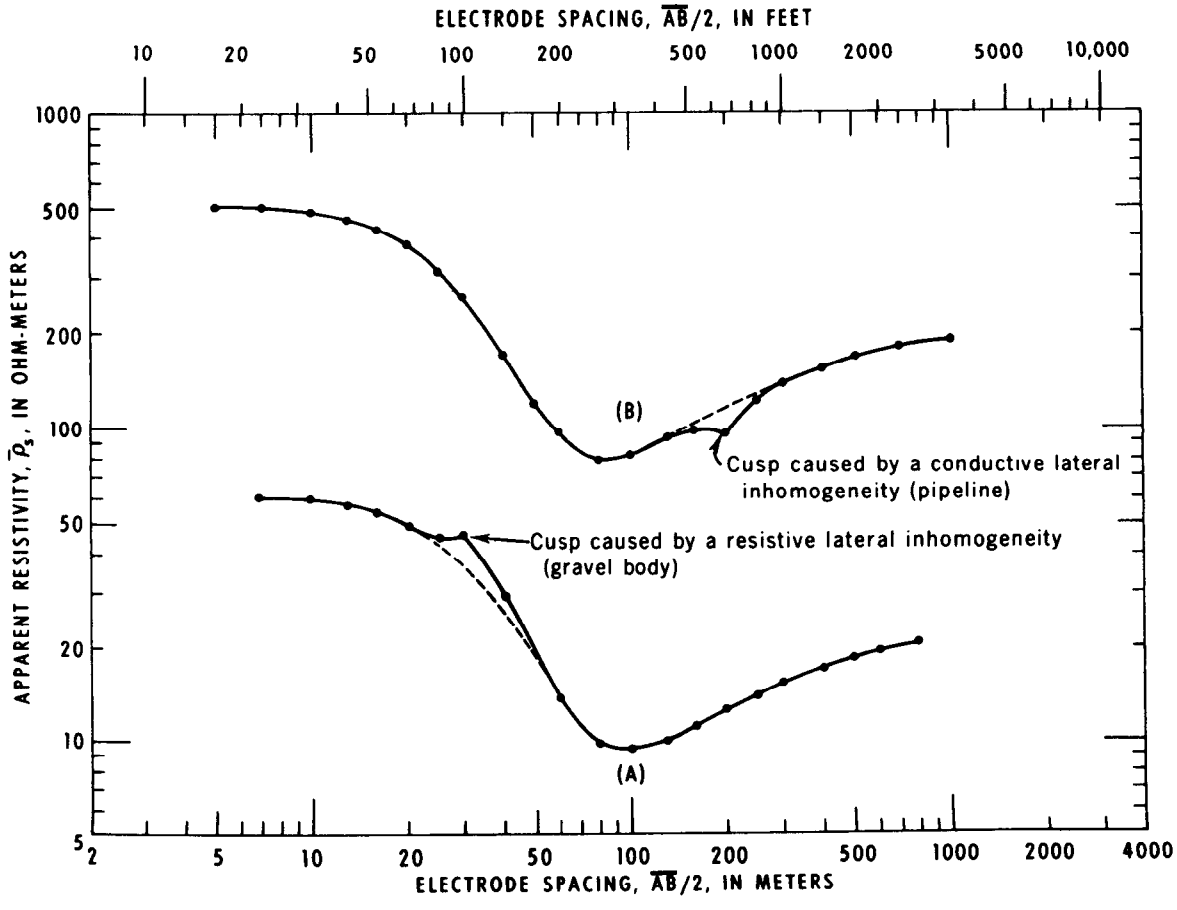

Figure 29.—Distortion of sounding curves by cusps caused by lateral inhomogeneites.

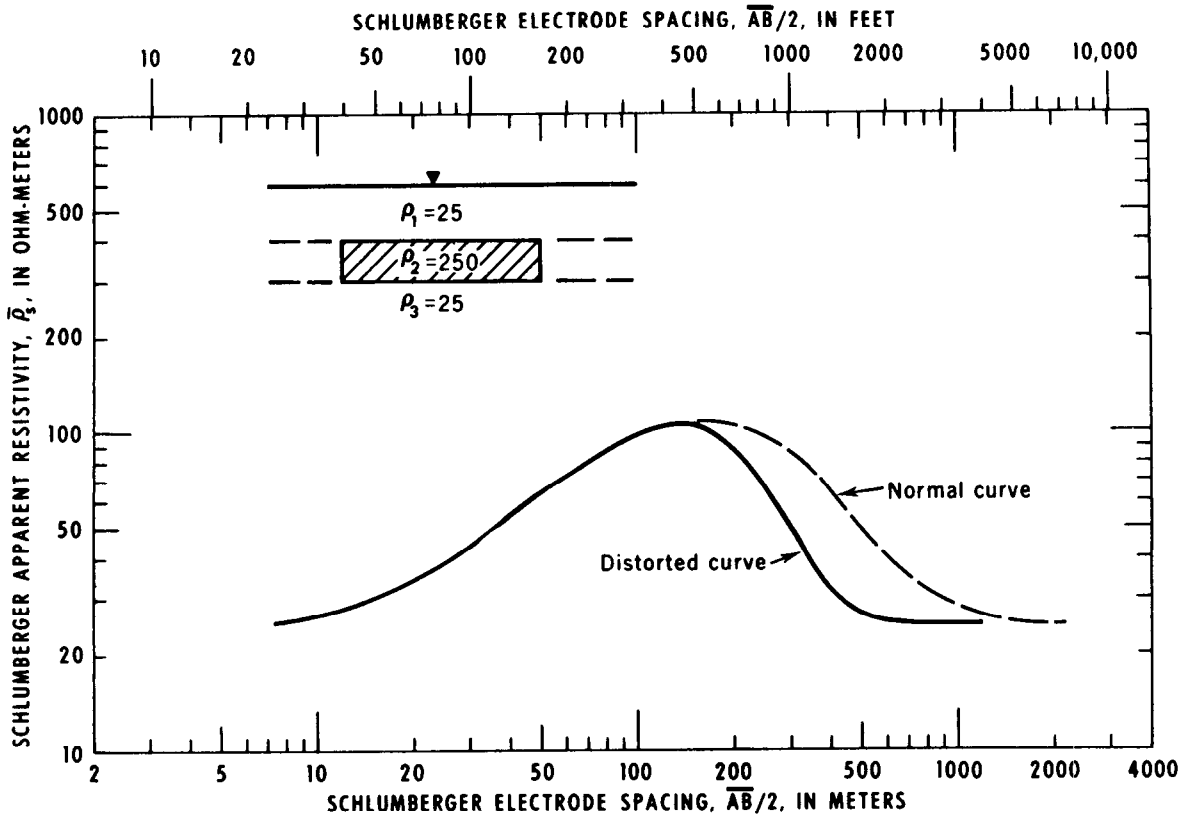

Figure 30.—Example of a narrow peak on a K-type curve, caused by the limited lateral extent of a resistive middle layer (after Alfano, 1959). Reproduced with permission of "Geophysical Prospecting."

Recently, however, the calculation of VES (vertical electrical sounding) curves of the Schlumberger type for horizontally stratified media was simplified and greatly accelerated through the use of the method of convolution (Ghosh, 1971).

The second difficulty in the calculation of theoretical curves is that in multilayer Earth models, the possible combinations of resistivity contrasts and layer thicknesses are infinite. Even in a simple two-layer Earth model, there are three variable parameters, ρ_1, ρ_2, and h_1. With ρ_1, ρ_2, and h_1 as variables there are an infinite number of possible sounding curves for the two-layer geoelectric section. However, by considering the resistivity and thickness of the first layer as unity and by plotting the theoretical sounding curves on a set of logarithmic coordinates with the dimensionless variables $\overline{AB}/2\ h_1$ (Schlumberger), a/h_1 (Wenner), or r/h_1 (dipole-dipole), on the abscissa; and $\bar{\rho}_s/\rho_1$, $\bar{\rho}_w/\rho_1$, or $\bar{\rho}_d/\rho_1$ on the ordinate, a simple family of curves is obtained. These two-layer curves vary in shape, in a unique manner, and in accordance with the infinite number of values that the ratio ρ_2/ρ_1 may attain. A set of two-layer master curves for the Schlumberger array is shown in figure 33; two-layer master sets of other arays may be different in shape.

In three-layer Earth models, there are five variable parameters: ρ_1, ρ_2, ρ_3, h_1, and h_2. By using the dimensionless variables

$$\mu_1 = \rho_2/\rho_1,\ \mu_2 = \rho_3/\rho_1,\ \upsilon_1 = \frac{h_2}{h_1}$$

and by plotting the theoretical sounding curves on logarithmic coordinates, the result is still an infinite number of curves (Cagniard, 1952).

The limitations on the calculation and application of theoretical sounding curves should not discourage their use. Several

graphical methods have been devised for the construction of electrical sounding curves of $\mu_1 = \rho_2/\rho_1$, $\mu_2 = \rho_3/\rho_1$, and $v_1 = h_2/h_1$ that have not been thoretically calculated (Kalenov, 1957; Matveev, 1964). The graphical construction of a given sounding curve is done by using the available theoretically calculated curves in conjunction with special nomograms. The graphical interpretation of sounding curves often is checked by calculating the exact sounding curve for the derived model on a digital computer.

Before interpretation is made with the master sets for horizontal layers, the interpreter must be satisfied with the form of the sounding curve, in that it is sufficiently smooth and not severely distorted by sharp cusps or discontinuities. A certain amount of smoothing generally is required. The type of curve (such as H, A, K, Q, HA, HK) and the minimum number of layers it seems to represent can be determined by visual inspection. Because of the principles of suppression and equivalence, certain three-layer curves may resemble two-layer ones and four-layer curves may resemble three-layer curves. The estimated number of layers is generally considered to be the minimum number.

Two-layer Interpretation

If the field curve, which is plotted on logarithmic transparent paper of the same module as the master curves, seems to represent a two-layer Earth model, we superpose the transparent sheet with the field curve over the two-layer master set, and move the transparent paper up, down, right, or left (maintaining the coordinate axes of the two sheets parallel) until a best fit of the field curve against one of the theoretical curves is obtained. Occasionally the field curve may have to be matched by interpolation between two of the master curves.

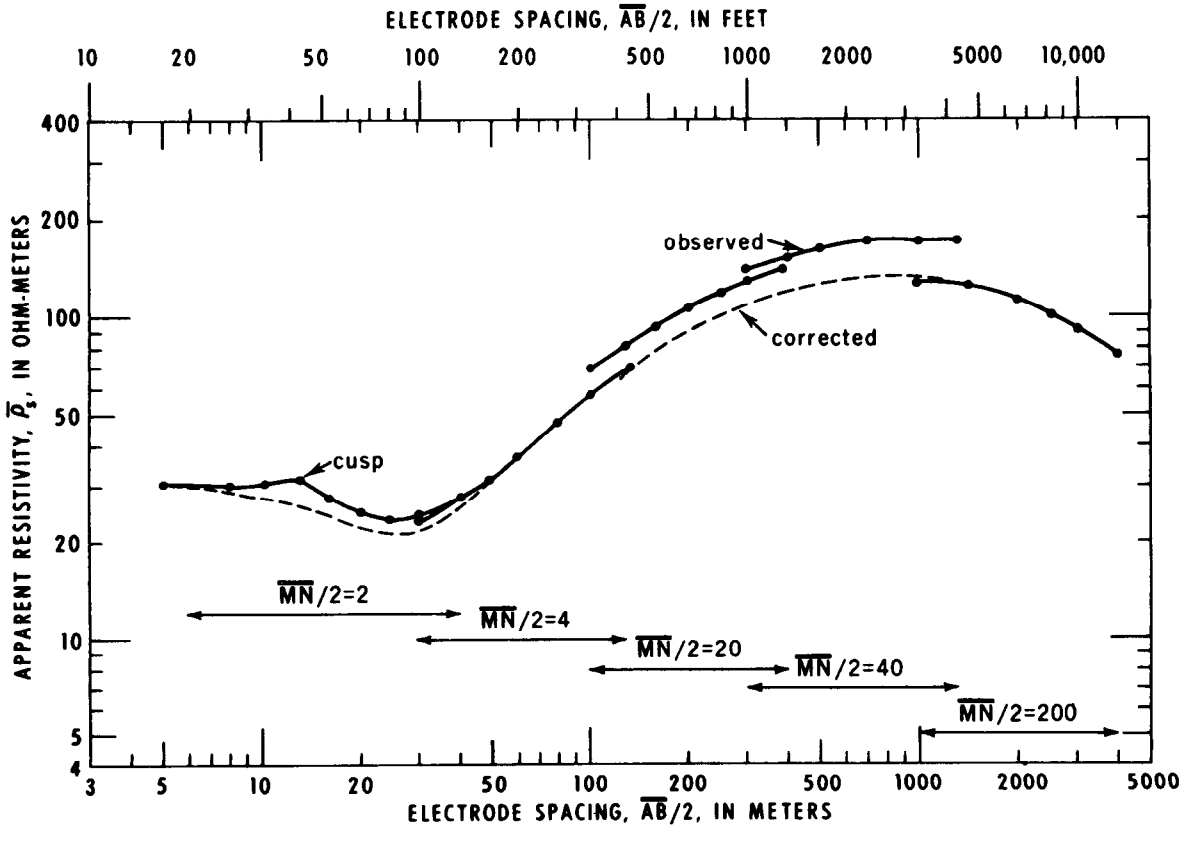

Figure 31.—Example of a distorted HK-Schlumberger curve and the method of correction.

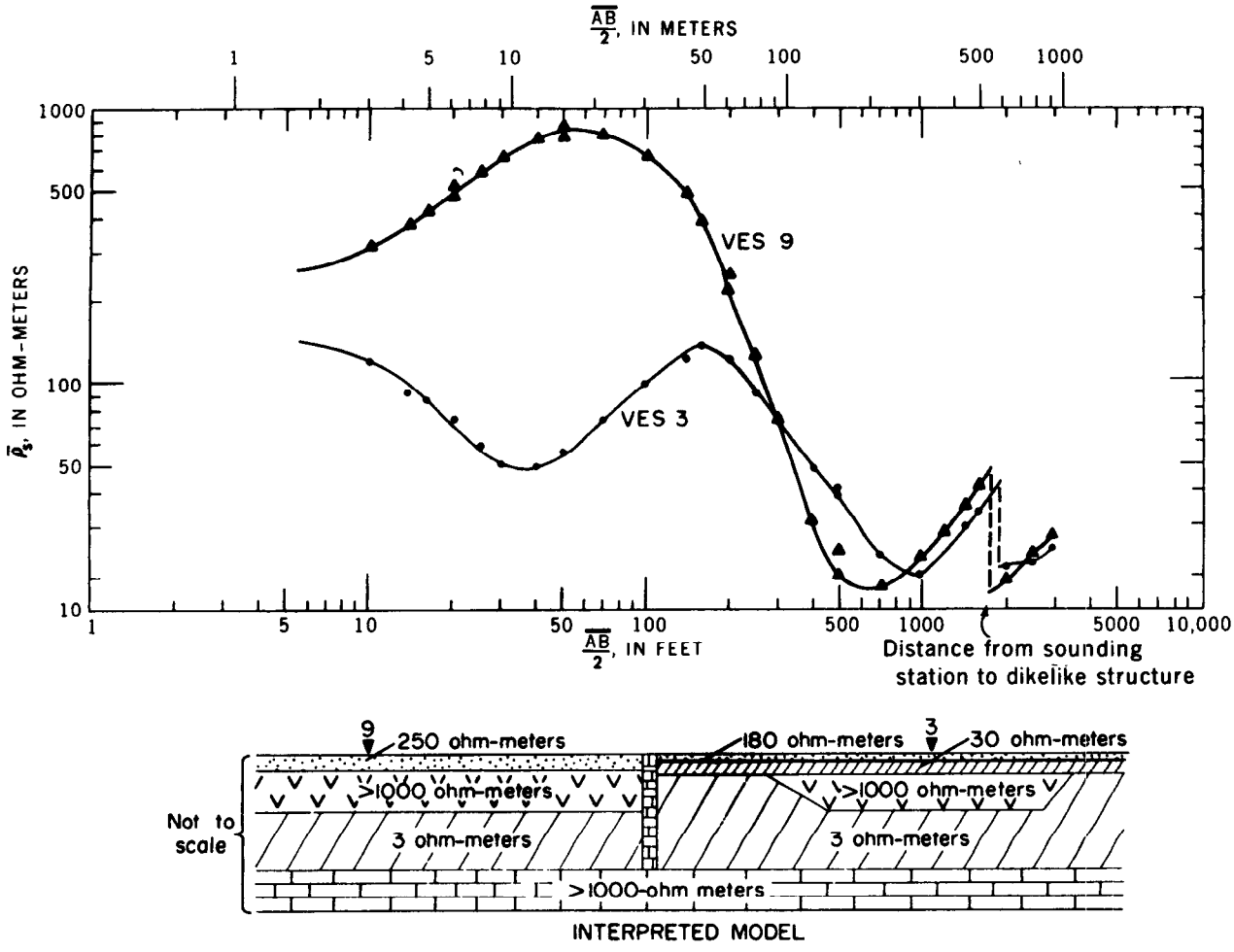

Figure 32.—Examples of tares (discontinuities) on Schlumberger curves caused by a near vertical dikelike structure. (after Zohdy, 1969a). Reproduced with permission of "Geophysics."

Determine the position of the cross, which is the origin of coordinates of the theoretical curve, and trace it on the sheet of the field curve. Also determine the resistivity of the second layer (ρ_2) by tracing the asymptote to the theoretical two-layer curve.

The abscissa value ($\overline{AB}/2$, a, or r) of the "cross" equals the thickness of the first layer and the ordinate value ($\bar{\rho}$) of the "cross" equals the true resistivity, ρ_1, of the first layer. The trace of the asymptote to ρ_2 on the field sheet equals the true resistivity, ρ_2, of the second layer (fig. 34).

Three-layer Interpretation

Determine the type of three-layer curve (H, A, K, Q) by inspection and select the applicable set of theoretical master curves.

Although one of the values of $\mu_1 = \rho_2/\rho_1$ in a set of theoretical curves may correspond to the real value of $\mu_1 = \rho_2/\rho_1$ of the field curve (or although a value of $\mu_1 = \rho_2/\rho_1$ in the album fits the observed curve through the principle of equivalence by T or by S), the value of $\mu_2 = \rho_3/\rho_1$ for the field curve may not be among those for which the theoretical curves were computed. Therefore, the first closest fit of the field curve should not be relied on. Better interpretations generally are obtained by enveloping the field curve between two three-layer curves having the same value of $\mu_1 = \rho_2/\rho_1$ and the same value of $\nu = h_2/h_1$ but different values of $\mu_2 = \rho_3/\rho_1$ (fig. 35). If the values of $\mu_2 = \rho_3/\rho_1$ for

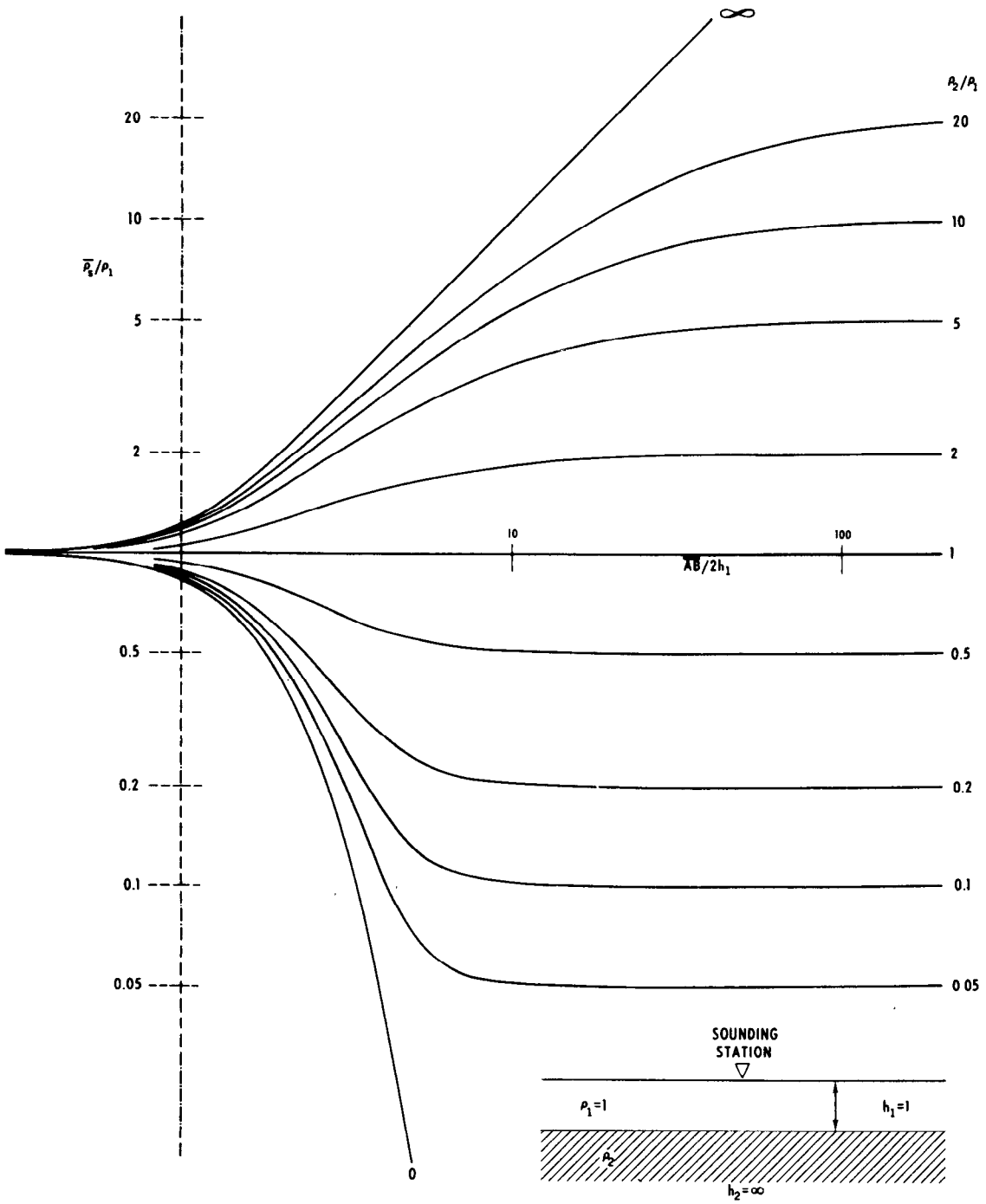

Figure 33.—Two-layer master set of sounding curves for the Schlumberger array (adapted from Orellana and Mooney, 1966).

the field curve and the theoretical curve are equal, then complete curve matching may be attained.

Maintaining parallelism between the axes of the field curve and the theoretical curve, determine the position of the cross on the field curve, note the value of $v_1 = h_2/h_1$ designating the theoretical curve, and note the values of $\mu_1 = \rho_2/\rho_1$ and $\mu_2 = \rho_3/\rho_1$.

Knowing h_1 and ρ_1 from the abscissa and ordinate of the cross, the values of ρ_2, h_2, and ρ_3 can be calculated from the values of $\mu_1 = \rho_2/\rho_1$, $v_1 = h_2/h_1$, and $\mu_2 = \rho_3/\rho_1$, respectively. The determined values of h_2 and ρ_2 may not be equal to the real values in the geologic section because of the principle of equivalence. Consequently the Pylaeve equivalency diagram (Dakhnov, 1953; Kalenov, 1957; Keller and Frischknecht, 1966; Bhattacharya and Patra, 1968) should be consulted for the section (H, A, K, or Q) under consideration, and the minimum and maximum values of h_2 and ρ_2 determined.

If a satisfactory match between the field curve and a theoretical three-layer curve is impossible, then either the curve represents more than three layers, or it is a three-layer curve with a large value of $v = h_2/h_1$ and values of $\mu_1 = \rho_2/\rho_1$ or $\mu_2 = \rho_3/\rho_1$ that are not in the album. The interpretation then is made using the two-layer curves in conjunction with auxiliary point diagrams (Orellana and Mooney, 1966; Zohdy, 1965) or by graphically constructing (Bhattacharya and Patra, 1968; Matveev, 1964; Kalenov, 1957) or numerically calculating (Ghosh, 1971) sets of three-layer master curves for the required values of v_1, μ_1, and μ_2.

Four-layer (or more) Interpretation

In practice, especially with large spacings, four or more layers may be distinctly reflected on the curve. The maximum number of layers detected by the curve with the electrode spacing $\overline{AB}/2$ of as much as 10,000 m (32,800 feet) generally does not exceed eight layers. Four- and five-layer curves are often encountered. The graphical interpretation (fig. 36) of multilayer sounding curves is made by using the three-layer curves and the auxiliary point diagrams (Bhattacharya and Patra, 1968; Kalenov, 1957; Orellana and

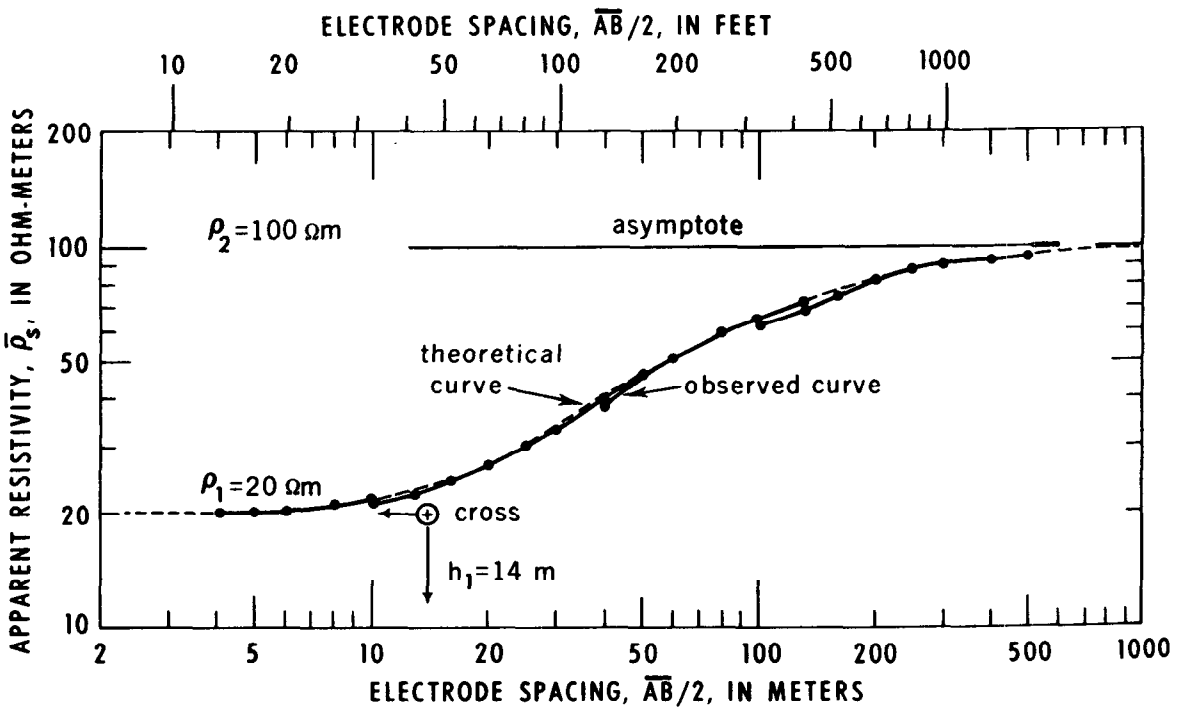

Figure 34.—Interpretation of a two-layer Schlumberger curve ($\rho_2/\rho_1 = 5$).

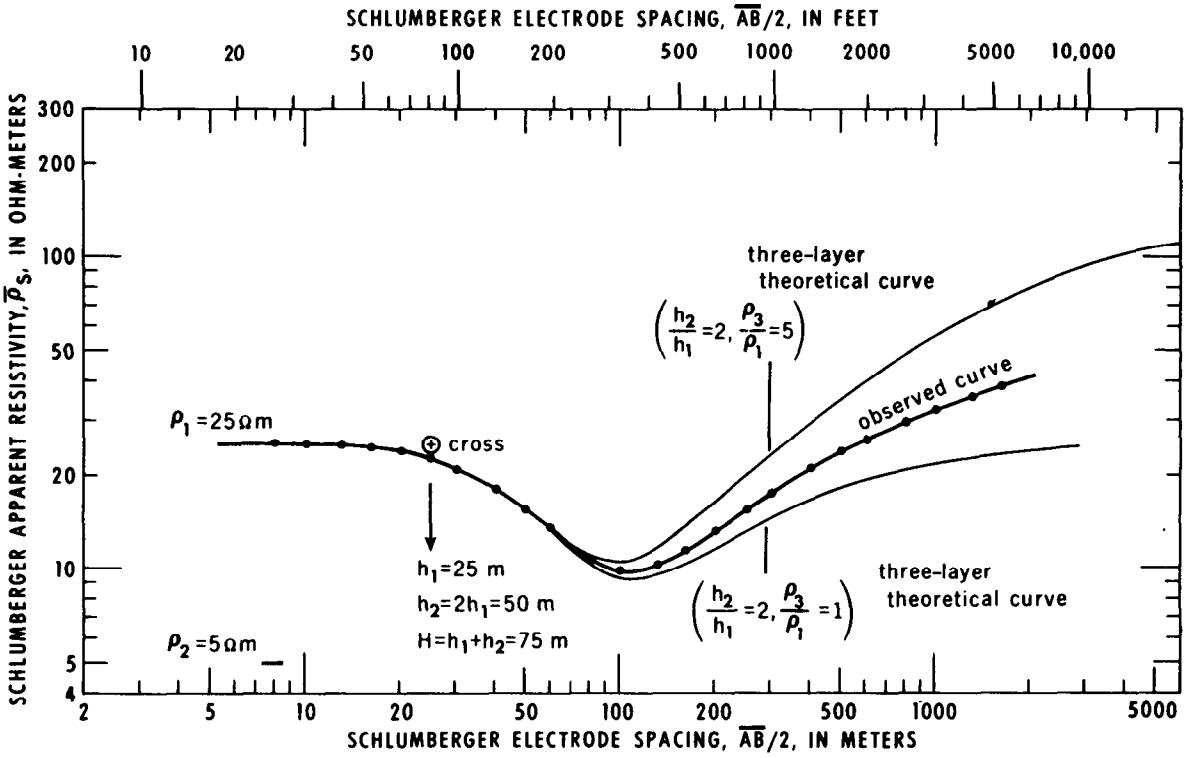

Figure 35.—Interpretation of a three-layer Schlumberger H-type curve.

Mooney, 1966; Zohdy, 1965). The accuracy of the interpretation depends on the effective relative thickness of the layers and the experience of the interpreter. It is suggested that the interpreted model be checked by (1) reconstructing the curve graphically using the method described by Matveev (1964), (2) reconstructing the first part of the curve by graphical methods and calculating the second part of the curve using the methods of Flathe (1955), Van Dam (1964, 1965), or Tsekov (1957), or (3) calculating the entire curve on a high-speed digital computer.

Empirical and Semiempirical Methods of Interpretation of Sounding Curves

Several empirical methods were invented because of the lack of calculated sets of master curves and these methods are still used by some investigators.

Moore's Cumulative Resistivity Method

Moore (1945, 1951) developed the so-called "Cumulative resistivity method," which is an empirical method for determining the depth (but not the resistivity) to horizontal layers from Wenner soundings. The method has been the subject of much discussion and has received both praise and condemnation (Muskat, 1945; Wantland, 1951).

The cumulative resistivity curve is constructed by plotting

$$\sum_{a=a_1}^{a=n} \bar{\rho}_w(a)$$

as a function of the Wenner electrode spacing a. The points on the curve will have the coordinates $(\bar{\rho}_w(a_1), a_1)$; $(\bar{\rho}_w(a_1) + \bar{\rho}_w(a_2), a_2)$; $(\bar{\rho}_w(a_1) + \bar{\rho}_w(a_2) + \bar{\rho}_w(a_3), a_3)$; . . . ; $(\bar{\rho}_w(a_1) + \rho_w(a_2) + \ldots + \rho_w(a_n), a_n)$, where $a_2 - a_1 = a_3 - a_2 = a_n - a_{n-1} =$ contant. This curve consists of straight line segments intersecting at points where the abscissa values, according to Moore are equal to the depths of horizontal boundaries. The method can be tested easily by using the theoretical data published in the Orellana-Mooney tables (Orellana and

Mooney, 1966) for Wenner curves. However, interpolation between the values given in the tables is necessary because the tables are based on electrode spacing values that increase at a logarithmic rate (1, 1.2, 1.4, 1.6, 2, 2.5, 3, 4, . . .), whereas Moore's method assumes a constant linear increase (1, 1.1, 1.2, 1.3, 1.4, 1.5, 1.6, 1.7, . . .). It is found that for horizontal two-layer Earth models the method gives reasonably accurate results provided the contrast in resistivity is moderate. If the contrast is large $(\rho_2/\rho_1) \rightarrow \infty$ or 0, the depth to the interface is underestimated by as much as 50 percent, whereas if the contrast is small, $(\rho_2/\rho_1) \cong 1$, the depth is overestimated by as much as 50 percent. This explains why Moore's method seems to work in certain areas and fails in other areas. The use of the method to interpret three-, or more, layer curves is highly questionable. Furthermore, the method does not give an estimate of the resistivities of the layers.

Barnes' Layer Method

Barnes (1952, 1954) developed an empirical method for the interpretation of electrical sounding data. The method, now known as "Barnes' layer method," is based on the erroneous assumption that the electrode spacing in the Wenner array is equal to the layer thickness. The "layer resistivity" as defined by Barnes, however, has interesting possibilities, especially if the Schlumberger array is used in lieu of the Wenner array, and provided curve-matching interpretation is used in lieu of Barnes' empirical approach (Keller, 1968).

All empirical methods either are rejected or improved by testing them with theoreti-

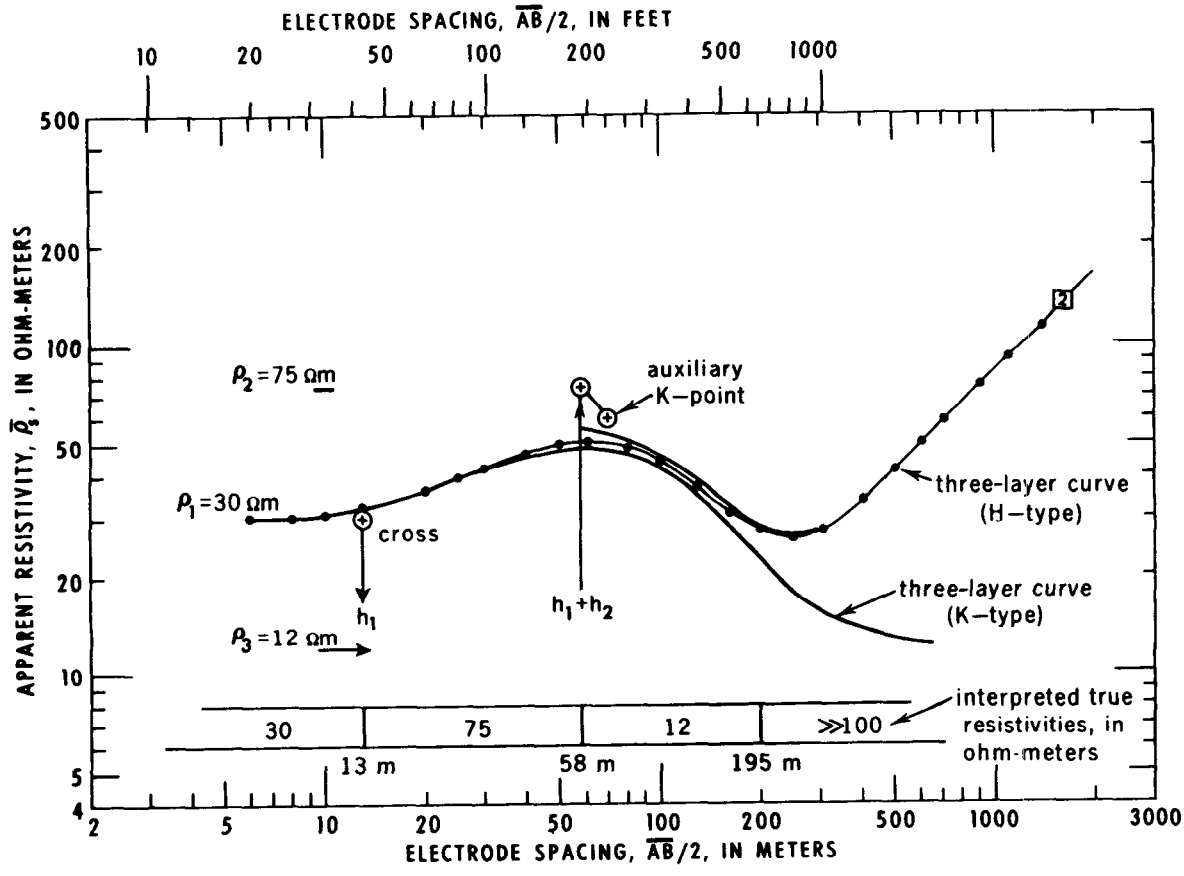

Figure 36.—Interpretation of a four-layer Schlumberger curve by the auxiliary point method using two three-layer curves. The numeral 2 on the upper curve indicates that the thickness of the third layer is twice as great as the abscissa of the auxiliary K point. (For details of method, see Bhattacharya and Patra, 1968; Zohdy, 1965.)

cally exact calculations. By testing empirical methods against tested theoretical curves, semiempirical methods are evolved. The conditions for which such semiempirical relations are valid generally are well defined, and for many of these relations rigorous mathematical formulations proving their approximate validity can be derived. Examples of these methods are: the determination of the value of T from K-type Schlumberger sounding curves, and the evaluation of ρ_L from polar dipole-dipole sounding curves. The Russian literature is richly endowed with such methods (Abdullaev and Dzhafarov, 1964; Kalenov, 1957). Many of these methods resulted in the development of useful nomograms. The general goal of all such methods is to avoid complete curve-matching procedures; consequently, only a part of the information contained in a sounding curve is utilized in interpretation, and large errors sometimes occur. Semiempirical methods, however, are useful in preliminary interpretations and in supplementing the final interpretation.

The empirical and semiempirical methods of interpretation are not recommended except in the preliminary examination of sounding curves. Considerable work has been done using these methods and some of it has been effective in ground-water studies. However, in almost every survey where the interpretation has been based on empirical and semiempirical methods only, more complete and accurate information could have been obtained using analytical methods.

Applications of Resistivity Surveys in Ground-Water Studies

In ground-water studies, the resistivity method can furnish information on subsurface geology which might be unattainable by other geophysical methods. For example, electrical methods are unique in furnishing information concerning the depth of the fresh-salt water interface, whereas neither gravity, magnetic, nor seismic methods can supply such information. A thick clay layer separating two aquifers usually can be detected easily on a sounding curve but the same clay bed may be a low velocity layer in seismic refraction surveys and cause erroneous depth estimates.

Mapping Buried Stream Channels

Buried stream channels, which often can be mapped accurately by the resistivity method, are favored targets for exploration. Horizontal profiling, electrical soundings, or both are used in their mapping.

In the San Jose area, California (fig. 37), knowledge of the presence and extent of shallow permeable layers is important in planning ponds for artificial recharge of ground water. Several buried stream channels were discovered by Zohdy (1964, 1965) and by Page (1968), using the combined techniques of horizontal profiling using the Wenner array and electrical sounding using the Schlumberger and Wenner arrays. Some of these channels were also investigated by use of induced polarization (Bodmer and others, 1968).

The buried stream channel in the Peñitencia area was discovered by making a few electrical soundings, the curves of which were distorted by the effect of lateral heterogeneities. The area was covered then by horizontal profiling using a Wenner electrode spacing of $a = 6.1$ m (20 feet). The result was an isoresistivity map (fig. 38) that clearly delineated the course of the buried channel. A cross section based on the interpretation of four sounding curves, the apparent resistivity profile, and subsequent drilling data are shown in figure 39.

According to information from the Santa Clara Valley Water Conservation District, the water table at one well near the percolation ponds subsequently developed in this area rose from a depth of about 73 m (240 ft) to a depth of about 37 m (130 ft) in two years.

In the area near Campbell, Calif., an apparent-resistivity map (fig. 40) was drawn on the basis of horizontal profiling using the Wenner array with spacing of $a = 9.15$

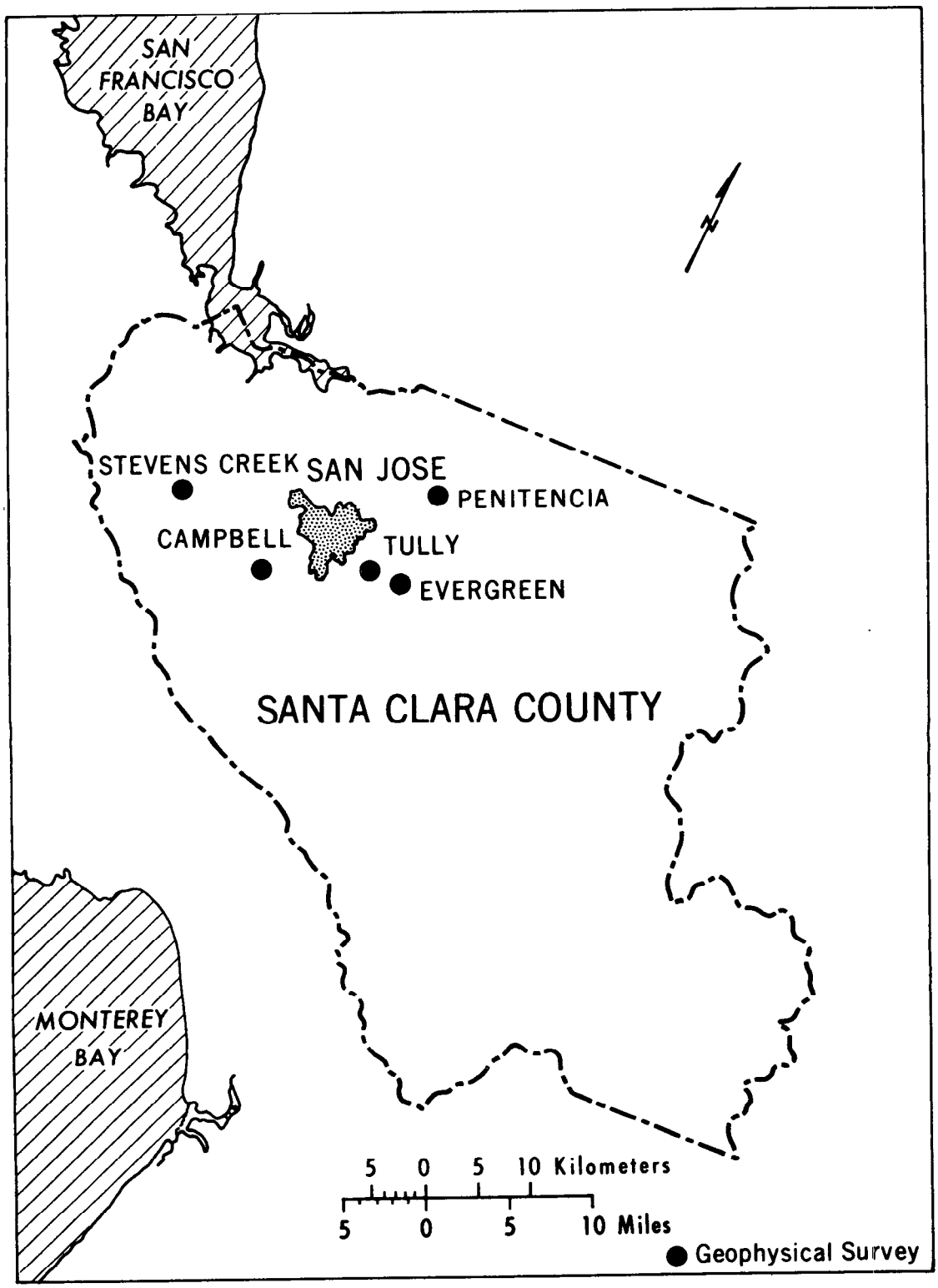

Figure 37.—Map of San Jose area, California, showing areas studied.

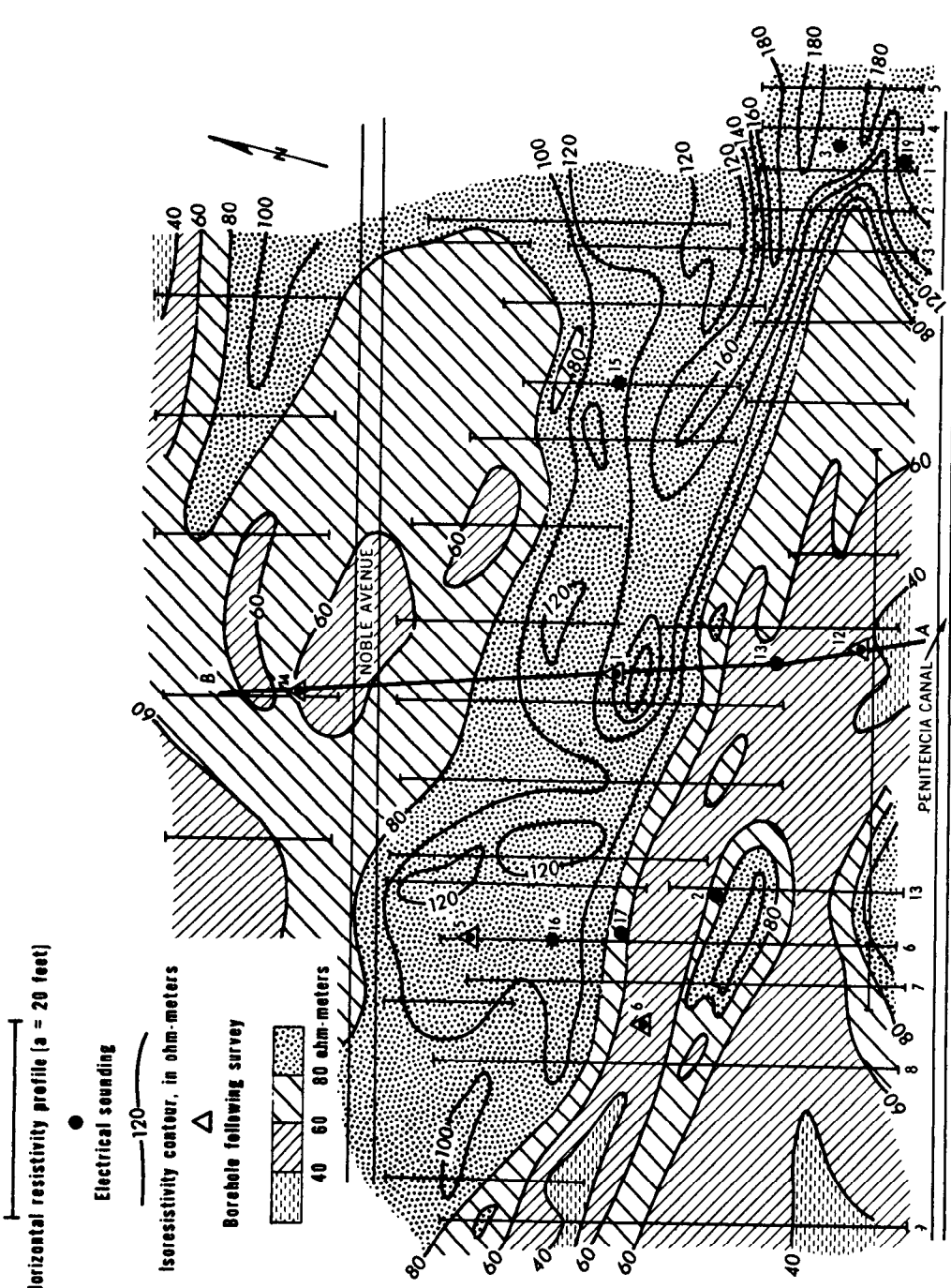

Figure 38.—Apparent-resistivity map, Penitencia, Calif. (after Zohdy, 1964, 1965), showing location of resistivity profile and geologic section, AB.

m (30 feet). The map indicated the presence of high resistivity layers at shallow depth but did not delineate the trend of a buried stream channel as directly and as clearly as in the Penitencia area. A cross-section based on the interpretation of electrical sounding data is shown in figure 41. The drilling of a well by the Santa Clara Water Conservation District near sounding 5 proved that the interpretation of the sounding curves was in excellent agreement with observed geologic conditions.

A buried stream channel saturated with fresh water was discovered near Salisbury, Md., by drilling (Hansen, 1966; Weaver and Hansen, 1966). A resistivity survey was made in the area of the channel using Schlumberger soundings and horizontal profiling ($\overline{AB}$ = 122 m (400 feet), $\overline{MN}$ = 24.4 m (80 feet)). A remarkable anomaly was obtained by horizontal profiling at right angles to the known strike of the channel (fig. 42). The interpretation of depth from the electrical soundings was in general agreement with drilling data.

From these three examples, we may conclude that, in shallow exploration, horizontal profiling can furnish information on the presence or absence of shallow buried stream channels and that elcctrical soundings for the determination of depth should precede and follow the horizontal profiling survey.

There are several examples in the literature (Denozier and others, 1961; Hallenbach, 1953) where courses of buried channels were mapped on the basis of electrical soundings and were subsequently verified by drilling. A map of interpreted true resistivities at a depth of 40 meters (131.2 ft) obtained north of Bremerhaven, West Germany, is shown in figure 43. The map was constructed on the basis of the interpretation of Schlumberger electrical soundings.

Geothermal Studies

In the Bad-Krozingen, Baden geothermal area in West Germany (Breusse and Astier, 1961) electrical soundings and horizontal profiling were made to delineate a fault zone where steam can be tapped for energy. An apparent-resistivity map was obtained

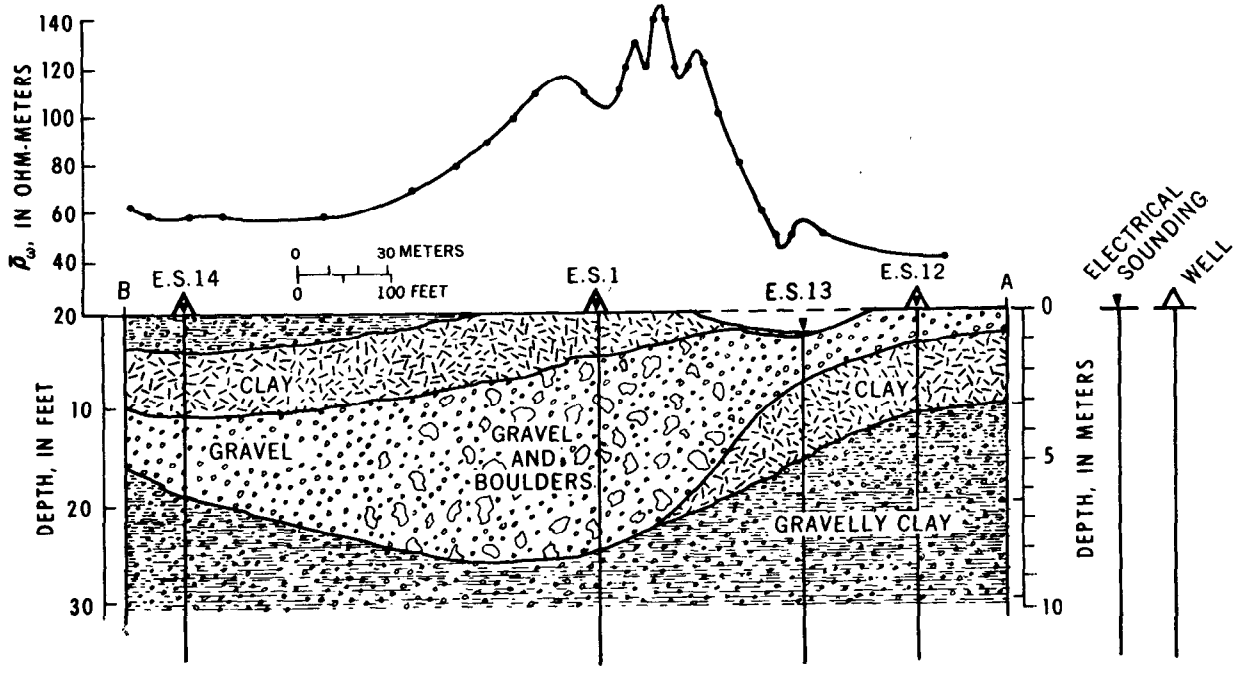

Figure 39.—Resistivity profile and geologic section, Penitencia, Calif. (after Zohdy, 1964, 1965). Horizontal profile obtained using Wenner array with electrode spacing a = 6.1 m (20 feet).

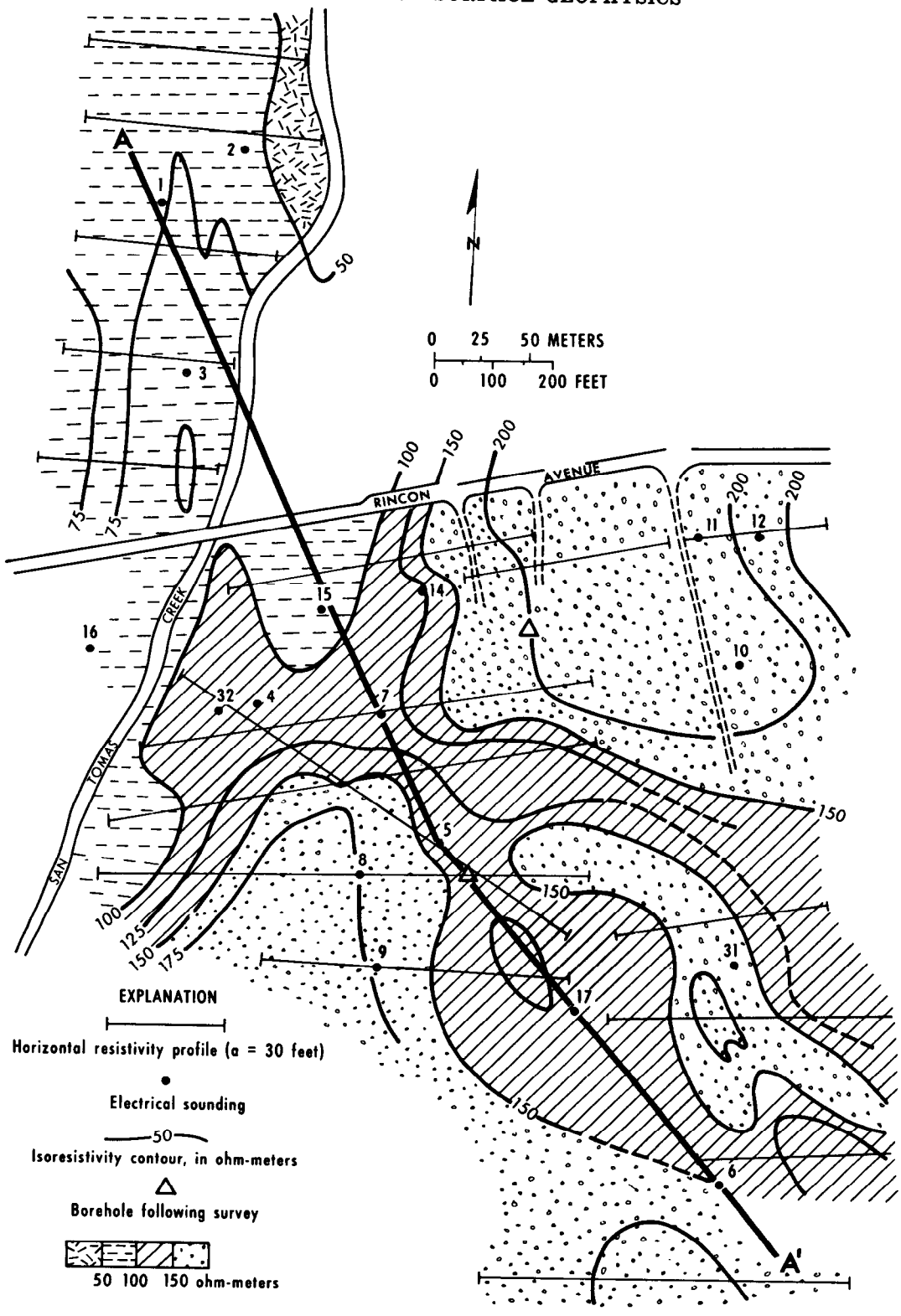

Figure 40.—Map of apparent resistivity near Campbell, Calif., obtained with Wenner array at a = 9.15 m (30 feet) and showing location of section AA'. (Unpub. data obtained by Zohdy, 1964.)

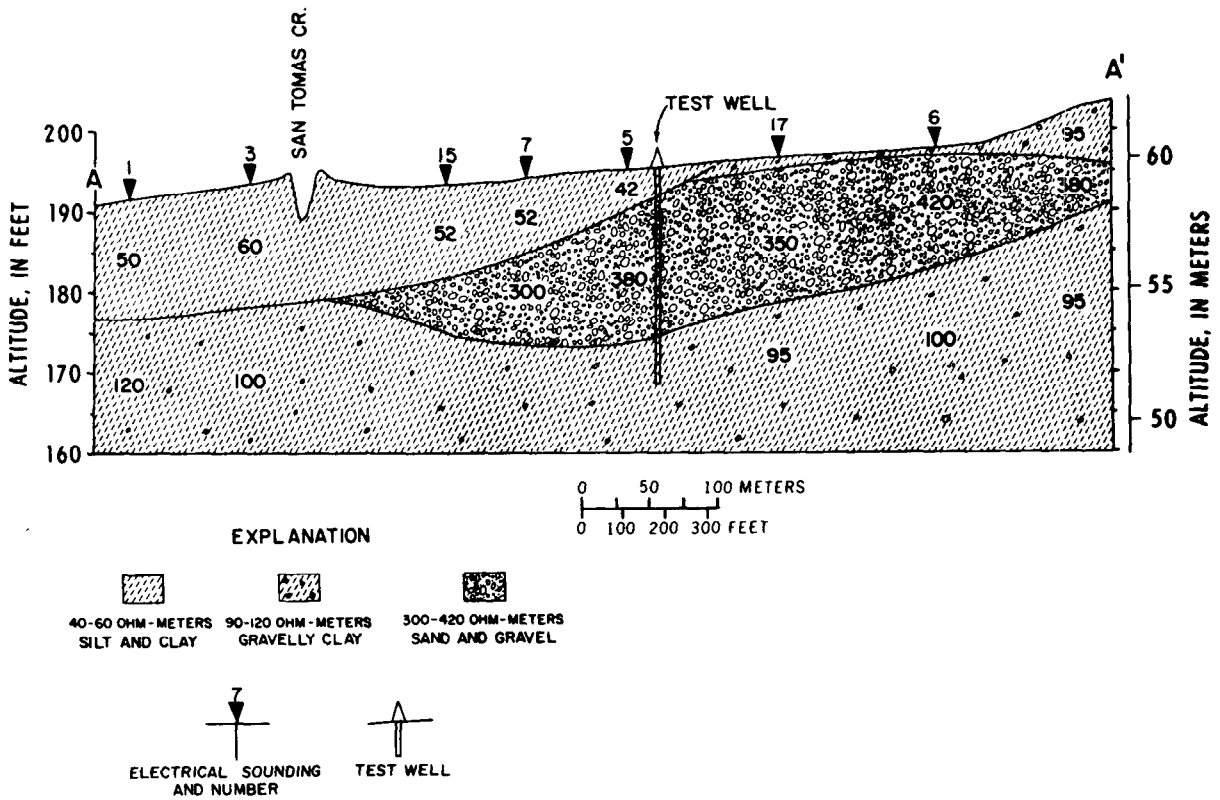

Figure 41.—Geoelectric section and drilling results near Campbell, Calif. Numbers in layers designate interpreted true resistivities. (Unpub. data obtained by Zohdy, 1964.)

by making horizontal profiling using the Schlumberger AB profile technique (see fig. 10a). In this survey the AB line was 4,000 m (13,120 feet) long. Eleven parallel profiles spaced 100 m (328 feet) apart were made, each of which consisted of 111 measurements spaced at 100 m (328 feet) intervals. The apparent-resistivity map obtained from this survey (fig. 44) was used to delineate the traces of the faults.

In New Zealand, Banwell and MacDonald (1965) and Hatherton and others (1966) reported on the successful use of Wenner sounding and horizontal profiling for delineating geothermal areas. Figure 45 shows an apparent-resistivity map prepared from Wenner horizontal profiling data using an electrode spacing of $a = 549$ m (1,800 feet). The two low-resistivity areas outlined by the 5 ohm-meter contour are believed to delineate the hottest ground. The northern area at the Wairakei Geyser Valley was already noted for its geothermal power production, but the large low-resistivity area southeast of Wairakei and northeast of Taupo was discovered by resistivity measurements. A test well (well 225) was drilled in that area, and a temperature of 220°C was recorded at a depth of 256.2 m (840 feet) where a well-marked structural discontinuity is encountered between relatively impermeable mudstones and a permeable pumice breccia. The geothermal power potential in this newly discovered area is probably considerable.

Other studies of geothermal areas were made in Italy by Alfano (1960) and by Breusse and Mathiez (1956).

Mapping Fresh-Salt Water Interfaces

From 1965 to 1969, the U.S. Geological Survey made several resistivity surveys in the southwestern United States where fresh-salt water interfaces were mapped successful-

ly with Schlumberger and equatorial electrical soundings. The apparent-resistivity map (fig. 46) was obtained with $\overline{AB}/2 = 305$ m (1,000 feet) in the White Sands Missile Range area (Zohdy and others, 1969). The apparent-resistivity contour of 10 ohm-m delineates, qualitatively, the area where mineralized groundwater is to be expected at shallow depth. Quantitative interpretation of the electrical sounding curves, using a digital computer for calculation of multilayer curves, resulted in the map shown in figure 47. The isobath lines on the map indicate depths at which the true resistivity of the rocks is less than 10 ohm-m (saline ground water) or more than 500 ohm-m (crystalline basement). Examples of electrical soundings obtained in the White Sands Missile Range area are shown in figure 48.

The literature is rich with case histories of areas in many parts of the world where the resistivity method was successfully used for mapping the fresh-salt water interface (Breusse, 1950; Flathe, 1967, 1968; Flathe and Pfeiffer, 1964; Van Dam and Meulenkamp, 1967; Zohdy, 1969a).

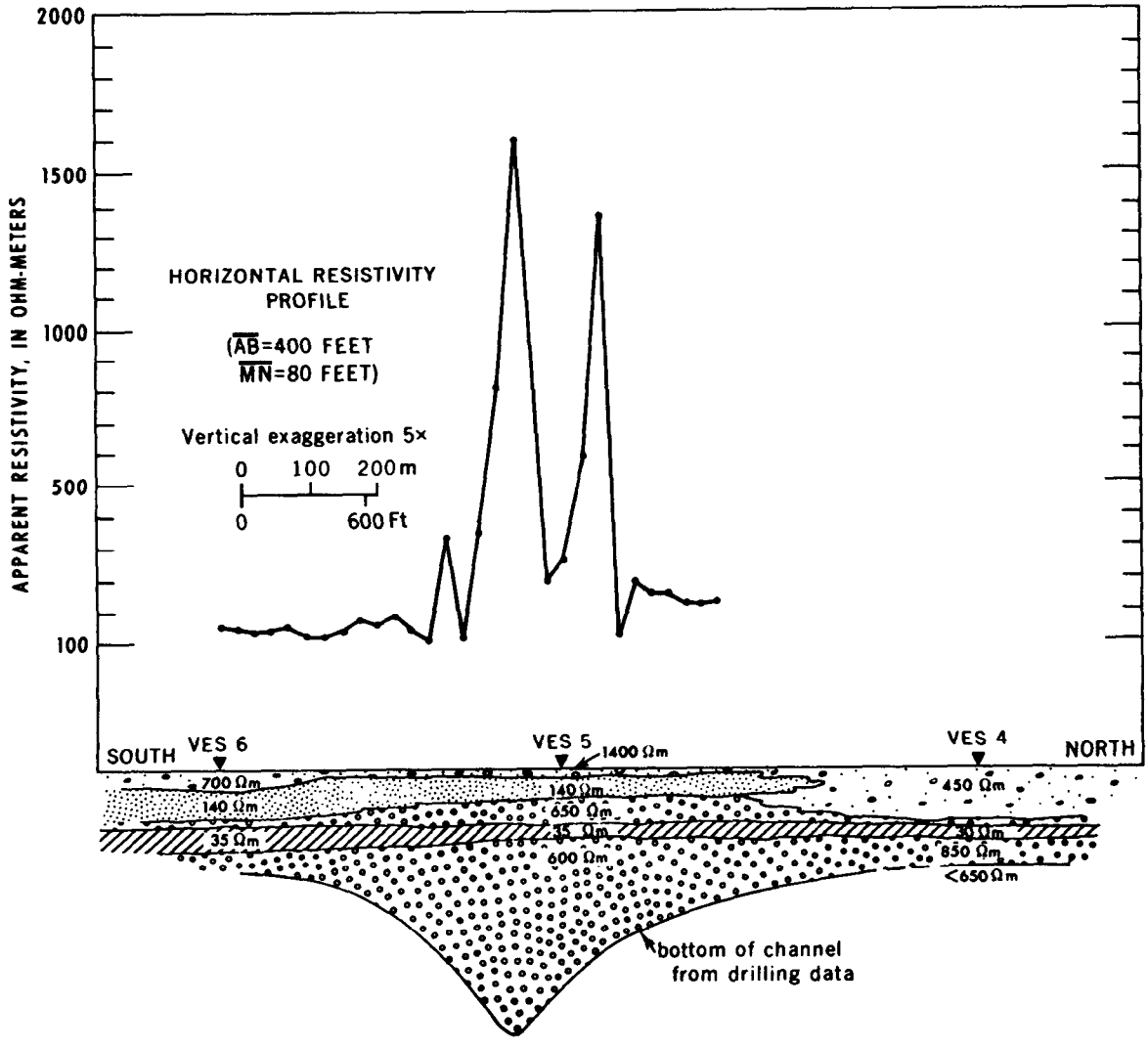

Figure 42.—Apparent-resistivity profile and geologic interpretation over buried channel, near Salisbury, Md. Data obtained by Zohdy and Jackson in 1966.

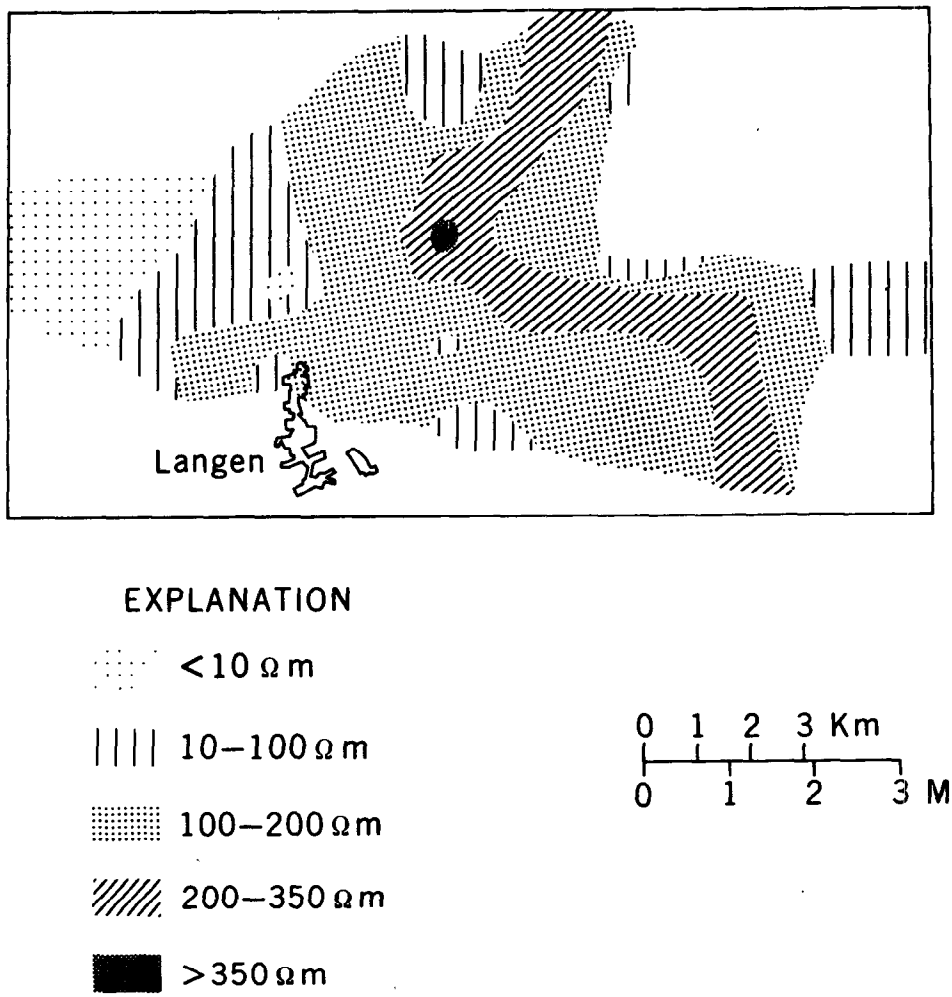

Figure 43.—Buried stream channel near Bremerhaven, West Germany, mapped from electrical sounding (after Hallenbach, 1953). Resistivities of more than 200 ohm-m were interpreted to be within the buried channel. Reproduced with permission of "Geophysical Prospecting."

Mapping the Water Table

Unlike the mapping of the fresh-salt water interface, the determination of the depth to the water table is generally a more difficult problem. Deppermann and Homilius (1965) investigated the geoelectric conditions where the water table can be detected on an electrical sounding curve. Wherever the water table is overlain and underlain by several layers of different resistivities, its detection on a sounding curve may be virtually impossible. Under favorable conditions the water table can be detected on a sounding curve as a conductive layer.

On the island of Hawaii, Zohdy and Jackson (1969) made several deep electrical soundings to determine the depth to low-resistivity layers that may represent basaltic lava saturated wih water. They concluded that the minimum depth to such a layer is of the order of 900 m (3,000 feet) (the survey was made at an average elevation of about 1,900 m (6,200 feet) above sea level). A block diagram based on the interpretation of electrical soundings in the Pohakuloa-

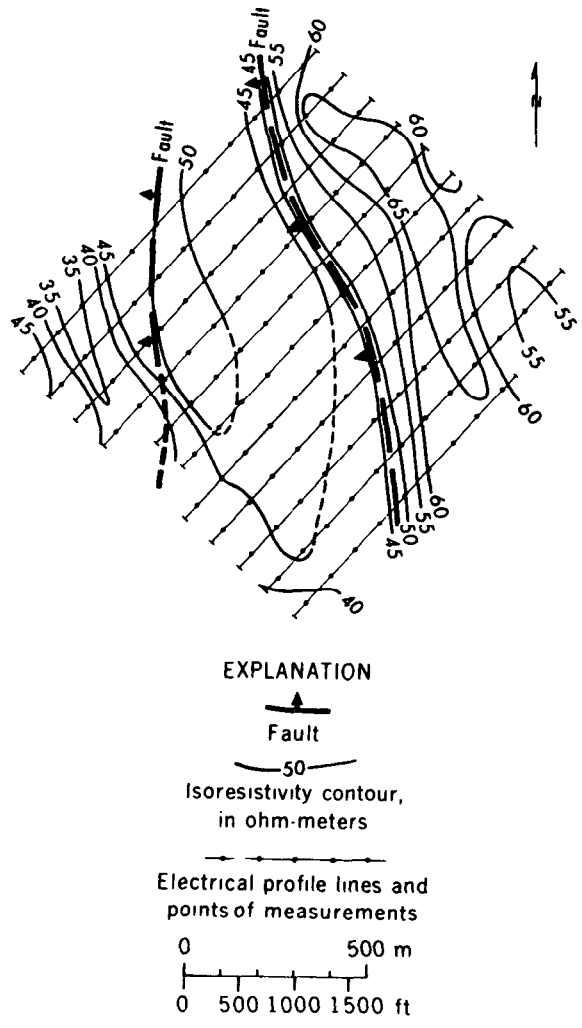

Figure 44.—Map of apparent resistivity in the Bad-Krozingen geothermal area, Germany. AB = 4,000 m (13,120 feet) (after Breusse and Astier, 1961).

Humuula area is shown in figure 49. The top of the layer with resistivity of less than 1,000 omh-m presumably may represent the water table. The ground water in this part of the island probably is partly impounded by dikes.

Mapping Clay Layers

Near Bowie, Ariz., a blue-clay layer separates two aquifers. The lower aquifer is artesian. The resistivity of this clay was found to be in the range of 0.5–7.0 ohm-m. The cross section shown in figure 50 is based on the interpretation of electrical soundings in that area. In places near VES 7 (fig. 51) where the clay is covered by less than 9 m (30 feet) of soil, and where it has very low resistivity (<1 ohm-m) and great thickness 275 m (900 feet), the lower aquifer acts as an electric basement.

Electromagnetic Methods

Electrical surveys also are made using a time-varying electromagnetic field as an energy source. These electromagnetic or induction methods generally use frequencies in the range between 100 and 5,000 Hz, but radio waves of higher frequencies are also used.

The magnetic field is produced by passing an alternating current through a wire loop. When this primary field is imposed on Earth materials a flow of electrical current results. The amount of current flow, as in other electrical surveys, depends on the conductivity of the layers. The current flow produces a secondary magnetic field which has the same frequency as the primary field, but not the same phase or direction. The secondary magnetic field can be detected at or above the ground surface by measuring the voltage induced in another loop of wire, the receiver.

Electromagnetic surveys can be made either on the ground or from a low-flying aircraft. The effective depth at which conductive bodies can be detected with electromagnetic methods is dependent upon both the frequency and spacing between the transmitter and the receiver loops. Thus, electromagnetic measurements can be used in the same manner as resistivity measurements to obtain horizontal profiles and depth soundings. In general, electromagnetic surveys lack the resolution and depth penetration of resistivity surveys but have the advantage of being rapid and less expensive. Results of electromagnetic surveys generally are presented in profile form. Measurements may be made at one or several frequencies. Interpretation usually is accomplished by curve matching or modeling. The technique is very effective in locating conductive bodies within

a few hundred feet of the surface, but has found only limited use in ground-water investigations. The technique has been used effectively in mapping buried channels where the channel-filling material has a resistivity contrast with the enclosing medium (Collett, 1967).

In recent years several powerful radio transmitters have begun broadcasting at frequencies of a few tens of kilo-Hertz. Radio waves at these frequencies penetrate the Earth to sufficient depths to be of use in geophysical exploration. Both ground and airborne detection systems have been developed. The measurements consist of one or more components of the electrical and magnetic fields. This method, which is undergoing rapid development, has proved effective in detecting near-surface highly conductive deposits, but quantitative interpretation techniques are not yet available.

A description of inductive methods is contained in Keller and Frischknecht (1966).

Induced Polarization Method

The induced electrical polarization method is widely used in exploration for ore bodies, principally of disseminated sulfides. Its use in ground-water exploration has been limited. The origin of induced electrical polarization is complex and is not well understood. This is primarily because several physico-chemical phenomena and conditions are responsible for is occurrence.

Conrad Schlumberger (Dobrin, 1960) probably was first to report on the induced polarization phenomenon, which he called "provoked polarization." While making conventional resistivity measurements, he noted that the potential difference, measured be-

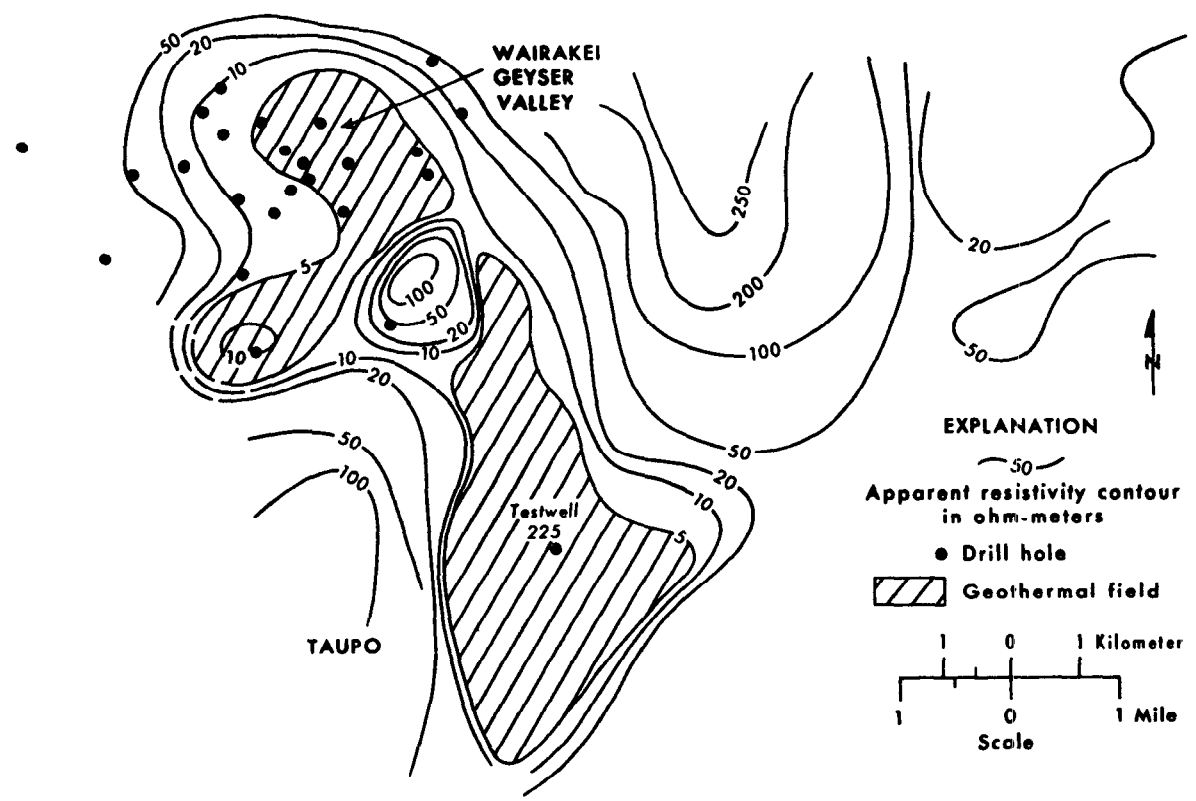

Figure 45.—Map of apparent resistivity in geothermal areas in New Zealand. Wenner spacing a = 549 m (1,800 feet). After Banwell and MacDonald (1965). Reproduced with permission of Commonwealth Mining and Metallurgical Congress.

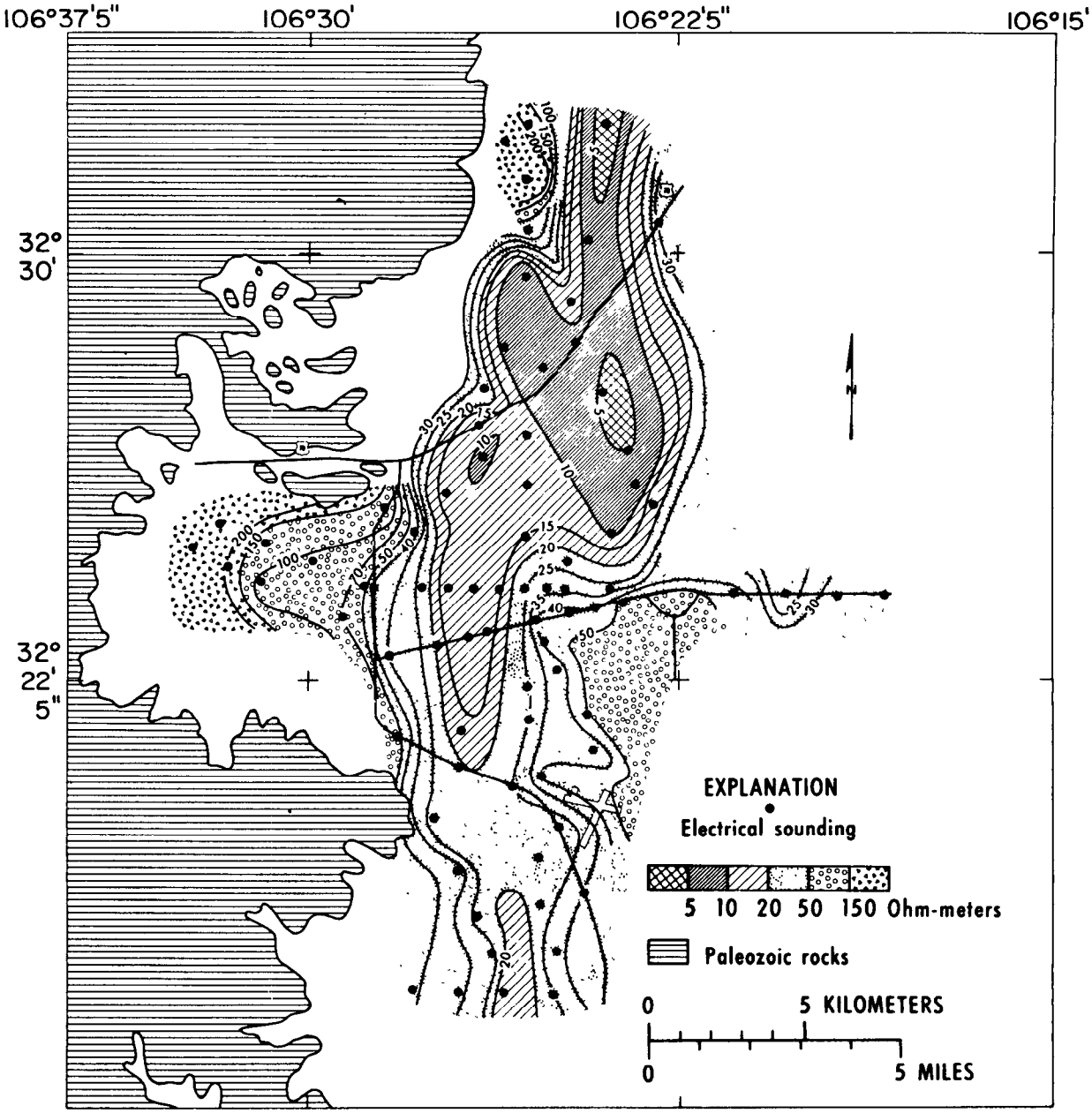

Figure 46.—Map of apparent resistivity in White Sands area, New Mexico, for electrode spacing $\overline{AB}/2 = 305$ m (1,000 feet) (after Zohdy and others, 1969).

tween the potential electrodes, often did not drop instantaneously to zero when the current was turned off. Instead, the potential difference dropped sharply at first, then gradually decayed to zero after a given interval of time. Certain layers in the ground became electrically polarized, forming a battery when energized with an electric current; upon turning off the polarizing current, the ground gradually discharged and returned to equilibrium.

The study of the decaying potential difference as a function of time is now known as the study of IP (induced polarization) in the "time domain." This type of study requires heavy and generally bulky equipment in the

field; to avoid this limitation, mining geophysicists began to study the effect of alternating currents on the measured value of resistivity. This is known as IP in the "frequency-domain."

Ground-water studies generally have been made with time-domain IP. In the time-domain IP, several indices have been used to define the polarizability of the medium. Seigel (1959) defined the "chargeability" (in seconds) as the ratio of the area under the decay curve (in millivolt-seconds) to the potential difference (in millivolts) measured before switching the current off. Komarov and others (1966) define the "polarizability" as the ratio of the potential difference after a given time from switching the current off to the potential difference before switching the current off. The polarizability is expressed as a percentage.

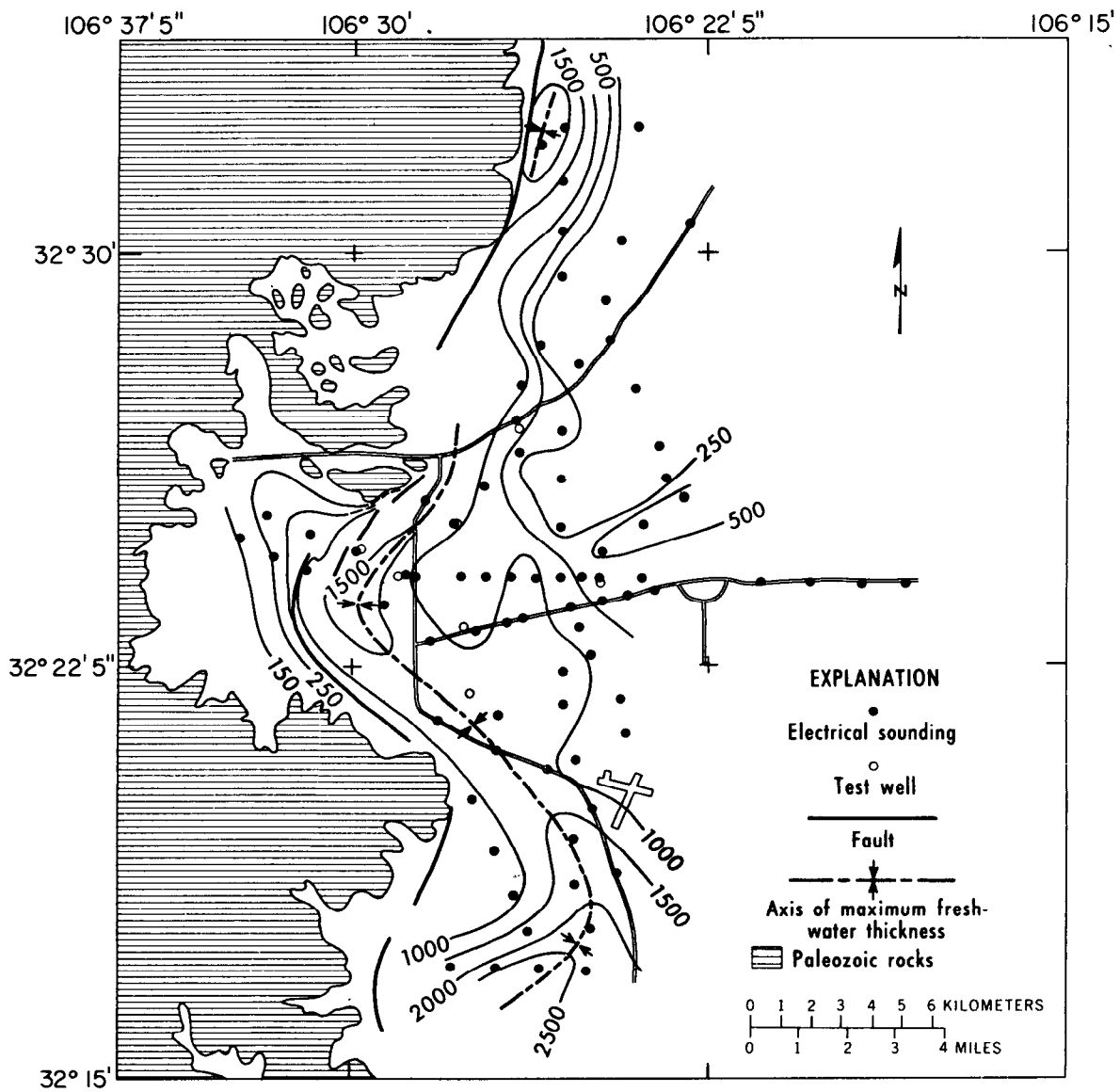

Figure 47.—Map of White Sands area, New Mexico, showing isobaths of the lower surface of fresh-water aquifer. Datum is land surface (after Zohdy and others, 1969).

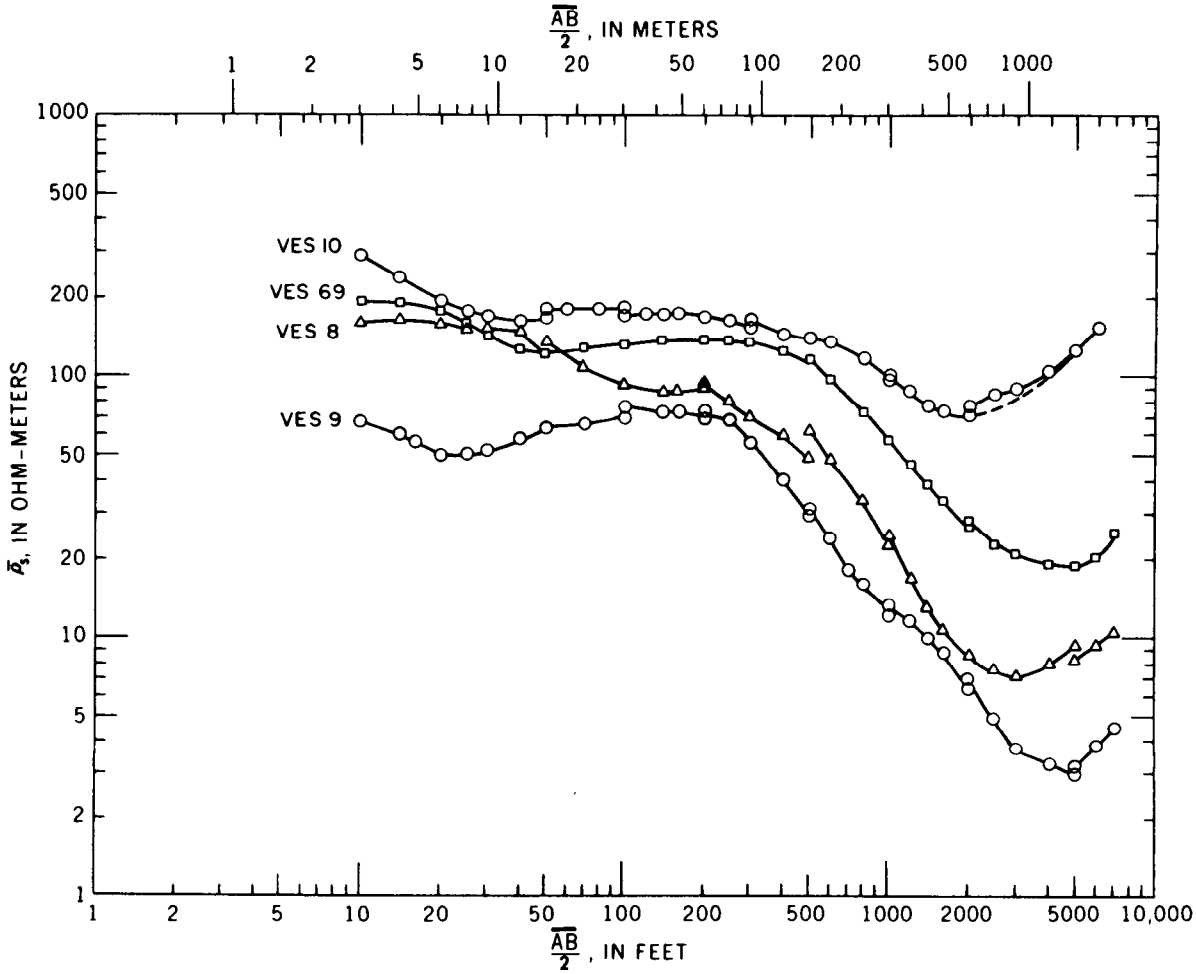

Figure 48.—Examples of Schlumberger sounding curves obtained in the White Sands area, New Mexico (after Zohdy and others, 1969).

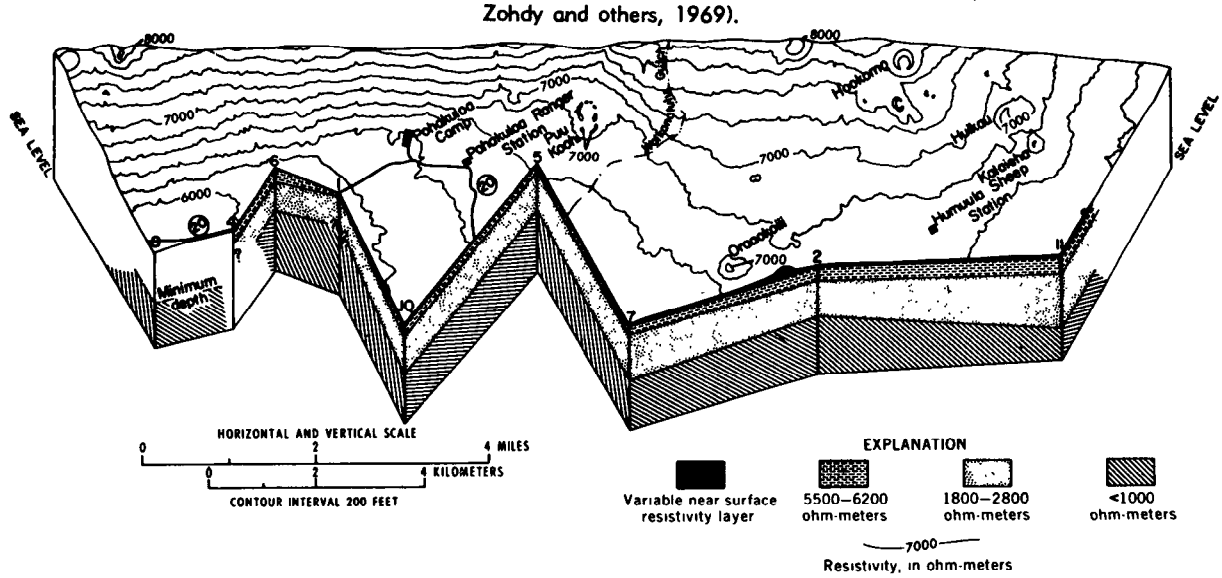

Figure 49.—Block diagram of Pohakuloa-Humuula area, Hawaii (after Zohdy and Jackson, 1969). Reproduced with permission of "Geophysics."

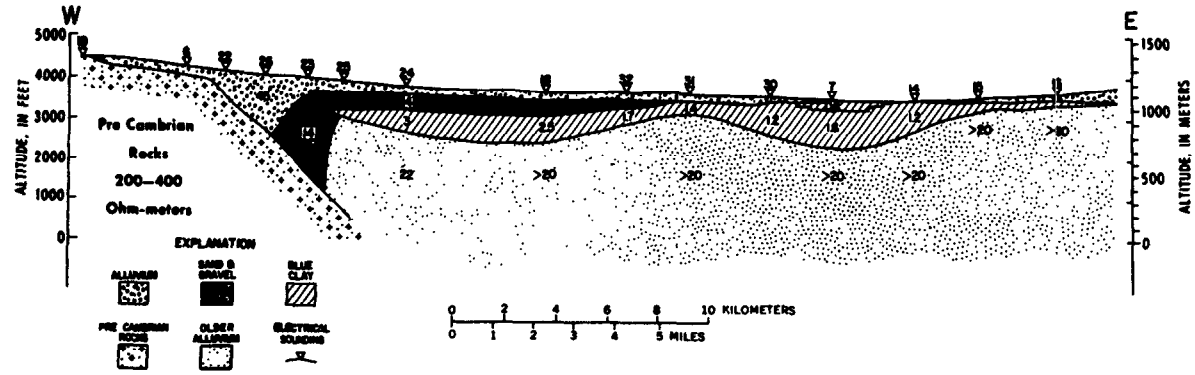

Figure 50.—Geoelectric section north of Bowie, Ariz. Numbers in layers designate true resistivities. Data obtained by Zohdy and Eaton, 1969.

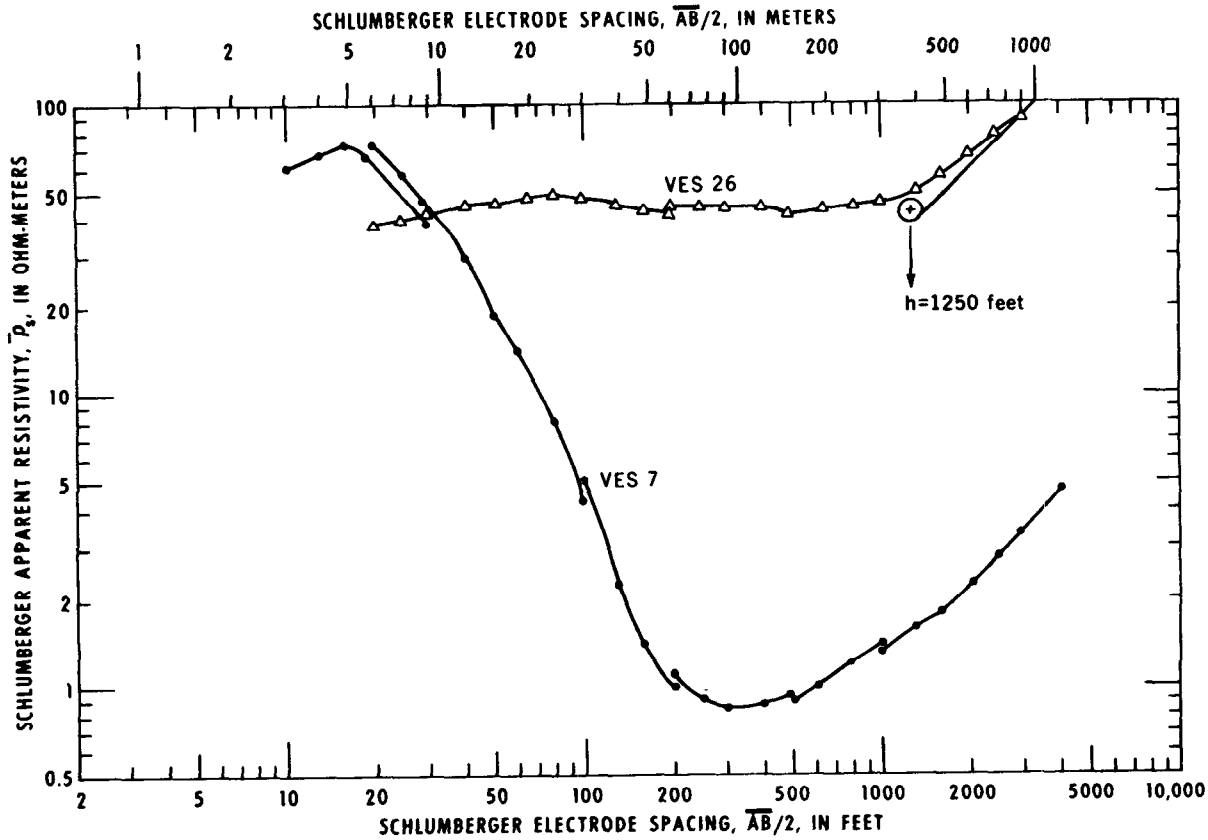

Figure 51.—Examples of Schlumberger sounding curves obtained near Bowie, Ariz. VES 26 shows homogeneous sediments (45 ohm-m) underlain by high resistivity Precambrian rocks at a depth of about 380 m (1,250 feet). VES 7 shows the presence of a thick section 275 m (900 feet) of low resistivity clay (<1 ohm-m). Data obtained by Zohdy and Eaton, 1969.

Relationship between apparent chargeability and apparent resistivity

Seigel (1959) showed that over a heterogeneous medium comprised of n different materials, the apparent chargeability, $\overline{\eta}$, is related to the apparent resistivity by

$$\overline{\eta} = \sum_{i=1}^{n} \eta_i \frac{\partial \log \overline{\rho}}{\partial \log \rho_i}, \qquad (1)$$

where η_i and ρ_i are the chargeability and resistivity of the i^{th} material. He also showed that the relation

$$\sum_{i=1}^{n} \frac{\partial \log \overline{\rho}}{\partial \log \rho_i} = 1, \qquad (2)$$

is valid. From equations 1 and 2 we can write the useful formula:

$$\frac{\overline{\eta}}{\overline{\eta}_1} = 1 + \sum_{i=2}^{n} \frac{\partial \log \overline{\rho}}{\partial \log \rho_i}\left(\frac{\eta_i}{\eta_1} - 1\right). \qquad (3)$$

If the theoretical expression for the apparent resistivity, $\overline{\rho}$, is known, then the corresponding expression for the reduced apparent chargeability $\frac{\overline{\eta}}{\eta_1}$, can be derived easily.

Induced Polarization Sounding and Profiling

The techniques of sounding and profiling, used in resistivity measurements, are also used in the IP method. IP sounding can be made using the Schlumberger, or Wenner array (in time-domain measurements). The apparent chargeability, $\overline{\eta}$, versus the electrode spacing, $\overline{AB}/2$ or $\overline{AB}/3$, is plotted on logarithmic coordinates. The IP sounding curve is interpreted by curve matching procedures using sets of IP sounding master curves.

At present, only a few two-layer master curves (for the Wenner array) have been published in the United States (Seigel, 1959; Frische and von Buttlar, 1957) but three-layer and four-layer curves have been published in the Soviet Union.

An IP sounding curve can be of significant value in complementing a resistivity sounding curve. For example, the resistivity and IP sounding curves for the following four-layer geoelectric section are shown in figure 52:

Layer	Thickness (m)	Thickness (ft)	Resistivity (ohm-m)	Chargeability (seconds)
1	10	32.8	10	1
2	10	32.8	160	1
3	5	16.4	40	10
4	∞	∞	160	1

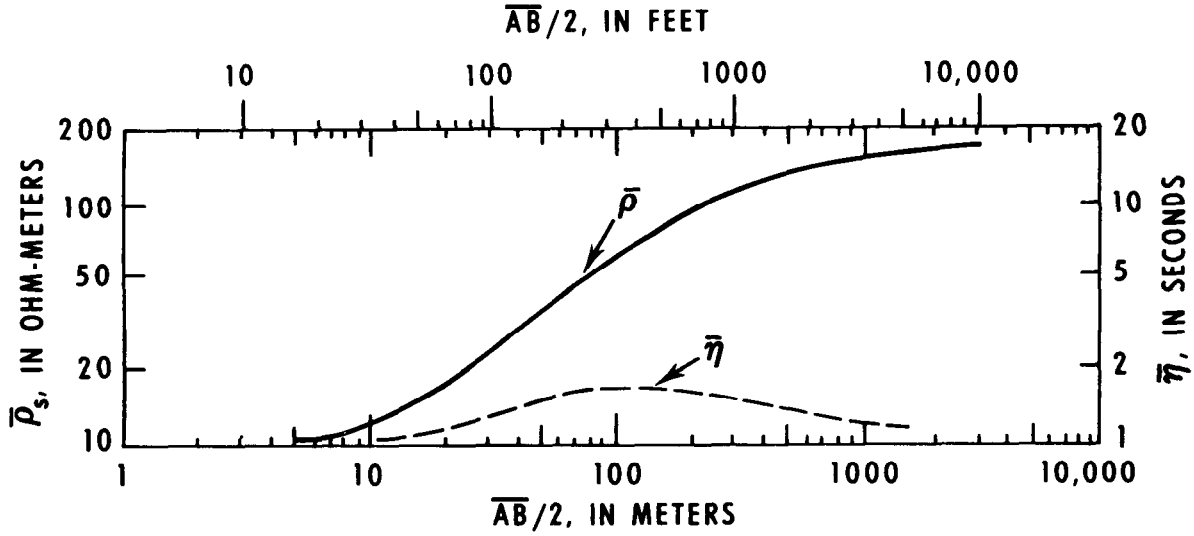

Figure 52.—Apparent resistivity and apparent chargeability (IP) sounding curves for a four-layer model (modified after Vanyan and others, 1961).

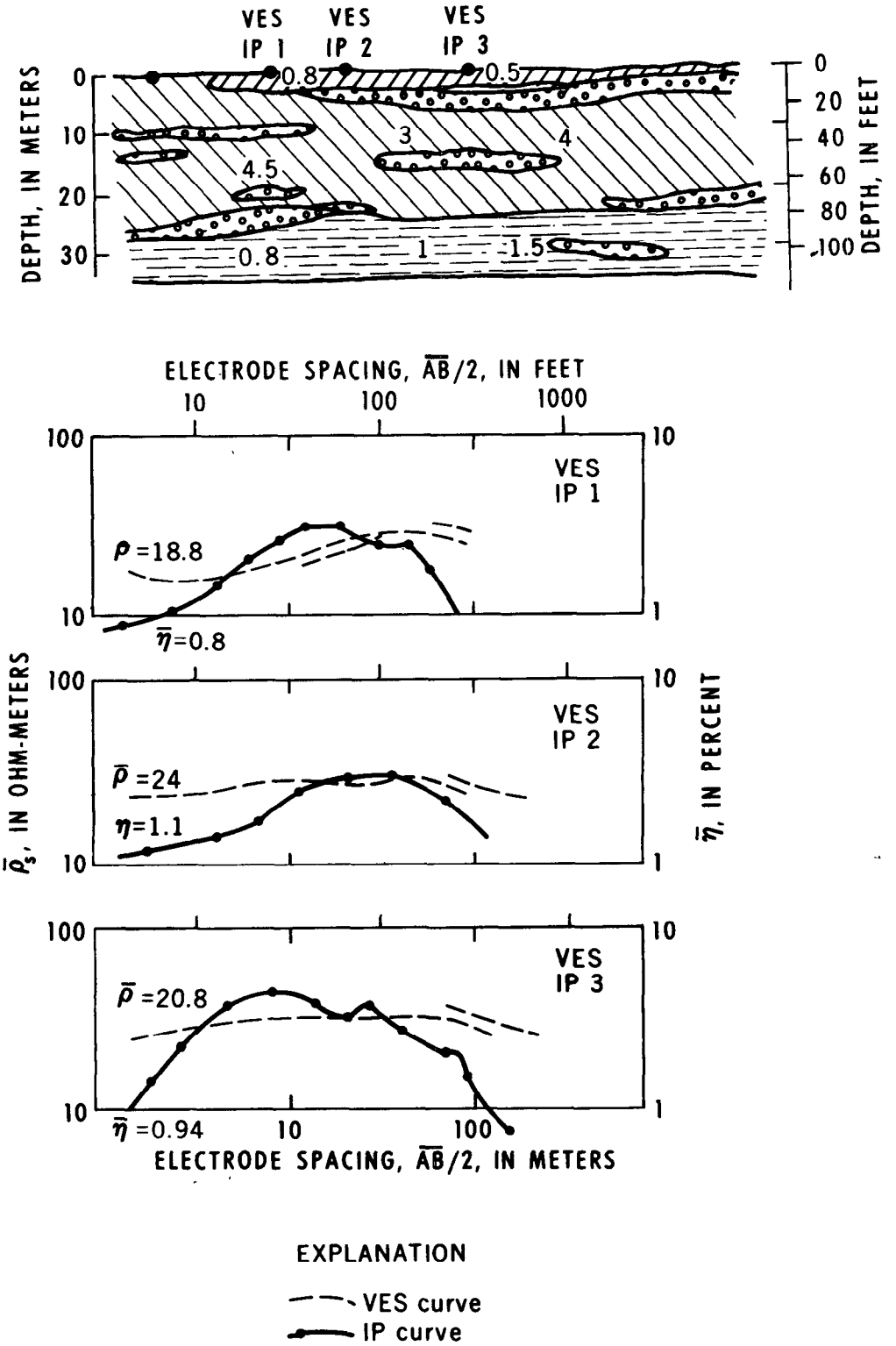

Figure 53.—Geoelectric section, VES and IP sounding curves of alluvial deposits in Crimea (after Kuzmina and Ogil'vi, 1965).

It is obvious that layer 3 cannot be distinguished on the four-layer resistivity curve (which resembles a two- or three-layer curve). But layer 3 is characterized by a different chargeability from the surrounding layers and its presence is indicated clearly by the IP sounding curve.

Applications of Induced Polarization in Ground-Water Surveys

Only a few IP surveys have been made for ground-water exploration, but there are three noted examples in the literature: Vacquier and others (1957); Kuzmina and Ogil'vi (1965); and Bodmer and others (1968). Kuzmina and Ogil'vi reported on work done near the Sauk-Soo river in Crimea and in the Kalinino region of Armenia. In Crimea the IP work consisted essentially of IP sounding (time domain) using the Wenner array. The alluvial deposits in the studied area were poorly differentiated by their resistivities, but three horizons were clearly distinguished by their polarizabilities (fig. 53). The section consisted of a top layer of weak polarizability (h_1 = 2–4 m (6.5–13 ft); η_1 = 0.8–1.5 percent), which represents a dry loamy layer; a second layer of strong polarizability (h_2 = 18–20 m (60–64 ft), η_2 = 3–5 percent), which represented a clayey sand layer saturated with fresh water; and a third layer of weak polarizability ($h_3 \rightarrow \infty$, η_3 = 1 percent), which represents impervious siltstones. The survey in this area demonstrates that the IP work provided more complete information about the ground-water occurrence than did the resistivity soundings alone.

References Cited

Abdullaev, R. A., and Dzhafarov, Kh. D., 1964, Theory and practice of the interpretation of geophysical observations (in Russian): Baku, Azerbaydzh. Gosudarst. Izd. (State press of Azerbaydzhan), p. 117–119.

Alfano, Luigi, 1959, Introduction to the interpretation of resistivity measurements for complicated structural conditions: Geophys. Prosp., v. 7, p. 311–366.

——— 1960, Geoelectric exploration for natural steam near Monte Amiata: Quaderni de Geophysica Applicata, v. 21, p. 3–17.

Al'pin, L. M., 1950, The theory of dipole sounding: Moscow, Gostoptekhizdat, 89 p. [Translation *in* Dipole methods for measuring earth conductivity]: New York, Plenum Press, 1966, p. 1–60.

——— 1958, Transformation of sounding curves: Prikladuaya Geofizika, v. 19, p. 23–46. [Translation *in* Dipole methods for measuring earth conductivity]: New York, Plenum Press, 1966, p. 61–78.

Banwell, C. J., and MacDonald, W. J. P., 1965, Resistivity surveying in New Zealand thermal areas: Eighth Commonwealth Mining and Metallurgical Congress, Australia and New Zealand, New Zealand Section, paper no. 213, 7 p.

Barnes, H. E., 1952, Soil investigations employing a new method of layer value determination for earth resistivity investigation: Highway Research Board Bull. 65, p. 26–36.

Barnes, H. E., 1954, Electrical subsurface exploration simplified: Roads and Streets, v. 97, p. 81–84.

Berdichevskii, M. N., 1957, On the determination of the total longitudinal conductance of sediments above a basement (in Russian): Razved. i promysl. geofiz., v. 19, p. 25–28. English translation by A. Zohdy, 1967, U. S. Geol. Survey Library, Denver, 7 p.

——— 1960, Electrical surveying by means of telluric currents: Moscow, Gostoptekhizdat. (English translation by Bradley, J. E. S., 1963, Boston Spa, England, National Lending Library; also by Keller, G. V., 1965, Quarterly of the Colorado School of Mines, v. 60, no. 1, 216 p.)

Berdichevskii, M. N., and Petrovskii, A. D., 1956, Methods of bilateral equatorial sounding: Prikladnaya Geofizika, v. 14, p. 97–114. [Translation by Ivan Mittin, U.S. Geol. Survey Library, Denver, 37 p.].

Berdichevskii, M. N., and Zagarmistr, A. M., 1958, Problems of interpretation of bilateral dipole electrical soundings of dipole arrays: Prikladnaya Geofizika, v. 19, p. 57–108. [Translation *in* Dipole methods for measuring earth conductivity: Plenum Press, 1966, p. 79–113.]

Bhattacharya, P. K., and Patra, H. P., 1968, Direct current geoelectric sounding, principles and interpretation: New York, Elsevier, 135 p.

Blokh, I. M., 1957, Dipole electroprofiling (in Russian): Moscow, Gosgeoltekhizdat, 191 p.

——— 1962, The resistivity method of electroprofiling (in Russian): Moscow, Gosgeoltekhizdat, 239 p.

Bodmer, René, Ward, S. H., and Morrison, H. F., 1968, On induced electrical polarization and

ground water: Geophysics, v. 33, no. 5, p. 805–821.

Breusse, J. J., 1950, La prospection électrique appliquée aux recherches hydrologique dans la presequ'île de Dakar: Internat. Geol. Cong., pt. V, p. 16–25.

——— 1961, Ground water geological surveys of the area east of Rome: Bull. de D'Association International des Hydrologeolgues, Rome Convention, Aug. 1961, 11 p.

——— 1963, Modern geophysical methods for subsurface water exploration: Geophysics, v. 28, no. 4, p. 633–657.

Breusse, J. J., and Mathiez, J. P., 1956, Application of electrical prospecting to tectonics in the search for natural steam at Larderello (Italy): Geophysical Case Histories, v. 2, p. 623–630.

Breusse, J. J., and Astier, J. L., 1961, Etude des diapirs en Alsace et Baden-Wurtemberg par la method du rectangle de resistivite: Geophys. Props., v. 9, p. 444–458.

Cagniard, Louis, 1953, Basic theory of the magnetotelluric method of geophysical prospecting: Geophysics, v. 18, p. 605–635.

——— 1956, Electricité tellurique, *in* Encyclopedia of Physics: Berlin, Springer-Verlag, v. 47, p. 407–469.

Collett, L. S., 1967, Resistivity mapping by electromagnetic methods: Mining and Groundwater Geophysics/1967, Geol. Survey of Canada, Economic Geology Rept. 26, p. 615–624.

Compagnie Générale de Géophysique, 1955, Abaques de sondage électrique: Geophys. Prosp., v. 3, supplement 3.

——— 1963, Master curves for electrical sounding (2nd revised edition): Leiden, Eur. Assoc. of Explr. Geophys.

Dakhnov, V. N., 1953, Electrical prospecting for petroleum and natural gas deposits: Moscow, Gostoptekhizdat, 497 p.

Denozière, P., Hirtz, J. M., Astier, J. L., Millot, G., and Simler, L., 1961, Étude hydrogeologique par prospection électrique du cône de déjection de L'Andlau (environs d'Anlau, Bas-Rhin): Strasbourg, Bull. Serv. Carte géol. Als. Lorr., v. 14, pt. 2, p. 27–37.

Deppermann, Karl, 1954, Die Abhangigkeit des scheinbaren Widerstandes von Sondenabstand bei der Vierpunkt-Method: Geophys. Prosp., v. 2, p. 262–273.

Deppermann, Karl, and Homilius, Joachim, 1965, Interpretation geoelektrischer Sondierungskurven bei Tiefliegender Grundwasseroberfläche: Geologisches Jahrbuch, v. 83, p. 563–573.

Dobrin, M. B., 1960, Introduction to geophysical prospecting (2nd edition): New York, McGraw-Hill Book Co., Inc., 446 p.

Dzhafarov, Kh. D., and Bairamova, R. A., 1965, The interpretation of four-layer VES curves of the HK-type (in Russian): Razvedochnaya Geofizika, v. 3, p. 78–82. English translation by Rhoda Robinson, U.S. Geol. Survey Library, Denver, 8 p.

Evjen, H. M., 1938, Depth factors and resolving power of electrical measurements: Geophysics, v. 3, p. 78–98.

Flathe, H., 1955, A practical method of calculating geoelectrical model graphs for horizontally stratified media: Geophys. Prosp., v. 3, p. 268–294.

Flathe, H., 1958, Geoelectrical investigations on clay deposits in Western Germany: Leiden, European Assoc. Explor. Geophysicals. Geophysical surveys in mining, hydrological, and engineering projects, p. 170–185.

——— 1963, Five-layer master curves for the hydrogeological interpretation of geoelectric resistivity measurements above a two-story aquifer: Geophys. Prosp., v. 11, p. 471-508.

——— 1964, New ways for the interpretation of geoelectrical resistivity measurements in the search for and delimitation of aquifers: Internat. Assoc. of Sci. Hydrology Bull. 9th year, no. 1, p. 52–61.

——— 1967, Interpretation of geoelectrical resistivity measurements for solving hydrogeological problems: Mining and Groundwater Geophysics/1967, Geol. Survey of Canada, Econ. Geol. Report 26, p. 580–597.

——— 1968, Geoelecktrische Untersuchung der Grundwasserversalzung im südlichen Jordantal: Geologisches Jahrbuch, v. 85, p. 767–782.

Flathe, Herbert, and Pfeiffer, D., 1964, Outlines on the hydrology of the isle of Madura (Indonesia): Internat. Assoc. of Sci. Hydrology, Berkeley, 1963, no. 64, p. 543–560.

Frische, R. H., and Von Buttlar, Haro, 1957, A theoretical study of induced electrical polarization: Geophysics, v. 22, no. 3, p. 688–706.

Genslay, R., and Rouget, F., 1937, Sur l'anisotropie électrique des terrains et la pseudo-anisotropie: World Petroleum Cong. 2d, p. 723–731.

Ghosh, D. P., 1971, Inverse filter coefficient for the computation of apparent resistivity standard curves for a horizontally stratified earth: Geophys. Prosp., v. 19, no. 4, p. 769–775.

Golovtsin, V. N., 1963, Elecktrorazvedka (Electrical prospecting): Kiev, Akademiya Nauuk Ukrainiskoi, SSR, 361 p.

Hallenbach, F., 1953, Geo-electrical problems of the hydrology of West German areas: Geophys. Prosp., v. 1, no. 4, p. 241–249.

Hansen, H. J., III, 1966, Pleistocene stratigraphy of the Salisbury area, Maryland, and its relationship to lower eastern shore: a subsurface approach: Maryland Geol. Survey, report of investigations no. 2, 27 p., 5 tables.

Hatherton, T., Macdonald, W. J. P., and Thompson,

G. E. K., 1966, Geophysical methods in geothermal prospecting in New Zealand: Bull. Volcanol., v. 29, p. 485–498.

Hedstrome, H., 1932, Electrical prospecting for auriferous quartz veins and reefs: Mining Mag., v. 46, p. 201–213.

Homilius, J., 1961, Über die Auswertung geoelektrischer Sondierungskurvon im Falle eines vielfach geschichteten Untergrundes: Zeitschrift für Geophysik, v. 27, p. 282–300.

——— 1969, Geoelectrical investigations in East Afghanistan: Geophys. Prosp., v. 17, p. 449–487.

Hummel, J. N., 1932, A theoretical study of apparent resistivity in surface potential methods: Trans. A.I.M.E., Geophys. Prosp., v. 97, p. 392–422.

Jakosky, J. J., 1950, Exploration Geophysics: Los Angelos, Trija, 1,195 p.

Kalenov, E. N., 1957, Interpretation of vertical electrical sounding curves: Moscow, Gostoptekhizdat, 472 p.

Keller, G. V., 1968, Discussion on "An inverse slope method of determining absolute resistivity" by P. V. Sanker Narayan and K. R. Ramanujachary (Geophysics, v. 32, p. 1036–1040, 1967): Geophysics, v. 33, p. 843–845.

Keller, G. V., and Frischknecht, F. C., 1966, Electrical methods in geophysical prospecting: New York, Pergamon Press, 519 p.

Komárov, V. A., Pishpareva, H. N., Semenov, M. B., and Khloponina, L. S., 1966, (Sheinmanna, S. M., editor), Theoretical fundamentals for interpretation of survey data obtained with the induced polarization method: Leningrad, Isdatel'stov "Nedra," 203 p.

Kreines, I. I., 1957, On the distortion of VES curves in the presence of a vertical electrical contact separating different media: Prikladnaya Geofizika, v. 17, p. 152–161.

Kunetz, Géza, 1955, Einfluss vertikaler Schischten auf elektrische Sondierungen: Zeitschr. Geophysik, v. 21, p. 10–24.

——— 1957, Les courants telluriques et leur application á la prospection: Ciel et Terre, LXXIII[e] année, no. 7–8, July-August issue, 32 p.

——— 1966, Principles of direct current resistivity prospecting: Berlin, Gebrüder Borntraeger, 103 p.

Kuzmina, E. N., and Ogil'vi, A. A., 1965, On the possibility of using the induced polarization method to study ground water: Razvedochnaya i Promyslovaya Geofizika, no. 9, p. 47–69.

Lasfargues, Pierre, 1957, Prospection électrique par courants continus: Paris, Masson et Cie, 290 p.

Logn, O., 1954, Mapping nearly vertical discontinuities by earth resistivities: Geophysics, v. 19, p. 739–760.

Maillet, R., 1947, The fundamental equations of electrical prospecting: Geophysics, v. 3, p. 529–556.

Matveev, B. K., 1964, Methods of graphical construction of electrical sounding curves: Moscow, [Publishing house] Nedra, 72 p. [English translation by I. Mittin, 1967, U.S. Geol. Survey Library, Denver, Colorado, 116 p.]

Migaux, León, 1946, A new method of applied geophysics: prospecting by telluric currents (in French): Annales Geophysique, v. 2, p. 131–146.

——— 1948, Practical applications of the telluric method (in French): Internat. Geol. Cong. Proc., pt. V, p. 85–95.

Migaux, León, Bouchon, R., and Repal, S. N., 1952, Telluric study in the Hodna Basin (in French): Internat. Geol. Cong. Proc., pt. IX, p. 231–243.

Migaux, León, and Kunetz, Géza, 1955, Apports des methodes electriques de surface a la prospection petroliere: World Petroleum Cong., 4th, Proc., Sec. I, p. 545–574.

Mooney, H. M., and Wetzel, W. W., 1956, The potentials about a point electrode and apparent resistivity curves for a two-, three-, and four-layer earth: Minneapolis, University of Minnesota Press, 145 p., 243 plates.

Mooney, H. M., Orellana, Ernesto, Pickett, Harry, and Tornheim, Leonard, 1966, A resistivity computation method for layered earth models: Geophysics, v. 31, p. 192–203.

Moore, W., 1945, An empirical method of interpretation of earth resistivity measurements: A.I.M.E. Geophys. Prosp. Trans., v. 164, p. 197–223.

——— 1951, Earth resistivity tests applied to subsurface reconnaissance surveys: Am. Soc. for Testing Materials, Spec. Tech. Publ. 122, p. 89–103.

Muskat, M., 1933, Potentials about an electrode on the surface of the earth: Physics, v. 4, p. 129–147.

——— 1945, The interpretation of earth resistivity measurements: A.I.M.E. Geophys. Prosps. Trans., p. 224–231.

Muskat, M., and Evinger, H. H., 1941, Current penetration in direct current prospecting: Geophysics, v. 6, p. 297–427.

Ogilvy, A. A., Ayed, M. A., and Bogorlovsky, V. A., 1969, Geophysical studies of water leakages from reservoirs: Geophys. Prosp., v. 27, no. 1, p. 36–62. [Netherlands].

Orellana, Ernesto, 1960, Algunas cuestiones de prospeccion geolectrica: Revista de Geofisica, v. 19, p. 13–28.

——— 1961, Criterios erróneos en la interpretación de sondeos eléctricos: Revista de Geofísica, v. 20, p. 207–227.

——— 1966, Notas sobre a la interpretacion de

sondeos electricos verticalés: Revista de Geofísica, v. 25, p. 1–40.

Orellana, Ernesto, and Mooney, H. M., 1966, Master tables and curves for vertical electrical sounding over layered structures: Madrid Interciecia, 150 p., 66 tables.

Page, L. M., 1968, The use of the geoelectric method for investigating geologic and hydrologic conditions in Santa Clara County, California: Jour. Hydrology, v. 7, no. 2, p. 167–177.

Rabinovich, B. I., 1965, Fundamentals of the method of field difference [in Russian]: Prikladnaya Geofizika, v. 43, p. 47–59. [English translation by I. Mittin, U.S. Geol. Survey Library, Denver, Colorado, 21 p.]

Schlumberger, Marcel, 1939, The application of telluric currents to surface prospecting: Am. Geophys. Union, Trans. part 3, p. 271–277.

Seigel, H. O., 1959, Mathematical formulation and type curves for induced polarization: Geophysics, v. 24, no. 3, p. 547–565.

Stefanesco, S. S., Schlumberger, Conrad, and Schlumberger, Marcel, 1930, Sur la distribution electrique potentielle autor d'une prix de terre ponctuelle daus un terrain a couche horizontales, homogenes et isotrope: Jour. de Physique et le Radium, v. 11, no. 1, p. 132–140.

Unz, M., 1963, Relative resolving power of four point resistivity configurations: Geophysics, v. 28, p. 447–456.

Vacquier, Victor, Holmes, C. R., Kintzinger, P. R., and Lavergne, Michel, 1957, Prospecting for ground water by induced electrical polarization: Geophysics, v. 12, no. 3, p. 660–687.

van Dam, J. C., 1964, A simple method for the calculation of standard graphs to be used in geoelectrical prospecting: Delft, Uitgeverij Waltman, 87 p.

——— 1965, A simple method for the calculation of standard graphs to be used in geo-electrical prospecting: Geophys. Prosp., v. 13, no. 1, p. 37–65.

van Dam, J. C., and Meulenkamp, J. J., 1967, Some results of the geo-electrical resistivity method in ground water investigations in the Netherlands: Geophys. Prosp., v. 15, no. 1, p. 92–115.

Van Nostrand, R. G., and Cook, K. L., 1966, Interpretation of resistivity data: U.S. Geol. Survey Prof. Paper 499, 310 p.

Vanyan, L. L., Morozova, G. M., and Lozhenitsyna, L. V., 1961, On the theoretical curves of the induced polarization method [in Russian]: Geologiya i Geofizika, no. 10, p. 118–123.

Vedrintsev, G. A., and Tsekov, G. D., 1957, Procedure for obtaining multilayer theoretical VES curves by the decomposition method in conjunction with the graphical method [in Russian]: Razvedochnaya i Promyslovaya Geofizika, v. 20, p. 36–46. [English translation by A. A. R. Zohdy and R. Robinson, 1968, U.S. Geol. Survey Library, Denver, Colorado, 19 p.]

Wantland, Dart, 1951, Geophysical measurements of the depth of weathered mantle rock: Am. Soc. Testing and Materials Spec. Tech. Pub. 122, p. 115–135.

Weaver, W., 1929, Certain applications of the surface potential method: A.I.M.E. Geophys. Prosp. Trans., v. 81, p. 68–86.

Weaver, K. N., and Hansen, H. J., III, 1966, An ancient buried river channel is discovered: The Maryland Conservationist, v. 43, no. 2, p. 9–11.

Wenner, Frank, 1916, A method of measuring earth resistivity: U.S. Bureau of Standards Bull., v. 12, p. 469–478.

Yungul, S., 1968, Measurement of telluric "relative ellipse area" by means of vectograms: Geophysics, v. 33, no. 1, p. 127–131.

Zagarmistr, A. M., 1957, Utilization of the increased resolving power of dipole-axial soundings in investigating a "Type-H" section (in Russian): Prikladnaya Geofizika, v. 16, p. 130–144. [Translation by Ivan Mittin, U.S. Geol. Survey Libraray, 1966, Denver, Colorado, 21 p.]

Zohdy, A. A. R., 1964, Earth resistivity and seismic refraction investigations in Santa Clara County, California: Unpub. Ph.D. thesis, Stanford Univ., 132 p.

——— 1965a, The auxiliary point method of electrical sounding interpretation, and its relationship to the Dar Zarrouk parameters: Geophysics, v. 30, p. 644–660.

——— 1965b, Geoelectrical and seismic refraction investigations near San Jose, California: Ground Water, v. 3, no. 3, p. 41–48.

——— 1968a, A rapid graphical method for the interpretation of A- and H-type electrical soundings: Geophysics, v. 33, p. 822–833.

——— 1968b, The effect of current leakage and electrode spacing errors on resistivity measurements, *in* Geological Survey Research 1968: U.S. Geol. Survey Prof. Paper 600–D, p. D258–D264.

——— 1969a, The use of Schlumberger and equatorial soundings in ground-water investigations near El Paso, Texas: Geophysics, v. 34, p. 713–728.

——— 1969b, A new method for differential resistivity sounding: Geophysics, v. 34, p. 924–943.

——— 1970, Variable azimuth Schlumberger sounding and profiling near a vertical contact: U.S. Geol. Survey Bull. 1313–B, 22 p.

Zohdy, A. A. R., and Jackson, D. B., 1969, Application of deep electrical soundings for ground water exploration in Hawaii: Geophysics, v. 34, p. 584–600.

Zohdy, A .A. R., Jackson, D. B., Mattick, R. E. and Peterson, D. L., 1969, Geophysical surveys for ground water at White Sands Missile Range, New Mexico: U.S. Geol. Survey open file rept., 31 p.